PARTICLE TRAJECTORIES IN A HYDROCYCLONE

A THESIS

Presented to

The Faculty of the Graduate Division

by

Charles Wesley Bouchillon

In Partial Fulfillment

of the Requirements for the Degree

Doctor of Philosophy in the

School of Mechanical Engineering

Georgia Institute of Technology

June, 1963

In presenting the dissertation as a partial fulfillment of the requirements for an advanced degree from the Georgia Institute of Technology, I agree that the Library of the Institution shall make it available for inspection and circulation in accordance with its regulations governing materials of this type. I agree that permission to copy from, or to publish from, this dissertation may be granted by the professor under whose direction it was written, or, in his absence, by the dean of the Graduate Division when such copying or publication is solely for scholarly purposes and does not involve potential financial gain. It is understood that any copying from, or publication of, this dissertation which involves potential financial gain will not be allowed without written permission.

PARTICLE TRAJECTORIES IN A HYDROCYCLONE

Approved:

Date approved by Chairman: May 21, 1963

ACKNOWLEDGMENTS

Assistance and encouragement for the completion of this investigation has been derived from many sources and omission of any of them here is the result of space limitation rather than lack of appreciation. An expression of gratitude to Dr. C. W. Gorton for his counsel in this investigation successive to his generous advice and encouragement during my overall program of graduate study is made with cognizance of the inadequacy of the requital. My sincere appreciation is given to Dr. Thomas W. Jackson for his counsel and encouragement in this investigation as well as the invaluable advice relating to research endeavors which he has generously supplied from time to time. Dr. Clyde Orr rendered a valuable service in reading and commenting on this presentation before its final preparation. I am very grateful to Dr. Homer S. Weber for his interest and encouragement during my program of graduate study.

Thanks are given to Mr. John Martin for assistance in hydrocyclone fabrication, to Mr. H. O. Foster for assistance in material procurement, to Mr. R. S. Cantrell for assistance in collection of the data, to Messrs. R. S. Johnson and Ralph Loftin for assistance in obtaining the analog computer solutions, to the staff of the Rich Electronic Computer Center for assistance in obtaining the numerical solutions, and to numerous others who had a share in the completion of this work.

I would like to express my gratitude to Barbara, my wife, Leslie, my daughter, and Rusty, my son, for the inspiration they furnished, and for their forbearence in yielding to the schedule necessary for completion of this program.

TABLE OF CONTENTS

TABLE OF CONTENTS (Continued)

LIST OF TABLES

LIST OF ILLUSTRATIONS

LIST OF ILLUSTRATIONS (Continued)

SUMMARY

The conventional hydrocyclone has been successfully employed for many years as a separation or classification device. The exact nature of the flow of a fluid through a hydrocyclone has not been obtained theoretically because of the complexity of the boundary conditions on the flow region. A description of the fluid flow is essential to the prediction of its operating characteristics. This work extends the knowledge of the nature of the flow in a hydrocyclone by means of an order of magnitude analysis of the equations of motion for an incompressible fluid in conjunction with application of some experimental observations. This analysis resulted in the division of the hydrocyclone into five regions of flow for separate consideration. In terms of the nomenclature in general use in the literature, these were the entrance-buffer region, the outer-core region, the inner-core region, the apex region, and the short-circuit flow region.

Fluid velocity components were predicted from the analysis for the inner and outer core regions. The predicted free vortex outer core circumscribing the forced vortex inner core agrees reasonably well with experimental observations. The fluid velocity component distribution is discussed in detail in Chapter II.

Particle trajectories in viscous fluids have been of interest for many years. Discussions in the literature have previously been limited to two-dimensional cases. Approximate equations of motion for spherical particles in a three-dimensional sheared viscous fluid flow field were

developed in this work in order to predict the trajectory of a spherical particle admitted into the hydrocyclone flow field previously discussed. In that the flow in the hydrocyclone is shear flow, spherical particles would experience rotation. When this is coupled with the relative motion of the particle with the fluid, a transverse force results in addition to the usual drag force. Because of the complexity of the flow, simplifying assumptions become necessary in order to obtain first approximations to the forces experienced by the particles. Details of these assumptions and the resulting equations are presented in Chapter III.

Analytical predictions of the separation characteristics were made from the particle trajectories obtained from numerical solutions of the equations of motion of spherical particles in hydrocyclone flow. A postulated set of fluid velocity components was employed for the numerical examples in that the air or vapor core was not accounted for in the theoretically predicted fluid velocities.

A transparent hydrocyclone three inches in diameter was fabricated to allow observation of the particle trajectories. Slit illumination normal to the observer gave good definition to a cross sectional view of the particle trajectories. The repeated entry of the particle into the illuminated slit gave several images on a time exposure photograph.

Separation efficiency was determined experimentally and predicted analytically for various specific gravity differences in the particles and slurry. The predictions were consistently high in the region studied. Unfortunately, the equations would not yield to generalization by non-dimensionalization, thereby necessitating trajectory calculations for each condition of operation for each hydrocyclone configuration.

The results of this work are of a dual character. The nature of the flow within the hydrocyclone has been explained by theoretical analysis, and approximate equations of motion for a sphere in a three-dimensional sheared flow field have been established. Visual observation of the particle trajectories furnished information about the apex region and inner core which led to the suggestion of a configuration modification which potentially would eliminate a source of inefficiency.

NOMENCLATURE

Symbol	Description	Units
a	Radius of Spherical Particle	ft
b	Cone Half Angle	radians
C	Drag Coefficient	--
C_n	Constants	appropriate
D	Diameter of Spherical Particle	ft
e	Separation Efficiency	per cent
F	Force	lbf
$G(\ )$	Arbitrary Functions	appropriate
g	Gravitational Acceleration	ft/sec^2
i	Unit Vector in r Direction	--
j	Unit Vector in θ Direction	--
k	Unit Vector in z Direction	--
M	Mass of Displaced Fluid	lbm
M_s	Mass of Spherical Particles	lbm
P	Pressure	lbf/ft^2
Q_i	Inlet Flow Rate	ft^3/sec
Q_u	Underflow Flow Rate	ft^3/sec
Q_n	Downward Inlet Flow Rate Outside the Neutral Trajectory	ft^3/sec
r	Coordinate Direction from Axis of Symmetry	ft
r_c	Radius of Air or Vapor Core	ft
r_i	Outer Radius of Inner Core	ft

R	Particle Reynolds Number (VD/ν)	--
R_c	Hydrocyclone Cylinder Radius	ft
R_m	Machine Parameter for r	appropriate
S	Particle Specific Gravity with Respect to the Slurry	--
t	Time	sec
u	Fluid Velocity Component in r Direction	ft/sec
U	Particle Velocity Component in r Direction	ft/sec
(vol)	Volume of the Spherical Particle	ft^3
v	Fluid Velocity Component in θ Direction	ft/sec
v_c	Fluid Velocity at Cylinder Wall	ft/sec
v_i	Inlet Fluid Velocity	ft/sec
V	Particle Velocity Component in θ Direction	ft/sec
$\bar{V}$	Relative Velocity of Particle with Respect to the Fluid $\bar{V} = i(u-U) + j(v-V) + k(w-W)$	ft/sec
$\bar{\bar{V}}$	Total Fluid Velocity $\bar{\bar{V}} = iu + jv + kw$	ft/sec
w	Fluid Velocity Component in z Direction	ft/sec
W	Particle Velocity Component in z Direction	ft/sec
x	Dummy Variable	sec
z	Coordinate Direction Along Axis of Symmetry	ft
z_2	Cone Height	ft
α	Velocity Loss Ratio—v_c/v_i	--
β	Constant of Proportionality in Newton's Second Law of Motion	lbm ft/lbf sec^2
δ	Order of Magnitude ($\delta \ll 1$)	--
ρ	Slurry Density	lbm/ft^3

ρ_s	Particle Density	lbm/ft^3
θ	Coordinate Direction Orthogonal to r and z Directions	radians
ν	Fluid Viscosity	ft^2/sec
ν_t	Apparent Turbulent Viscosity	ft^2/sec

Subscript notation of partial differentiation will be used. For example

$$u_z = \frac{\partial u}{\partial z} \quad .$$

CHAPTER I

INTRODUCTION

Background

The conventional hydrocyclone has been successfully employed for many years as a separation or classification device. A cross section sketch of a conventional hydrocyclone is presented in Figure 1.* The fluid slurry to be treated is admitted into the hydrocyclone through a tangential entrance which is usually of circular cross section. The entrance is located as near to the roof of the hydrocyclone as practical design limitations permit. The majority of the slurry moves down the outer area of the cylindrical section and into the outer portion of the inverted cone. In this region, the slurry begins to feed across toward the center of the cone and up the overflow tube. The overflow tube is concentric with the hydrocyclone geometric axis and extends the length of the cylindrical section of the hydrocyclone body. A small fraction of the slurry is removed from the apex end of the cone and is referred to as the underflow.

A secondary flow moves across the roof of the hydrocyclone to the base of the overflow tube, downward along the outer wall of the tube, and into the mouth of the tube. The general character of the flow in the hydrocyclone is presented in Figure 2.

Centrifugal effects generated by the rotating fluid coupled with the fluid motion in the hydrocyclone serve to separate large-heavy particles

---

*All figures appear in Appendix A, pp. 81-113.

from the slurry or to classify particles according to shape-density relationships. The large-heavy particles report to the underflow and the fine-light particles report to the overflow.

Separation efficiency is generally the primary operating characteristic of interest in the application of the hydrocyclone. The fluid flow characteristics are necessary for the prediction of particle trajectories and subsequently the separation efficiency. The exact nature of the flow in a hydrocyclone has not been obtained from theoretical considerations due to the inherent complexities of the flow system. The entrance system is related to a turbulent jet issuing into a stagnant fluid with the additional complexities of wall effects and swirling of the fluid in the vicinity of the entrance jet. The secondary flow over the roof is related to the rotary motion of semi-infinite fluid with a stationary boundary; however, entrance turbulence seriously affects the behavior of this flow. The apex region is subject to strong viscous effects and the exact nature of the main stream motion approaching this region is not presently known.

Experimental evaluation of the flow in a hydrocyclone is similarly a difficult task. Broer (1)* suggests that systematic observations of cyclone flow, separation characteristics, and pressure losses be made with attempts to interpret these data for the determination of the design criteria for various applications. These suggestions are well taken if primary consideration is being given to the evaluation of the overall behavior of the hydrocyclone as opposed to focusing attention on the basic mechanisms involved in its operation. Because of the three-dimensional

---

*Numbers in parentheses refer to the "Literature Cited" section of the Bibliography, p. 129.

character of the flow, instrumentation to measure the velocity and pressure distributions must be appropriate for the task. Various techniques have been developed for measurements in three-dimensional fluid flow situations. Winternitz (2) reviewed the use of probes to determine flow conditions in three-dimensional fields. A single probe with five pressure leads allows the determination of the total velocity, direction of the total velocity, static pressure, and consequently the velocity components. The use of a spherical pitot probe in a dust collecting air cyclone was employed by Ter Linden (3) in a rather comprehensive investigation of the flow. Difficulties inherent in the probing method include the possibility of large perturbations due to the deceleration of the rotation as a result of the presence of the sensing element in the flow. This would be of particular significance in probing the inner core of the vortex in that the probe would be residing in the stem wake. Large radial pressure gradients of the total and static pressures demand extensive calibration procedures to eliminate errors introduced by the pressure gradients. This is necessary due to the finite distances between the sensing ports on probes. If these effects were not accounted for, significant errors in direction and magnitude could result.

A somewhat cruder method was used by Shepherd and Lapple (4) to obtain results for the flow in an air cyclone. They found the flow direction by streamers and the speed with a pitot tube. The same inherent difficulties accompany this method as with the measurements discussed in the preceding paragraph.

A specific cylindrical cyclone separator design was used by Smith (5) to investigate the flow of air through a vortex. He used a stretch

probe which consisted of a 0.032 inch O. D. tube stretched across the diameter of the cylinder. The cobra head was mounted in the center with pressure leads at either end. The probe could be traversed and rotated in order to obtain the magnitude and direction of the velocity components provided the radial components were neglected. The tension on the probe allowed a much smaller stem to be used without the flutter generally accompanying a thin cantilevered probe.

The methods of velocity measurement in three dimensions presented above suffer the additional detrimental effects of higher drag in a hydrocyclone and are consequently not suitable for highly accurate experimental investigation of the flow in a hydrocyclone.

A comprehensive qualitative study of the flow in a hydrocyclone was presented by Bradley (6). Dye injection at various points was used to determine the general character of the flow and to study the effects of various overflow nozzle configurations. The concept of the "mantle" in the hydrocyclone was presented in this work. This suggests that the general flow pattern in the radial and vertical directions is as shown in Figure 2. The "mantle" is a region of zero radial velocity and appears to be a circulation cell buffering the downward moving outer vortex and the upward moving inner vortex. Its location may have a significant effect on the magnitude of the radial velocity components.

An optical method for the study of the motion of solid particles in a small hydrocyclone was used by Kelsall (7) for the determination of the approximate nature of the flow in the hydrocyclone. An agreement of less than 5 per cent deviation of the vertical and horizontal velocity components of the tracer particles from those of the fluid components at a given

point was claimed in this work. The results of trajectory calculations made during the present investigation indicate that this is a resonable estimate for the accuracy of the method. Support for this conclusion will be asserted later in the discussion of trajectory calculations.

Separation characteristics of hydrocyclones were studied by Moder and Dahlstrom (8). They executed an extensive experimental program to determine the feasibility of fine-size, close-specific gravity solid separation with the hydrocyclone. Both sink and float particles were used. Variations in the slurry split to underflow, specific gravity difference in the particles and liquid, and particle size were considered. A three-inch diameter hydrocyclone was used for the evaluation studies. Their results indicate that the slurry split to underflow is an important variable in the separation characteristics of a hydrocyclone.

A theoretical prediction of the 50 per cent separation sized particle was presented by Bradley (9) for a conventional hydrocyclone. The 50 per cent separation sized particle implies that 50 per cent of the particles in the inlet slurry report to the underflow and 50 per cent to the overflow.

The concept of the equilibrium surface for particles in hydrocyclone flow is the criterion most generally applied to prediction of the separation characteristics of a hydrocyclone. The equilibrium surface is defined as the surface at which the particles in the hydrocyclone would have no radial velocity or acceleration; i.e., the drag and centrifugal forces are in balance. Tarjan (10) introduces the consideration of resistances to particle motion in a fluid extending beyond the range of application of Stoke's prediction. This results in a more realistic prediction of the

equilibrium surfaces. The equilibrium surface concept of efficiency prediction depends on the further assumption that the particles will have sufficient time to reach their equilibrium position in the hydrocyclone before being carried out by the overflow stream and that they will report to the underflow unless the equilibrium surface is smaller than the overflow diameter.

Lapple and Shepherd (11) developed equations of motion for particles in a viscous fluid for various special cases considering drag as determined for steady state, inertial and buoyant effects. One of these cases was two-dimensional motion in a centrifugal field which would correspond to hydrocyclone flow neglecting the vertical velocity components.

The motion of spherical particles injected at the center of a cylinder of gas in solid body rotation was considered by Kriebel (12). The time for centrifugation to the outer wall as well as the deposition angle on the outer wall were found to be largely dependent on the particle diameter. Performance limitations for an idealized hydrocyclone and a centrifugal particle size analyzer were predicted by the results of the analysis. The predicted results were essentially verified by using an air centrifuge that closely approximated the analytical model. Limitations of these results include the assumption of Stokes law for the drag force evaluation.

Particle trajectory predictions for a horizontal rotating drum aerosol chamber were presented by Calder (13). This was almost the same problem as considered by Kriebel (12) with the exception of the additional consideration of the gravity force. The method of analysis differed; however, in that vector analysis was employed by Calder while Kriebel adhered to more elementary mathematical concepts. The vector analysis

approach allowed separation of the gravity and centrifugal effects by a suitable transformation to yield a solution for particles remaining in the Stokes law regime.

A transverse force is produced if a particle is spinning in addition to having relative motion to the surrounding fluid. A summary of works in this area was presented by Swanson (14). A theoretical prediction of the transverse force on a spinning sphere based on an extension of Oseen's approximation was presented by Rubinow and Keller (15). This force has not previously been considered in the prediction of particle trajectories in hydrocyclone flow.

The drag force on a spherical particle experiencing an arbitrary acceleration in laminar flow was presented by Rayleigh (16), in a study of the drag force prediction for various configurations. The "added mass" term is included in this development as a portion of the acceleration contribution to the total drag force.

Purpose and Objective

Application of hydrocyclones to various separation or classification processes is generally done on an empirical basis. A theoretical approach to the prediction of separation efficiency would be desirable. In arriving at a method of efficiency prodiction, it is necessary to determine the flow in the hydrocyclone and the trajectories of particles introduced into the flow.

The objective of this work was to extend the knowledge of the nature of fluid flow in a hydrocyclone, to develop the equations of motion for particles in a three-dimensional flow field, to solve these equations for particle trajectories in a hydrocyclone for particular cases, and then to

apply the results to the prediction of separation efficiency for a given hydrocyclone with certain operating conditions. The experimental phase of the work was directed primarily toward verification of individual trajectory prediction by visual observation and photographic technique. Separation efficiency predictions were compared to experimental results for the same operating conditions.

CHAPTER II

ANALYSIS OF THE FLUID FLOW IN A HYDROCYCLONE

The Analytical Model

The flow of a viscous incompressible fluid through the boundary configuration described by the conventional hydrocyclone is quite complex and exact treatment is not feasible using techniques of analysis presently available. However, the general nature of the flow may be obtained from the construction of an analytical model based on intuitive reasoning and experimental evidence presented by various investigators. This analysis yields only a first approximation to the flow in that rather broad simplifying assumptions are made in arriving at the analytical model. The approximate results allow better understanding of the nature of the flow in the hydrocyclone and comparison of the approximate theoretical predictions with experimental observations indicate regions of refinement necessary in the analytical model for prediction of the actual flow.

The general nature of the flow through a conventional hydrocyclone suggests the assumption of rotational symmetry about the geometric axis of the body cone. The presence of the single tangential inlet at the upper part of the flow field introduces asymmetric conditions to the flow. Under the influence of turbulent entry conditions, large momentum interchanges in the vicinity of the entrance effects the uniformity of average flow conditions at distances sufficiently removed from the entrance. Consequently, the flow in the body cone approaches rotational symmetry about its geometric axis. Thus the assumption of axisymmetric flow is made with

some reservation but will be employed as a condition for the analytical model in order to simplify the analysis.

Variation of flow conditions are not generally made during short periods of time in the application of the hydrocyclone to the continuous separation or classification of particles in a slurry. Steady flow conditions will thus be assumed for the analytical model.

The conventional polar coordinate system (r, θ, z) was chosen for the analysis. The coordinate system orientation and the velocity vector assignments are presented in Figure 3.

The assumptions made for developing the analytical model indicate that consideration of steady, axisymmetric, incompressible flow with three-dimensional velocity aspects should lead to an approximate description of the flow.

Further refinements in the analysis of the flow may be made by division of the hydrocyclone into five regions of flow. These regions are shown in Figure 4 and were chosen in this fashion on the basis of experimental evidence along with intuitive reasoning. Each of the regions will be discussed in detail and approximate analyses will be made of the flow in the inner and outer core regions. The entrance region, apex region, and the buffer region will be discussed only qualitatively on the basis of existing analyses of related problems.

The Outer Core Region

The outer core region is considered to be the controlling influence in the overall flow characteristics of the hydrocyclone. The existence of the "mantle" as shown by Bradley (17) suggests that the outer core flow becomes fully established some distance below the bottom of the vortex

finder. Also since radial velocities are not present in the "mantle", it is necessary to consider a buffer region between the entrance section and the outer core region. The buffer region can be described better after the nature of the flow in the outer core has been established.

A first approximation to the flow in the outer core may be obtained by neglecting the wall boundary layer effects and assuming that the flow in the outer core is frictionless. Support of this assumption will be given later.

The equations of motion for a frictionless fluid in steady axisymmetric flow may be expressed in polar coordinates as

$$u\,u_r - v^2/r + w\,u_z = -\beta\,P_r/\rho \quad (1)$$

$$u\,v_r + u\,v/r + w\,v_z = 0 \quad (2)$$

$$u\,w_r + w\,w_z = \beta\,P_z/\rho - g \quad (3)$$

and the equation of continuity as

$$u_r + u/r + w_z = 0 \quad (4)$$

The boundary conditions to be satisfied are that at $r = 0$, $u = 0$ and at $r = z \tan b$, $u/w = \tan b$. The latter condition implies that the velocity vector component in the r-z plane is parallel to the wall and in a downward direction if the radial velocity is negative.

Additional conditions will be imposed later to evaluate some of the constants obtained in the solution for u, v, w, and P.

---

*Subscript notation of partial differentiation is used in this presentation.

A more general treatment can be realized by non-dimensionalization of the equations to be solved. This may be accomplished by setting

$$u' = u/v_i \tag{5}$$

$$v' = v/v_i$$

$$w' = w/v_i$$

$$P' = P\beta/\rho v_i^2$$

$$r' = r/z_2$$

$$z' = z/z_2$$

$$g' = g z_2/v_i^2$$

Substitutions of these non-dimensional variables into equations 1 through 4 reduces them to

$$u'u'_{r'} - v'^2/r' + w'u'_{z'} = - P'_{r'} \tag{6}$$

$$u'v'_{r'} + u'v'/r' + w'v'_{z'} = 0 \tag{7}$$

$$u'w'_{r'} + w'w'_{z'} = - P'_{z'} - g' \tag{8}$$

and

$$u'_{r'} + u'/r' + w'_{z'} = 0 \tag{9}$$

Consideration of the order of magnitude of the various terms in the equations of motion and continuity will sometimes result in a much simplified analytical model. In that the fluid is admitted tangentially into the hydrocyclone, the rotational velocity component is anticipated to be

considerably larger than the radial or vertical velocity components. This observation is corroborated by the results of Kelsall (18). Order of magnitude of

$$\begin{aligned} u' &-- \delta \\ v' &-- 1 \\ w' &-- \delta \\ r' &-- \delta \\ z' &-- 1 \end{aligned} \tag{10}$$

where $\delta << 1$ are suggested on the basis of experimental evidence and the restriction that the cone angle be reasonably small.

Application of these orders of magnitude to the terms of equations 6 through 9 gives

$$\underset{\delta}{u\,u_r} \; \underset{1/\delta}{-\,v^2/r} + \underset{\delta^2}{w\,u_z} = -P_r^{*} \tag{11}$$

$$\underset{1}{u\,v_r} + \underset{1}{uv/r} + \underset{\delta^2}{w\,v_z} = 0 \tag{12}$$

$$\underset{\delta}{u\,w_r} + \underset{\delta^2}{w\,w_z} = -P_z - g \tag{13}$$

and

$$\underset{1}{u_r} + \underset{1}{u/r} + \underset{\delta}{w_z} = 0 \tag{14}$$

*From this point on, primes will be omitted from the non-dimensional equations for simplicity.

Omitting the negligible terms from each group of inertia, pressure, and body force terms in equations 11 through 13, the approximate equations of motion for the flow in the outer core become

$$v^2/r = P_r \tag{15}$$

$$v_r + v/r = 0 \tag{16}$$

$$u\, w_r = - P_z - g \tag{17}$$

and all terms of equation 14 are retained for reasons of importance of satisfaction of the continuity equation for incompressible flow to give

$$u_r + u/r + w_z = 0 \tag{18}$$

Equation 16 contains v and r only and may be rewritten as

$$(vr)_r = 0 \tag{19}$$

and integrated with respect to r to give

$$vr = G_1(z) \tag{20}$$

Because the term v_z was of order δ, the assumption that v is independent of z is suggested. This reduces equation 20 to

$$vr = C_1 \tag{21}$$

which is recognized as the well known potential vortex motion with the accompanying singularity at $r = 0$.

Combination of equations 21 and 15 indicate that

$$P_{rz} = 0 \tag{22}$$

This observation suggests partial differentiation of equation 17 with respect to r in order to eliminate the pressure and gravity terms. This operation reduces equation 17 to

$$u_r w_r + u w_{rr} = 0 \tag{23}$$

to be solved simultaneously with equation 18 for u and w.

If a trial solution of

$$u = - C_3 r/z \tag{24}$$

is substituted into equation 18, there results

$$w_z = 2 C_3/z \tag{25}$$

This may be integrated with respect to z to give

$$w = 2 C_3 \ln z + G_2(r) \tag{26}$$

Where $G_2(r)$ may be evaluated from the wall boundary condition that $u/w = \tan b$ at $r = z \tan b$. This operation results in

$$G_2(r) = - C_3 - 2 C_3 \ln (r/\tan b) \tag{27}$$

The first approximations to the velocity components then become

$$u = - C_3 r/z \tag{28}$$

$$v = C_1/r \tag{29}$$

$$w = C_3 \{2 \ln [(z \tan b)/r] - 1\} \tag{30}$$

for the outer core region.

The first approximation to the pressure distribution in the outer core may now be determined from equations 15, 17, and 28 through 30. Combining equations 15 and 29,

$$P_r = C_1^2/r^3 \tag{31}$$

which may be integrated with respect to r to give

$$P = - C_1^2/2r^2 + G_3(z) \tag{32}$$

From equations 17 and 32,

$$G_3'(z)^* = - u w_r - g \tag{33}$$

Substituting the velocity component solutions for u and w,

$$G_3'(z) = - g - 2 C_3^2/z \tag{34}$$

Integrating

$$G_3(z) = - gz - 2 C_3^2 \ln z + C_2 \tag{35}$$

and the approximate distribution in the outer core becomes

---

*Primes on G( ) terms indicate total differentiation.

$$P = - C_1^2/2r^2 - gz - 2 C_3^2 \ln z + C_2 \qquad (36)$$

where C_2 may be evaluated from a known pressure at the wall.

Returning to the omission of the wall boundary layer from the analysis of the outer core, there now exists some plausible argument as to the validity of this omission.

The nature of turbulent boundary layers in the presence of a highly favorable pressure gradient is such that a very small mass defect occurs in the boundary layer. Velocity profiles presented by Schlichting (19) for turbulent flow in a convergent channel indicate decreasingly small mass defects with increasing convergence angles which correspond to more highly favorable pressure gradients. The tangential velocity component in the case under consideration causes an extremely favorable pressure gradient for the downward flow adjacent to the wall. The omission of the wall boundary layer in the analysis of the flow of the outer core should not introduce large errors in that extremely small mass defects are present in the boundary layer proceeding down the wall. It is expected that this boundary layer will be important in the determination of the particle trajectories in the vicinity of the wall.

The Inner Core Region

From the solution of the outer core flow it is observed that with decreasing r, the orders of magnitude initially assumed are no longer applicable to the flow. This renders the outer core solution inappropriate to the description of the inner core flow. A consideration of the orders of magnitude suggested by the limiting case of the outer core solutions

and the geometry of the situation will allow development of approximate equations for the flow in the inner core. It is observed that the velocity gradients become large as r is decreased. This suggests that viscous effects might be significant in the inner region. In that the flow is suspected to be turbulent in character, the non-dimensional equations of motion may be written as

$$u u_r - v^2/r + w u_r = - P_r + \nu_t (u_{rr} + u_r/r - u/r^2 + u_{zz}) \quad (37)$$

$$u u_r + uv/r + w v_z = \nu_t (v_{rr} + v_r/r - v/r^2 + v_{zz}) \quad (38)$$

$$u w_r + w w_z = - P_z - g + \nu_t (w_{rr} + w_r/r + w_{zz}) \quad (39)$$

and the non-dimensional continuity equation as

$$u_r + u/r + w_z = 0 \quad (40)$$

where ν_t is some non-dimensionalized apparent viscosity due to turbulence effects and is assumed to be constant in this analysis.

Orders of magnitude of

$$\begin{aligned} u &-- \delta \\ v &-- 1 \\ w &-- 1 \\ r &-- \delta \\ z &-- 1 \end{aligned} \quad (41)$$

$$\nu_t \text{ -- } \delta^*$$

where $\delta \ll 1$ applied to equations 37 through 39 give

$$u\,u_r - v^2/r + w\,u_z = -P_r + \nu_t\,(u_{rr} + u_r/r - u/r^2 + u_{zz}) \qquad (42)$$

$$u\,v_r + uv/r + w\,v_z = \nu_t\,(v_{rr} + v_r/r - v/r^2 + v_{zz}) \qquad (43)$$

$$u\,w_r + w\,w_z = -P_z - g + \nu_t\,(w_{rr} + w_r/r + w_{zz}) \qquad (44)$$

Omission of the negligible terms of each of these equations reduces them to

---

*The order of magnitude of δ for ν_t resulted on consideration that the non-dimensionalized apparent viscosity

$$\nu_t' = \frac{\nu_t}{v_i z_2} = \left(\frac{\nu_t}{\nu}\right)\left(\frac{\nu}{v_i z_2}\right)$$

where orders of magnitude of

$$\left(\frac{\nu_t}{\nu}\right) \text{ -- } \frac{1}{\delta} \quad \text{and} \quad \left(\frac{\nu}{v_i z_2}\right) \text{ -- } \delta^2$$

are anticipated, thus an order of magnitude of

$$\nu_t' \text{ -- } \delta$$

is assigned for this analysis.

$$v^2/r = P_r \tag{45}$$

$$v_{rr} + v_r/r - v/r^2 = 0 \tag{46}$$

$$w_{rr} + w_r/r = 0 \tag{47}$$

respectively.

Equations 45 through 47 and the equation of continuity

$$u_r + u/r + w_z = 0 \tag{48}$$

describe the flow in the inner core. A solution to equation 46 is

$$v = r\, G_5(z) \tag{49}$$

However, because the order of magnitude of the v_z term was insignificant in relation to the other terms of the θ momentum equation, the solution is reduced to

$$v = C_4\, r \tag{50}$$

where

$$C_4 = C_1\, (2r_c)^{-2}$$

This result is in keeping with the notion of solid body rotation in the inner core as discussed by Kelsall (20).

A solution to equation 47 is

$$w = G_6(z)\, \ln r + G_7(z) \tag{51}$$

Partial differentiation of equation 51 with respect to z gives

$$w_z = G_6'(z) \ln r + G_7'(z)$$

In combination with the equation of continuity this gives

$$(ur)_r = G_6'(z)\, r \ln r + G_7'(z)\, r \tag{52}$$

Integration with respect to r yields

$$u = 0.5\, G_6'(z)\, (r \ln r - r/2) + G_7'(z)\, r + G_8(z)/r \tag{53}$$

However with the condition that at $r = 0$, $u = 0$;

$$G_6'(z) = G_8(z) = 0$$

Therefore

$$G_6(z) = C_6$$

and equation 53 is reduced to

$$u = 0.5\, G_7'(z)\, r \tag{54}$$

For compatibility of the inner core and outer core solutions, if

$$G_7'(z) = -2\, C_3/z$$

then

$$G_7(z) = -2\, C_3 \ln z + C_7$$

and the velocity components in the r and z directions become

$$u = -C_3 r/z \tag{55}$$

and

$$w = C_3 \{2 \ln [(z \tan b)/r] - 1\} \tag{56}$$

for the inner core also.

The viscous contribution in the r momentum equation is reduced to zero by the form of the velocity component for u . The physical implication here is that the shearing stresses are constant throughout the inner core region in that each of the viscous terms is approximately equal to zero. In a highly turbulent flow with large momentum interchange, this condition would likely prevail in the absence of solid wall effects.

The pressure distribution in the inner core may be determined approximately from equations 45, 50, and 55. Combination of these equations give

$$P_r = C_4^2 r \tag{57}$$

Integration with respect to r yields

$$P = 0.5 C_4^2 r^2 + G_9(z) \tag{58}$$

Assuming that the pressure distribution in the z direction in the inner core is that impressed by the outer core at the junction of the two regions, the pressure distribution in the inner core is given by

$$P = 0.5\, C_4^2 (r^2 - r_i^2) - 0.5\, C_3^2/r_i^2 - gz - 2\, C_1^2 \ln z + C_2 \quad (59)$$

where r_i is the radius of the outer limits of the inner core.

Experimental evidence presented by Kelsall (21) suggests using

$$r_i \simeq 2.0\, r_c \quad (60)$$

as the outer limits of the inner core.

The Apex Region

Increasing influence of wall effects, uncertainty of the exact nature of the approaching and departing flow, and the turbulent character of the flow in the apex region are reasons for omission of this region from direct analysis. Because the air core diameter has been observed to be larger than the discharge opening at the apex of the core while some flow through the apex opening has been observed, viscous effects in this region seem to be of major significance.

Although this region is of considerable importance in the determination of the stream division, for the purposes of this investigation, the flow in this region will be assumed to be an extension of the flow in the inner and outer cores. This assumption will likely introduce error in the particle trajectory predictions in this region and may seriously affect the accuracy of overall separation efficiency predictions for the hydrocyclone. These effects will be discussed more completely in Chapter VII.

The Entrance and Buffer Regions

The slurry is admitted into the cylindrical portion of the hydrocyclone by means of a single tangential entry which is of circular cross

section. The entrance region has two major flows to be examined. These will be done only on a qualitative basis because of the complexity of the boundary and entry conditions of the region. The first to be considered is the secondary flow on the roof of the hydrocyclone.

The problem of a fixed solid boundary adjacent to a semi-infinite fluid undergoing solid body rotation at distances removed from the boundary is presented by Schlichting (22) for laminar flow. The results of that problem may be related in a qualitative sense to the conditions existing on the roof of the hydrocyclone. The implication is that boundary layer motion on the roof results in a secondary flow spiraling inward to the base of the overflow tube, downward along its outer wall, and into the open end of the overflow tube. This boundary flow has been discussed by many previous investigators and is identified in the literature as short circuit flow. Particles in the short circuit stream which do not experience sufficient forces to be separated from the fluid are carried into the overflow. This is undesirable and seemingly could be altered by proper baffling to eliminate the short circuit flow. However, according to Kelsall (23), most schemes to effect this result have caused a reduction in the separation efficiency of the hydrocyclone.

The other flow to be examined is the main flow in the cylindrical section. This flow can be best described if it is discussed in conjunction with the buffer zone and the results of the analysis of the outer and inner core flows. The turbulent character of the entrance render analytical treatment of the region in the immediate vicinity of the entrance jet of doubtful value. The assumption of zero radial velocity in the entrance region is made. This assumption neglects the short circuit flow region

and is based on the observation of Bradley (24) that the "mantle" extends below the overflow tube. The zero radial velocity assumption also is not completely in accord with the observation that recirculatory flow about the "mantle" may constitute as much as 25 per cent of the throughflow as determined from the results of Kelsall (25).

In view of the contradictions in the foregoing, particle trajectories will be considered only from regions of zero radial velocity in the entrance section downward into the hydrocyclone.

The buffer region is considered to be a region in which the flow changes into the form of flow pattern required in the outer core. A smooth transitional radial velocity component relationship will be postulated for the buffer region. This will result in a vertical velocity distribution for the entrance and buffer regions. The exact nature of these velocities are presented in later sections of this chapter.

The expression for the tangential velocity component is assumed to be the same for these regions as for the inner and outer cores.

Comparison of Predicted and Experimentally Observed Velocities

The nature of the flow in a hydrocyclone has been presented through analytical considerations with admittedly broad assumptions and qualitative observations based on existing solutions to some related problems. A more complete understanding of the reasons for the behavior of the fluid flowing through the hydrocyclone is possible through these approximate predictions even though they do not exactly describe the flow.

Comparison of the predicted velocity profiles with those observed by Kelsall (26) are presented in Figure 5. The deviation of the predicted vertical component and consequently the radial velocity component from

those presented by Kelsall as experimental observations is attributed to the coring phenomenon and the omission of viscous effects in portions of the analysis. The reasonably good agreement in the outer portion of the outer core substantially corroborate the observation that the mass defect in the turbulent flow of a fluid in a highly favorable pressure gradient is increasingly negligible with increasingly favorable pressure gradients impressed upon the boundary layer flow. In this particular case, the centrifugal effects make the pressure gradient in the direction of flow inordinately large for the throughflow under consideration.

The formation of the air or vapor core was not considered in the analytical model. The radius of the vapor core could be predicted from the pressure distribution given by equation 59. The vapor pressure of the liquid should be used to determine a value of r for which the fluid pressure in the hydrocyclone is equal to the vapor pressure. The coring phenomenon is observed to be predicted by the pressure distribution equation for all conditions of operation provided the wall pressure remains finite. Departure from this prediction has been observed experimentally provided the overflow pressure is sufficiently high and the flow rate sufficiently low. In this instance, the assumptions made in obtaining the solutions no longer apply in that different orders of magnitude prevail for the velocity components.

In that there is some deviation of the predicted velocity components from the observed velocity components in an actual hydrocyclone, a better prediction of the trajectories of particles in a hydrocyclone may be made by postulation of velocity components which more closely approximate the observed flow.

Postulation of Fluid Velocity Components for Trajectory Calculations

After several trial velocity components which might represent the actual fluid flow in the main body of the hydrocyclone had been considered, the following fluid velocity components in the various regions were chosen as satisfactory approximations to represent the average flow conditions in the hydrocyclone.

For all five flow regions,

$$v = C_4 r = C_1 r/(2r_c)^{1.8} \tag{61}$$

for

$$r_c < r \leq 2r_c$$

and

$$v = C_1 r^{-0.8} \tag{62}$$

for

$$2r_c < r \leq z \tan b$$

For the outer and inner core regions,

$$u = -C_3 (1 - r_c/r) \tan b \tag{63}$$

$$w = C_3 [(z \tan b + r_c)/r - 2] \tag{64}$$

These components are presented in comparison with the experimental results of Kelsall (27) in Figure 6.

The postulated velocity components more nearly represented the experimental observations of Kelsall, especially in the vertical direction, and were used in particle trajectory calculations instead of the theoretical predictions obtained.

For the buffer region,

$$u = -C_3 \left(1 - r_c/r\right) \left[1 - \sin^2 \left(z - z_1\right) \pi/(z_2 - z_1)\right] \tan b \qquad (65)$$

$$w = C_3 \left\{(z \tan b + r_c')/r - 2 - (z_2 - z_1) \tan b/2r \right. \qquad (66)$$
$$\left. + \left[(z_2 - z_1)/2\pi\right] \sin \left[\pi \left(z - z_1\right)/(z_2 - z_1)\right]\right\}$$

For the entrance region,

$$u = 0 \qquad (67)$$

$$w = C_3 \left[(z_2 \tan b + r_c)/r) - 2 - \tan b \left(z_2 - z_1\right)/2r\right] \qquad (68)$$

The flow as postulated for all regions is presented in Figure 7. The vertical fluid velocity component in the buffer region is based on the postulated radial component variation. The equation of continuity was used to determine the vertical velocity variation. The radial and vertical velocities in the entrance region are extensions of the velocities in the buffer region evaluated at $z = z_2$. With this representation, the velocity components and velocity component gradients are equal both at the entrance-buffer and core-buffer region intersections, except for a discontinuity in u_z at $z = z_2$.

The buffer region was assumed to extend from z_2 downward to z_1. The latter was the level at which approximately 25 per cent of the downward moving fluid crossing the horizontal section at z_2 would have crossed over

into the upward moving portion of the outer core. This assumption was based on the concept of the recirculatory flow associated with the presence of the "mantle" in the hydrocyclone.

The constants in the velocity component relationships may be determined in the following manner. Because all of the inlet flow rate passes downward across the horizontal surface at z_1, the evaluation of C_3 may be accomplished from overall continuity considerations and is given by

$$C_3 = 2 Q_i/\pi (z_1 \tan b - r_c)^2 \tag{69}$$

The evaluation of C_1 depends on the design of the cleaner and the velocity loss of the inlet stream resulting from the wall viscous effects which retard the rotation of the bulk of the fluid. The velocity loss ratio is defined as

$$\alpha = v_c/v_i \tag{70}$$

where v_c is the tangential velocity component at the cylinder wall. From this definition and equation 62,

$$C_1 = \alpha v_i R_c^{0.8} \tag{71}$$

The velocity loss ratio was determined from the velocity component presentation of Kelsall (28) for this particular case to be 0.735. A compilation of the results of several investigations for the velocity loss ratio for different conditions of operation are presented by Bradley (29).

CHAPTER III

THE EQUATIONS OF MOTION OF A SPHERE IN THREE DIMENSIONAL MOTION IN A MOVING VISCOUS FLUID

Background

The hydrocyclone is generally applied to the classification or separation of particles that have dimensions several orders of magnitude smaller than the radius of the hydrocyclone. This condition suggests that wall effects will not be of great importance to particle motion except as the particle comes into close proximity to the wall.

In this analysis, the flow about the particle will be assumed to be approximated by the equations developed for a particle moving in an infinite stagnant fluid. A further assumption is that the level of the macroscopic turbulence in the hydrocyclone is sufficiently low to be negligible in the particle trajectory determination.

In situations involving particle motion in a moving fluid, the relative velocity of the particle with respect to the fluid is used in the determination of the force effects. A further assumption is that the forces predicted by unidirectional evaluations will be satisfactory approximations to instantaneous forces for varidirectional cases.

This approach has been employed by Lapple and Shepherd (30) in the evaluation of particle trajectories in two-dimensional studies.

Drag Force

Experimental efforts by numerous investigators have produced a fairly complete knowledge of the drag coefficient as a function of Reynolds number for spheres, discs, cylinders, and other bodies in steady flow. Average values of the drag coefficient of spheres in steady flow for various Reynolds number are presented by Lapple and Shepherd (31) based on the combined results of 17 investigators. These values will be used as the basis for an approximation to the portion of drag force prediction due to steady flow. It is anticipated that the range of Reynolds number of interest in the application of the hydrocyclone will be $0.01 < R < 10^5$. This range extends beyond the limit of Oseen's prediction and thereby necessitates an approximation to the drag coefficient as a function of Reynolds number for trajectory calculations.

A first approximation to the drag coefficient as a function of Reynolds number for steady flow may be expressed as piecewise continuous functions over three intervals. These are given by

$$C = 24.0/R \tag{72}$$

for

$$0.01 < R \leq 1.0 \ ,$$

$$C = 19.5/R^{4/7} \tag{73}$$

for

$$1.0 < R \leq 10^3$$

and

$$C = 0.44 \tag{74}$$

for

$$10^3 < R \leq 10^5$$

These approximations are shown in comparison to the values presented by Lapple and Shepherd (32) in Figure 8.

The relative motion of a particle with respect to the fluid in a hydrocyclone is not independent of time. The effects of accelerations on the drag force on spheres in unsteady laminar flow were considered by Stokes as reported in Lamb (33) in the case of a sphere undergoing harmonic motion in an infinite fluid. He was able to obtain the force on the sphere due to the presence of the surrounding fluid. This analysis led to the work of Basset and Boussinesq for arbitrary accelerations of a sphere which is reiterated in a study of the motions of solid bodies through viscous liquids by Lord Rayleigh (34).

The total drag force on a sphere is given by

$$F_d = - M \left\{ 4.5 \nu \bar{V}/a^2 + 0.5 V_t + (4.5/a)(\nu/\pi)^{0.5} \int_{-\infty}^{t} (t - x)^{-0.5} \bar{V}_x(x)\, dx \right\} \tag{75}$$

where x is a dummy variable of integration. The first term is the steady state portion of the drag. The second term is generally referred to as the "added mass" effect due to the inertia of the fluid.

The results of this analysis are limited to very small Reynolds number applications.

Lift Force

A rotating body moving through a fluid such that the axis of rotation is at an angle with the relative velocity vector of the particle with respect to the fluid will experience a transverse force component in a direction perpendicular to the plane containing the rotational axis and the relative velocity vector. The magnitude of this force is a function of the angular velocity of the particle, the relative velocity of the particle with respect to the fluid, and the shape of the body. This is generally referred to as Magnus effect for two-dimensional cases.

A summary of the investigations of the Magnus effect is presented by Swanson (35). A few of the earlier major contributions are presented here essentially as given by Swanson. The phenomenon of the drift of a sliced tennis ball was recorded by S. T. Walker as early as 1671. G. Magnus performed crude experiments to account for the drift of spinning missiles with unbalanced musket balls and an air jet. He was successful in predicting the direction of the drift. Lord Rayleigh was the first to establish the ideal flow representation of the two-dimensional case of the potential flow around a cylinder with circulation. Early quantitative data were obtained by Lafay around 1910. He reported the peculiarity of negative lift forces for low rotative speeds. This observation was later corroborated by the results of Swanson (36).

An extensive discussion of more recent investigations of the Magnus effect are presented in the work of Swanson with the exception of the work of Rubinow and Keller (37) which had not been published at the time. Their investigation relates to the transverse force on a spinning sphere moving in a viscous fluid. The flow about a spinning sphere moving in a viscous

fluid was determined for small Reynolds number. The transverse force and the torque on a sphere may be evaluated from the solution obtained.

For the case of the spinning sphere moving steadily through an unbounded incompressible viscous fluid, the lift component of force is given by Rubinow and Keller (38) as

$$F_L = \pi a^3 \rho \Omega \times \bar{V} [1 + O(R)] \tag{76}$$

where $O(R)$ is negligible for $R < 1.0$.

The results of Rubinow and Keller indicate that the rotation causes no corrections to the drag of order R. According to Einstein as given by Rubinow and Keller (39), a sphere in shear flow $\bar{\bar{V}}$ rotates with angular velocity

$$\Omega = 0.5 \nabla \times \bar{\bar{V}} \tag{77}$$

An attempt to solve the case of a spinning sphere in Poiseuille flow was made by Rubinow and Keller (40) in the same manner in which they were successful in obtaining the solution just discussed. The additional complexities of the problem expanded the required effort for obtaining a solution beyond reasonable bounds. This case was then considered by them in an approximate fashion and satisfactory order of magnitude results were obtained from application of equation 76 to a sphere in Poiseuille flow.

Buoyant Force

Buoyant forces are generally defined as the net force acting on a body submerged in a fluid due to the pressure gradient in the fluid in the vicinity of the body due to body forces on the fluid. Applying this

general definition to the case being considered, the components of the buoyant force are given approximately by

$$F_{b_r} = - \rho \, (\text{vol}) \, v^2/r \tag{78}$$

and

$$F_{b_z} = \rho \, (\text{vol}) \, g \tag{79}$$

There is no component acting in the θ direction because of axial symmetry. The contribution of the radial and vertical velocity gradients to the pressure distribution as determined in Chapter II are neglected here.

Application to Spherical Particles in Hydrocyclone Flow

The equations of motion of a particle may be developed from a consideration of the forces acting on the particle. The net force is related to the resulting motion of a particle through Newton's second law.

The relative motion of the particle with respect to the fluid in a hydrocyclone is of an unsteady nature and thereby necessitates consideration of the effects of acceleration on the drag forces involved. A first approximation to this effect may be obtained from consideration of the second term of equation 75 which is the resultant force predicted by classical hydrodynamics and generally known as the "added mass" effect.

The direction of the drag force is assumed to be in the direction of the relative velocity vector of the particle with respect to the fluid. The drag force component magnitude and sense for the various coordinate directions may be determined by multiplying the drag force by $(u-U)/\bar{V}$, $(v-V)/\bar{V}$, and $(w-W)/\bar{V}$ for the r, θ, and z directions respectively.

The lift force for this application may be approximated by equation 76 if the influence of large Reynolds number is neglected. The fluid velocity components were developed in Chapter II and may be employed to determine the angular velocity of the sphere as given by equation 77.

From the generalized curvilinear coordinate development of Rouse (42), the particle angular velocity may be obtained from the observation that

$$\nabla \times \bar{\bar{V}} = i[w_\theta - (rv)_z]/r + j[u_z - w_r] + k[(rv)_r - u_\theta]/r \qquad (80)$$

The assumption of axial symmetry and the velocity components of equations 62 through 64 reduces equation 80 to

$$\nabla \times \bar{\bar{V}} = j[C_3(z \tan b + r_c)/r^2] + k(0.2\, C_1/r^{1.8}) \qquad (81)$$

The relative velocity is given by

$$\bar{V} = i(u-U) + j(v-V) + k(w-W) \qquad (82)$$

Combination of equations 76, 81, and 82 with the omission of O(R) from equation 76 results in

$$\begin{aligned} F_L = {} & 0.5\, \pi\, \rho\, a^3 \{ i\, [C_3(z \tan b + r_c)(w-W)/r^2 \\ & - (0.2\, C_1/r^{1.8})(v-V)] + j\,[(0.2\, C_1/r^{1.8})(u-U)] \\ & - k\, [C_3(z \tan b + r_c)(u-U)/r^2]\} \end{aligned} \qquad (83)$$

An order of magnitude analysis of the lift force in relation to the drag force indicated that the lift forces should be included in the prediction of the particle trajectories.

Newton's second law of motion may now be applied in the three coordinate directions to give three equations of motion. In polar coordinates they are

$$M_s \left(r_{tt} - V^2/r\right) = \Sigma F_r \tag{84}$$

$$M_s \left(r\theta_{tt} + 2UV/r\right) = \Sigma F_\theta \tag{85}$$

$$M_s z_{tt} = \Sigma F_z \tag{86}$$

where

$$\Sigma F_r = F_{d_r} + F_{b_r} + F_{L_r} \tag{87}$$

$$\Sigma F_\theta = F_{d_\theta} + F_{L_\theta} \tag{88}$$

$$\Sigma F_z = F_{d_z} + F_{b_z} + F_{L_z} + F_{g_z} \tag{89}$$

remembering that the force components of drag may be obtained by the direction cosines and the total drag force.

CHAPTER IV

SOLUTION OF THE EQUATIONS OF MOTION FOR SPHERES IN HYDROCYCLONE FLOW

Statement of the Problem

The fluid velocity components for flow in a hydrocyclone were developed in Chapter II and the equations of motion for particles in three-dimensional flow were developed in Chapter III. Trajectories of individual spheres in a hydrocyclone will allow the prediction of separation characteristics for given operating conditions in a particular hydrocyclone. All attempts to non-dimensionalize the equations of motion of the sphere in order to present a generalized trajectory were unsuccessful. This means that trajectory calculations must be made for each condition of operation for each hydrocyclone in order to predict the separation characteristics. A hydrocyclone configuration was chosen identical to the one used by Kelsall (41) for determining velocity components except that a shorter accepts nozzle was used in this study. Good observation of the trajectories could not be obtained with the long accepts nozzle. This selection fixed the geometry of the flow field and limited the study to a given hydrocyclone.

The equations of motion of particles in three-dimensional motion were recognized as three independent, second order, non-linear, ordinary differential equations to be solved simultaneously with time as the only independent variable. The solution was based on the assumption of initial conditions for the particle trajectory. The initial conditions will be

discussed in detail for each of the solutions obtained as they are developed in this chapter.

Several assumptions were necessary in the application of the equations of motion of a particle in three-dimensional fluid motion to the present case in order to implement an approximate solution. The first of these was that the presence of the particle would not affect the fluid velocity distribution in the hydrocyclone. It was assumed further that the particle would be sufficiently small in relation to the radius of the hydrocyclone so that wall effects would not interfere with particle motion as predicted by the drag, "buoyant", and lift forces determined for particles in an infinite fluid.

Thus the problem was resolved to obtaining the solution of an initial value problem of three, second order, non-linear, ordinary differential equations with time as the only independent variable.

Numerical Solutions

The three equations discussed above were transformed into six first order equations by observing that the particle velocity components may be written as

$$U = r_t \tag{90}$$

$$V = r\theta_t \tag{91}$$

$$W = z_t \tag{92}$$

Several standard techniques of numerical analysis were considered and the modified method of Euler was chosen as the method to be used on the basis of implementation of the simultaneous solution of six first

order differential equations having a variable parameter to be evaluated from the marching solution as it proceeds. This method simply uses the average value of the slopes at the ends of an interval to predict the function change over the interval. The initial conditions allowed a marching solution to be made without regard to the ultimate value of the functions at the end of the trajectory.

As a first estimate of the trajectories only the steady state drag force, buoyant force and the added mass term of the acceleration contribution to drag were considered. The lift force term was included in later solutions. The equations to be solved for this case were obtained from equations 84 through 89 and are given as

$$U_t = (V^2 - v^2/S)/r + 3\,C\bar{V}\,(u-U)/4\,SD + \bar{V}_t\,(u-U)/2\,S\bar{V} \qquad (93)$$

$$V_t = 3\,C\bar{V}\,(v-V)/4\,SD - UV/r + V_t\,(v-V)/2\,S\bar{V} \qquad (94)$$

$$W_t = (g/S) - g + 3\,C\bar{V}\,(w-W)/4\,SD + \bar{V}_t\,(w-W)/2\,S\bar{V} \qquad (95)$$

and

$$r_t = U \qquad (96)$$

$$\theta_t = V/r \qquad (97)$$

$$Z_t = W \qquad (98)$$

with the initial conditions

$$U_o = u_o \qquad r_o = r_o$$

$$V_o = v_o \qquad \theta = 0.0$$

$$W_o = w_o \qquad Z_o = Z_o$$

where C was approximated by

$$C = 24/R \qquad \text{for} \qquad 0 < R < 1.0$$

and

$$C = 19.5/R^{(4/7)} \qquad \text{for} \qquad 1.0 \leq R < 1000.0$$

Multiplying each equation through by dt and applying the modified method of Euler resulted in a system of equations suitable for solution on a digital computer. A calculation flow diagram for the sequence of the major operations being performed by the computer in executing the solution of the differential system is presented as Figure 28. An "Algol" program was written to implement the solution of these equations for the particle trajectories and is presented in Appendix B as used on the Burroughs 220 Data Processing System of the Rich Electronic Computer Center at the Georgia Institute of Technology.

The solution to the differential system displayed unstable characteristics with relatively large time intervals. This difficulty was circumvented by decreasing the time interval to a satisfactorily small value. This value was obtained by taking a trial problem and reducing the time interval by a factor of two to determine the relative accuracy of the results for the calculations. The maximum allowable time interval varied with the conditions of operation imposed on the system and were determined for each of the conditions of operation by trial and error.

In an effort to simplify the calculations, the further approximation of assuming that the particles attained the fluid velocities in the θ and z directions respectively was made. The results of this simplified system

agreed fairly closely with those of the previous differential system. This observation is offered in support of the 5 per cent agreement of particle and fluid radial and vertical velocities mentioned in Chapter I. The results are shown in Figure 9. This comparison indicates that the simplified system would yield a suitable approximation for the inlet trajectories of particles with similar operating conditions provided that the lift effects are negligible. The results of Lapple and Shepherd (42) indicate that a transverse velocity component will affect the rate of traverse in a given direction and the reasonable agreement of the above should not be construed to be a general statement valid throughout the hydrocyclone.

Case I. Particle Reynolds Number Less Than One

For small particles remaining in the Stokes flow regime, the time required to calculate a trajectory was prohibitively long on the Burroughs 220 machine with the method used because of the extremely short time interval required for stable computations. Only a partial trajectory was calculated for this case and is presented in Figure 10. The same hydrocyclone operating conditions were used in obtaining analog computer solutions which will be discussed later.

Case II. Particle Reynolds Number Greater Than One

The components of the lift force were added to the equations of motion and trajectories were calculated for spherical particles in the hydrocyclone for several conditions of operation. As an approximation to the lift force in the entrance and buffer regions, the equations for the lift components in the inner and outer cores were used. The time required to reach essentially steady state was extremely small so that only the

"added mass" term in equation 75 of the acceleration effects was used in the calculations for the drag force.

The predicted trajectories for several conditions of operation were obtained for comparison with the results of the experimental program. The three conditions of operation considered for the numerical calculations were taken as given below.

Condition I. Conditions of operation of

$b = 10$ $\quad\quad$ $\nu = 0.91 \times 10^{-5}$

$r_c = 0.0083$ $\quad\quad$ $D = 0.0014$

$Q_i = 0.0208$ $\quad\quad$ $g = 32.2$

$S = 1.01$

with consistent units were used for calculation of the particle trajectories. Results of these calculations are presented in Figure 11a.

Condition II. Conditions of operation were the same as those of Condition I except that $S = 1.0067$. The results of these calculations are presented in Figure 11b.

Condition III. Conditions of operation of

$b = 10$ $\quad\quad$ $\nu = 0.91 \times 10^{-5}$

$r_c = 0.0083$ $\quad\quad$ $D = 0.0024$

$Q_i = 0.0253$ $\quad\quad$ $g = 32.2$

$S = 1.0, 0.99, 0.98$

were used. The three specific gravity values were used successively in order to arrive at analytical predictions of the separation efficiency

for comparison with experimental observations which were taken over a wider range of specific gravity. The results of the separation efficiency predictions of Conditions I and II indicated that very small specific gravity differences would effect complete particle removal for the conditions used. The specific gravity values selected for Condition III were based on the trend established by them and the shape of the separation curve as determined experimentally and presented as Figure 27. Trajectory predictions for these conditions are presented in Figure 12.

Analog Computer Solutions

Case I. Particle Reynolds Number Less Than One; No Lift

With very small particles, the effect of lift and the relative velocities in the θ and z directions become negligible. The Reynolds number for this condition was considered to be less than one, consequently Stoke's prediction of the drag coefficient holds. Relative acceleration of the particle becomes negligible shortly after the beginning of the particle trajectory and was neglected in this case. As previously stated, the numerical solution for this case proceeded very slowly, thereby consuming excess computational time.

Consideration of the particle trajectories for only the outer core region for the special case described above rendered the problem ideally suited to application of the electrical analog computer as a means of determining the particle trajectory prediction. The machine time for solution was easily adjusted to a reasonable period by combination of transforming the equations into a machine parameter representation and adjustment of the computing time by changing the capacitance across the integrating amplifiers of the circuit.

The equations to be solved under the assumptions enumerated above were obtained from equations 84 through 89 and were reduced to

$$r_{tt} = C_1^2(1 - 1/S)\, r^{-2.6} - 18\, C_3[(\tan b)(1 - r_c/r) - r_t]/S\, D^2 \quad (99)$$

$$z_t = C_3[(z \tan b + r_c)/r - 2] \quad (100)$$

and

$$\theta_t = C_1\, r^{-1.8} \quad (101)$$

The circuit diagram for the analog computer used in obtaining solutions of these equations for various conditions is presented as Figure 29 in Appendix C. Conditions were imposed to make a base solution and individual parameter changes about this base condition presented the effects of variation of the individual parameters with minimum changes required in the program. The conditions for the base trajectory determination were

$b = 10$ $\qquad$ $\tan b = 0.1763$

$V = 1.0689 \times 10^{-5}$ $\qquad$ $Q_i = 0.0288$

$r_c = 0.01$ $\qquad$ $R_c = 0.125$

$z_2 = 0.7094$ $\qquad$ $z_1 = 0.6607$

$r_0 = 0.063125$ $\qquad$ $\theta_0 = 0.0$

$z_0 = 0.6607$ $\qquad$ $D = 0.0007382$

$S = 1.02$

with consistent units being used throughout. The solutions are shown as r versus z presentations for the case given above for several different initial conditions on r in Figure 10.

The different conditions for the numerical solution and the analog solution account for the deviation of the two trajectories. The entrance and buffer regions were not considered in the analog solution.

The effects on given trajectories produced by variation of flow rate, specific gravity of the particle with respect to the slurry, and sphere diameter were considered and the solutions obtained for these cases are presented in Figures 13 through 15.

Case II. Particle Reynolds Number Greater Than One, No Lift

A second series of analog computer solutions were obtained for the special case of steady state drag effects, tangential particle velocity component equal to the tangential fluid velocity component, no lift forces, and given operating conditions. The circuit diagram presented as Figure 30 in Appendix C was used on the analog computer in obtaining solutions of the following equations which were obtained from equations 84 through 89.

$$r_{tt} = C^2 (1 - 1/S)\, r^{-2.6} + 0.75\, C\bar{V}\, (u - r_t)/SD \qquad (102)$$

$$\theta_{tt} = 0.75\, C\bar{V}\, (w - W_t)/SD \qquad (103)$$

where

$$u = - C_3 \tan b\, (1 - r/r_c) \qquad (104)$$

and

$$w = C_3\, [(z \tan b + r_c)/r - 2] \qquad (105)$$

Some rather interesting trajectories were obtained from this program for some of the special conditions imposed on the operational parameters. After secondary trajectories had been experimentally observed in the visual studies of the particle trajectories, initial conditions were imposed to start the solution with the particle residing in the inner core of the hydrocyclone at the fluid velocity. Particle trajectories for a special case and the conditions imposed are presented in Figure 16 as a plot of the r versus z position of the particle. The trajectory prediction proceeded reasonably fast except in the vicinity of the equilibrium position indicated in Figure 16. The experimental counterpart of this observation will be discussed in Chapter VII.

Case III. Particle Reynolds Number Greater Than One, Lift Included

The complexity of the full equations of motion including the lift force components greatly increased the special equipment requirements for the application of the analog computer. The non-linear equipment then available would have been insufficient for the program requirements. In view of these limitations and the fact that numerical solutions would be obtained for the general case, the full equations were not solved by analog computer technique.

Comparison of Numerical and Analog Methods of Solution

Digital computing machinery is capable of performing a tremendous number of operations very accurately in a short time. This allows the application of various well known numerical techniques to obtaining the solution of differential systems. For the cases considered in this work, the numerical approach was readily implemented through the convenience and relative ease of programming presented by the "Algol" language for use with

the compiler for the Burroughs 220 data processing system. The numerical scheme exhibited unstable computational characteristics for time intervals too large for certain conditions of the problem. Trial techniques allowed the determination of the maximum satisfactory time interval which could be used in the calculations. Successive increases of the time interval exhibited the onset of instability of the solution. Provided this limit was not exceeded, the solution proceeded smoothly. The limitation of a maximum time interval rendered the technique undesirable from a computational time requirement point of view for some cases.

The electrical analog computer presents an excellent vehicle for the solution of ordinary differential systems having one independent variable. Auxiliary equipment for non-linear considerations is available in electronic or electro-mechanical components. Programming of the analog computer was readily accomplished by using the patchboard technique. This system allows several programs to be in various stages of progress simultaneously without tying up the computer components for each program being considered. The analog solution is generally implemented by transforming the equations in real parameters into equations of machine parameters which will remain in a satisfactory range for the voltage representation of the machine parameters. On vacuum tube machines this is usually -100 to +100 volts. The machine time for solution of a problem can be readily adjusted either in the transformation of the equations or by changing the capacitance across all of the integrating amplifiers. This solution time adjustment does not seriously affect the accuracy provided it remains within the response time capability of the electro-mechanical components. The latter operation does not affect any of the other values used in the

circuit and is especially convenient when the maximum rate of solution is appreciably different for various initial conditions. In the application of the analog computer to the determination of the secondary trajectories, this feature was very beneficial in that high velocities were experienced relative to those of the entry trajectories and the result was an overload in the velocity integrators for the same speed of solution used above. This condition was alleviated by slowing down the solution speed.

The non-linear equipment may introduce some error into the solution but this depends on the particular application and a first approximation to the error may be obtained by checking the program for repeatability characteristics.

A limitation of the program employed here was that the entire flow field was not described. This deficiency could have been overcome by limiting controls and auxiliary programs for these regions similar to those employed in the numerical solution. Because the major portion of the trajectory was in the outer core, the analog solutions were obtained using only the relations for the fluid velocity components for this region.

Both the analog and digital computers have desirable and detrimental characteristics which should be considered in the selection of the method by which a solution to a differential system is to be obtained. The digital computers have accuracy characteristics limited only by the number of digits that the programmer chooses to employ in the calculations. Errors in the solution of differential systems are introduced inadvertently through the numerical methods employed in obtaining the solutions. Proper interval selection and judicious choice of method for a particular problem generally produces satisfactory results. The analog method of solution is

continuous and represents the differential equations within a small degree of error but additional errors are introduced because of the physical limitations of linear amplification, precision resistance and capacitance components, and output equipment accuracy. Analog computer components are currently available with a precision of 0.1 per cent. As with the digital computers, the analog solutions can give quite satisfactory results; however, they are somewhat more dependent on the careful implementation of solution by the operator.

The overall accuracy of the analog solution is dependent on the quantity of components in the circuit, the cancellation of error effects which may occur, the precision to which each component is either made or adjusted, and the accuracy of the output. Obviously, no exact figure can be quoted for overall accuracy. This can best be determined by test cases for which a solution is known.

CHAPTER V

SEPARATION EFFICIENCY PREDICTIONS

Method of Prediction

The separation efficiency of a hydrocyclone applied to the removal of particles from a slurry may be defined as the per cent removal of particles from the stream. Particle trajectory solutions are readily amenable to the prediction of the separation efficiency of a hydrocyclone for particular operating conditions. Predictions made here will be only approximate because of secondary effects omitted from the particle trajectory calculations. In the apex region, the particles may be drawn into the inner core and be carried out the overflow tube resulting in a source of inefficiency that has been excluded from the particle trajectory prediction. Under certain conditions of operation, particles may be drawn out the overflow by the short circuit flow which has also been neglected in the trajectory calculations.

The separation efficiencies may be obtained from the predicted trajectories in the following manner. A particle distribution across the beginning section is assumed to be proportional to the volumetric flow rate across the area being considered; i.e., the particles are assumed to be uniformly distributed in the slurry at this level in the hydrocyclone. The distribution of the particles passing this area may be ascertained as an explicit function of r from the foregoing assumption and the relation

$$Q = 2\pi \int w\, r\, dr \qquad (106)$$

A neutral trajectory may be defined as the trajectory which terminates at the intersection of the air core with the core wall geometry. A particle trajectory starting at a radius larger than the initial radius of the neutral trajectory would intersect with the hydrocyclone wall and thereby be considered as particles reporting to the underflow. Trajectories starting at radii smaller than the initial radius of the neutral trajectory are assumed to represent particles that would report to the overflow.

The percentage of particles reporting to the underflow may then be determined by a consideration of the percentage of the particles introduced into the hydrocyclone through the area outside of the initial radius of the neutral trajectory.

The flow rate outside the neutral trajectory is given by

$$Q_n = 2\pi \int_{r_n}^{R_c} w\, r\, dr$$

The separation efficiency is then given by

$$e = (Q_n/Q_i)\ 100 \qquad (107)$$

The initial radius of the neutral trajectory may be determined approximately by calculation of several inlet trajectories for various initial radii and interpolation of the resultant trajectories for the initial radius of the neutral trajectory.

Application to Special Cases

Case I. Particle Reynolds Number Less Than One

The results obtained from the analog computer program for the special case of very small particle Reynolds number is readily amenable to the method of separation efficiency prediction outlined above. The approximations involved in obtaining these particle trajectories were discussed in the Analog Computer Solutions section of Chapter IV. The initial value of r for the neutral trajectory is 0.099 as observed in Figure 11.

In that centrifugation effects are relatively small in this case, it is assumed that the particles would be uniformly distributed in the slurry at the beginning section of the particle trajectory prediction, i.e., at $z = z_1$. Using the vertical fluid velocity component and equation 106, the flow rate across the horizontal section at $z = z_1$ is given by

$$Q = 2 C_3 [(z_1 \tan b + r_c) r - r^2] \qquad (108)$$

Using this flow rate distribution with the definition of separation efficiency given by equation 107 and the conditions of operation for this special case, the approximate predicted separation efficiency is 87 per cent.

Case II. Particle Reynolds Number Greater Than One

The results obtained from the digital computer solutions to the full equations of motion may be applied to the predictions of the approximate separation efficiency as defined by equation 107. The conditions of operation used in the trajectory calculations were discussed in the Numerical Solutions section of Chapter IV.

In this case it is assumed that the particles are uniformly distributed in the slurry at the initial value of z used in the trajectory calculations. Using the vertical fluid velocity component for this region and equation 106, the flow rate distribution across the horizontal section at $z = z_0$ is given by

$$Q = 2 C_3 [(z_2 \tan b + r_c) r - r^2] - \tan b [(z_2 - z_1) r/2] \quad (109)$$

Using this flow rate distribution with the definition of separation efficiency given by equation 107 and the conditions of operation for this special case, the predicted separation efficiency becomes 100 per cent for Condition I because all of the trajectories intersected with the cone wall geometry.

Employing the same procedure, the predicted separation for Condition II is similarly 100 per cent.

For the three specific gravities considered in Condition III, the predicted separation efficiencies are 0, 36, and 85 per cent. These values are shown in comparison with the experimental observations in Figure 27.

CHAPTER VI

EXPERIMENTAL PROGRAM

Description of the Apparatus

A transparent model was required to permit observation of individual particle trajectories by suitable illumination of the slurry moving through the hydrocyclone. After several possible means of construction were considered, plexiglass rod of appropriate diameter was carefully machined and polished to form the three inch hydrocyclone shown in cross section in Figure 17. The inherent refractory properties of a cylindrical exterior surface was detrimental to observation of the particle trajectories in the hydrocyclone. Because of the similarity of refractory properties of water and plexiglass, a square plexiglass box was constructed to surround the hydrocyclone and was filled with water. This eliminated refractory problems of any practical significance, automatically eliminating any cumbersome corrections in the interpretation of the observations of the particle trajectories.

An intense light source which could be used for long periods was required. A mercury vapor lamp afforded these characteristics and was housed in a suitably baffled and slitted chamber. A Ken-Rad, H 33-1-CD, 400 Watt, mercury vapor lamp was used. The ballast transformer required for the mercury arc vapor lamp was a Sola, 78-10-216, constant wattage transformer, single phase with a 110 volt primary supply requirement.

A schematic diagram of the flow system is presented in Figure 18. A hold tank of 30 gallons capacity was provided for the slurry. Gravity

drain of the hold tank was provided. Plastic piping with nylon fittings was used where feasible to prevent rust particles from clouding the flow in the model.

The slurry was drawn from bottom of the hold tank into the suction of a centrifugal pump rated at 40 GPM of water operating with a 110 foot head. The pump was driven by an integrally mounted one and one half horsepower 220 volt single phase motor. The discharge from the pump was divided in a tee into the inlet stream for the hydrocyclone and the recycle stream. The latter was utilized as a hydraulic agitator to maintain suspension of the particles in the hold tank. A gate valve was used to control the flow rate in the recycle line. The entry of the recycle line into the hold tank was fitted with a tee to divide the stream in order to prevent the formation of a vortex which would allow air entrainment in the suction flow to the pump. The inlet stream was throttled by a gate valve preceding the Schutte and Koerting, body 9655B, tube 9HCFB, Fig. 8-210, special float flowrater. The feed stream went directly from the flowrater discharge into the entry part of the hydrocyclone. The overflow tube was connected to a return line to the hold tank. A gate valve was used to control the back pressure on the overflow stream. The underflow tip was connected to a gravity drain line returning the underflow stream to the hold tank. The discharge end of the underflow line was open to the atmosphere, thus allowing air movement into the apex opening of the hydrocyclone.

Bourdon gages were used to measure the pressure of the feed (0-100 psi) and overflow (0-15 psi) streams. A mercury in glass thermometer (0-220° F) was used to measure the temperature of the water in the hold tank.

The spherical particles were DuPont, Pelaspan 8, polystyrene base, suspension polymerized particles. The expanding agent present in the particles did not activate until the particle reached approximately 200° F. The particles were sufficiently tough to withstand the rough treatment of passing through the pump rotor for several hours before fracture of the particles became evident. The specific gravity of the particles was found to be 1.039 ± 0.0005 by floatation and sinking observations in solutions of magnesium sulfate. The specific gravity of the magnesium sulfate solution was determined by a floatation gravitometer.

The particles were sized by screening and the size range giving the best trajectory trace was the -20 + 25 mesh U.S. sieve size range.

In order to obtain variations in the operating conditions, the specific gravity of the fluid was adjusted by addition of magnesium sulfate in the proper quantities. This scheme had been successfully employed by Moder and Dahlstrom (43).

A 4 x 5 Speed Graphic camera equipped with a Polaroid attachment was used to photograph the particle trajectories in the hydrocyclone. Polaroid Type 47 film with an ASA film speed rating of 3000 was used.

Experimental Procedure

The float for metering water with the flowrater was not readily available at the time the experiment was to be conducted. A float was fabricated in order to expedite the experimental phase of the work. Trial weights of the float were used to arrive at a reasonable deflection for the flow rate range anticipated. The flowrater was then calibrated by taking the average of two timed bucket samples for five different flow

rates. The calibration curve is presented in Figure 19. The float was satisfactory for the flow rates encountered in this application.

The hold tank was calibrated for water capacity by weighed bucket additions to the tank.

The specific gravities of aqueous magnesium sulfate solutions are presented for various concentrations in (44). It was observed that up to a specific gravity of 1.04 the relationship could be approximated as a linear increase in specific gravity with an increase in the percentage concentration of magnesium sulfate. Specific gravity values of the spheres with respect to the magnesium sulfate solution were selected for experimental investigation. The specific gravity of the spheres was 1.039 and the required specific gravity of the solution was easily determined.

The hold tank was filled with the desired amount of water and the required quantity of magnesium sulfate was added. The mixture was agitated by pumping it through the recycle line until a solution was formed. The solution was then allowed to remain quiescent for approximately two hours to allow the air bubbles entrained in the solution by the addition of the magnesium sulfate to escape from the surface in the hold tank.

The desired quantity of spheres were treated in a 100 ml beaker with a 5 per cent solution of Hyamine 2389 to render the surface hydrophilic. The supernatent liquid was decanted after the spheres had settled. The spheres were then washed to prevent formation of foam in the system from the addition of excess quantities of the surfactant when the spheres were added to the system.

Operating conditions were adjusted to the desired values by proper valve manipulation after the pump was started.

The operating conditions were recorded and particle trajectories were photographed. The operating conditions were numbered sequentially and a corresponding number for identification along with film exposure conditions were written on the back of the Polaroid prints as they were removed from the camera.

The first series of pictures were made with a one-eighth inch slit of light directed across the diameter of the hydrocyclone with the camera directed normal to the illuminated section. Consequently, the spheres were illuminated only as they crossed the slit of light and the result was a series of images indicating the intersection of the particle trajectory with the illuminated section. Particles were observed rotating in equilibrium circles as shown in Figure 26.

The second series of pictures were taken with the entire model illuminated in an effort to obtain the trace of the particle trajectory by a time exposure of the film. This method of illumination resulted in diminished contrast between the particles and the solution. One set of pictures in this series were made with the specific gravity of the slurry at 1.035. The results of this set were not satisfactory in that air entrainment became a serious problem with the increased salt concentration. The small air bubbles caused the slurry to be almost as reflective or refractive as the spheres, thus eliminating the necessary contrast for making suitable pictures. Another set of pictures were taken after the salt concentration had been decreased by dilution to a slurry specific gravity of 1.021. At this level of salt concentration, the air entrainment was not sufficient to appreciably increase the refraction of light by the slurry. The particle traces in this set were discernable for short lengths

of the trajectories. The trace length was shortened by the necessarily small time exposure for suitable contrast in the picture. An example of the results of this set of pictures is presented in Figure 20. The inadvertently large particle concentration caused these results to be only of qualitative value.

A third series of pictures were taken with the one-eighth inch slit of light across the diameter of the hydrocyclone for salt solution concentrations giving slurry specific gravities of 1.035 and 1.021. The difficulties encountered with the contrast of particles and slurry for good photographic results in the second series were also encountered with this lighting condition. For the slurry specific gravity of 1.035, no useful results were obtained. The set of pictures taken with the slurry specific gravity at 1.021 were reasonably satisfactory. An example of the results obtained in this set is presented in Figure 21.

A fourth series of pictures were taken with no salt in the solution in order to obtain good contrast between the particles and the slurry. An example of the results obtained in this series is presented in Figure 25. Considerable effort had been made to photograph the phenomenon of the particle entering the inner core in the vicinity of the apex region and being carried out through the overflow tube before it could escape from the inner core. A fortunate selection of the arbitrary time of tripping the shutter mechanism rather than some elaborate control scheme to capture the trajectory is responsible for the photograph presented in Figure 25. The uncertainties of initial starting time involved plus the short time duration of the trajectory in the inner core made this trajectory rather elusive from a photographic point of view.

Measurements were made for comparison of the separation efficiency with the analytical predictions. Conditions of operation were also established for experimental verification of some of the concepts of the mechanism of operation of the hydrocyclone as developed here. The data were collected in the following manner. The inlet stream flow rate was determined from the flowrater indication and the calibration curve presented as Figure 19. A timed sample of the underflow stream was collected, weighed on a 0.1 gram balance, and filtered. The filtered sample was then dried and weighed on a 0.0001 gram balance in order to ascertain the mass of the particles collected in the underflow sample. The overflow stream was passed through a No. 30, U.S. sieve size screen which caught the particles in the overflow stream during the same time interval as was used in obtaining the underflow sample; i.e., the samples were collected simultaneously. The time required to take the sample was of the order of 10 seconds. The particles from the overflow were then collected, dried, and weighed on a 0.0001 gram balance for the determination of the particle concentration in the overflow stream. Simple continuity relationships then allowed the determination of the inlet stream particle concentration.

Samples of the slurry were taken from the hold tank for subsequent determination of the specific gravity of the solution.

Having thus obtained the necessary data, the separation efficiency could be calculated from the average values of three samples taken for each run. It was necessary to add particles to the slurry hold tank intermittently because of the removal in the sampling process. No attempt was made to maintain the same inlet stream particle consistency throughout the investigation; however, the particle consistency did remain below one

per cent which is well below the maximum value allowable before the efficiency is affected by the increased particle consistency as suggested by Fontein, van Kooy, and Leninger (45). The results of the experimental investigation of separation efficiency are presented in Table I, below, and Figure 27.

Separation efficiency studies resulted in corroboration of the analytical predictions and visual observation of particles being carried out the overflow after having reached the vicinity of the underflow by the fluid moving up through the inner core. The low separation efficiencies noted for runs 2, 3, 6, and 28 are attributed to this phenomenon and proper adjustment of the operating pressures resulted in an improvement in the separating effectiveness at essentially the same flow rates. Increased overflow pressure decreased the diameter of the air or vapor core and consequently the diameter of the inner core, therefore fewer particles were carried out through the overflow by the means just described.

Accuracy of Measurements

Flowrater Calibration

Timed bucket samples were taken to calibrate the flowrater which was equipped with a special float for this experiment. Samples of the order of 23 pounds were taken over a time interval of as small as approximately 10 seconds. The weight was determined accurately within 0.04 lbm on a 0.1 lbm scale; the error being introduced by an estimated variation in the tare due to different amounts of residual slurry in the sample bucket. The time was recorded within 0.5 seconds from a stop watch with a 0.1 second scale; the error being introduced by reaction time in bucket removal. The reading on the flowrater scale was observed within 1.0 mm

TABLE I. EXPERIMENTAL RESULTS

RUN NUMBER	PRESSURES PSIG INLET	PRESSURES PSIG OVERFLOW	FLOW RATES LBM / SEC INLET	FLOW RATES LBM / SEC OVERFLOW	FLOW RATES LBM / SEC UNDERFLOW	RELATIVE SPECIFIC GRAVITY	TEMP DEG.F	PER CENT U-F SLURRY	SEP EFF PER CENT
1	5.0	0.5	0.71	0.701	0.009	1.039	78	1.27	99.9
2	29.0	1.5	1.65	1.637	0.013	1.039	81	0.79	2.1
3	13.1	1.0	1.06	1.049	0.011	1.039	81	1.04	14.6
4	7.5	0.6	0.75	0.742	0.008	1.039	81	1.07	97.1
6	11.0	0.8	0.99	0.979	0.011	1.010	81	1.11	1.9
7	18.0	9.0	0.93	0.892	0.038	1.010	81	4.09	90.9
8	32.0	15.0	1.30	1.267	0.033	1.010	80	2.54	94.3
10	32.0	15.0	1.30	1.272	0.028	1.039	80	2.15	99.0
11	32.0	15.0	1.30	1.271	0.029	1.007	81	2.23	52.5
20	29.0	8.0	1.62	1.455	0.165	1.016	82	10.18	97.3
21	29.0	8.0	1.62	1.450	0.170	1.008	82	10.49	89.4
22	29.0	8.0	1.62	1.455	0.165	1.003	82	10.18	43.4
23	29.0	8.0	1.62	1.460	0.160	0.996	82	9.88	16.2
24	29.0	8.0	1.62	1.461	0.159	0.989	81	9.81	7.6
25	29.0	8.0	1.80	1.621	0.179	1.003	82	9.94	55.9
26	29.0	8.0	1.80	1.620	0.180	0.996	82	10.00	21.8
27	29.0	8.0	1.77	1.600	0.170	1.010	82	9.60	94.8
28	25.0	1.2	1.77	1.662	0.108	1.010	82	6.10	64.7
29	34.0	12.0	1.85	1.604	0.246	1.010	82	13.30	94.0
30	43.0	15.0	2.07	1.776	0.294	1.010	82	14.20	97.1
31	27.0	6.0	1.65	1.540	0.110	1.000	84	6.67	17.4
32	32.0	9.0	1.65	1.480	0.170	1.000	84	10.30	23.9
33	38.0	12.0	1.65	1.422	0.228	1.000	84	13.85	23.5
34	41.0	15.0	1.65	1.326	0.324	1.000	84	19.64	27.8

from a scale of 1.0 mm divisions; the error being introduced by fluctuations in the flow conditions. Consequently, the calibration curve for the flowrater presented in Figure 19 is accurate within 5 per cent, with increasing accuracy for the higher readings. Applications in this experiment were in the region of one per cent error in the calibration curve.

Particle Specific Gravity Determination

The specific gravity of the particles was determined by suspension in a solution of magnesium sulfate. A floatation gravitometer with scale divisions of 0.002 was used. The temperature of the solution was 84° F. In that the specific gravity of the particles with respect to the slurry would be used in the calculations, the effect of temperature on the measurements would cancel. Particles were suspended in a 1000 ml cylinder and the concentration of the solution was adjusted so that the particles would sink at a specific gravity reading of 1.0395 and would float at a specific gravity reading of 1.0385; the readings being estimated from the scale divisions. The specific gravity of the particles was then taken as 1.039 for the calculations with an estimated error of 0.05 per cent.

Slurry Specific Gravity Determination

Samples of the slurry were taken from the hold tank during the runs. These samples were then sealed and marked for subsequent specific gravity measurements. The same floatation gravitometer as was used with the particle specific gravity evaluation was used to determine the specific gravity reading of the slurry at 84° F. The reading was taken within 0.0005 of the actual value suggesting accuracy of reading of the order of 0.05 per cent. Although the readings were taken very carefully and the error in each of the readings was very small, the difference in the specific

gravities is a parameter in the equations of motion and must be considered in the experimental investigation indicating a possible error of the order of 6 per cent in the specific gravity differences.

Slurry Split to Underflow

Timed samples of the underflow were taken for times of the order of 10 seconds having mass of the order of 1200 grams. The time was recorded within 0.5 seconds from a stop watch having 0.1 second divisions; the error being introduced by reaction time in taking the sample. The weight was determined within 1 gram on a 0.1 gram balance, the error being introduced by varying amounts of residual slurry in the sampling device. The underflow rate was thus determined within 5 per cent which would be coupled with the one per cent accuracy of the inlet flow rate measurements to give the per cent slurry to underflow measurements an estimated accuracy of the order of 5 per cent for the 10 per cent underflow conditions considered.

Per Cent of Particles Reporting to Underflow

The particles from the overflow stream were caught on a No. 30, U.S. sieve size screen and washed into a bottle for storage until they were filtered in a cloth for drying and subsequent weighing on a 0.0001 gram balance. Extreme caution was exercised in handling the particles to prevent losing some of the sample. The underflow sample was caught in a bottle and stored for the weighing operation just described. The sample weights were of the order of 2 grams and were balanced within 0.001 gram giving a weighing accuracy of approximately 0.05 per cent. Inadvertent washing out of the particles from the screen in the overflow sampling could conceivably have introduced an error of the order of 3 per cent in the weight of the overflow sample. In view of the foregoing and the

various percentages of particles leaving through the underflow is estimated to be accurately determined within 3 per cent with higher accuracy anticipated if the percentage of particles leaving through the underflow is greater than 70 per cent.

Qualitative Observations

Some quite interesting phenomena were noted from visual studies of the behavior of spherical particles in the transparent hydrocyclone. The most enlightening of these was the large percentage of spheres that were caught in the upward moving vortex and were then thrown back out before reaching the overflow entrance. The trajectories of particles experiencing this motion are referred to as secondary trajectories. This phenomenon caused an increased concentration of particles in the outer core region of the hydrocyclone and was detrimental to particle trajectory observation because of the large number of images presented.

With the slit light source as previously described, it was possible to follow the trajectories by visual observation. The majority of the particles did not stay in close proximity to the cone wall in the outer core even though they had been observed striking the wall previously.

Because of the short exposure time required by the film to obtain good contrast between the particles and the background and the relatively long times of the inlet trajectories, the photographic method did not yield useful results for the inlet trajectories. Consequently, a typical inlet trajectory as visually observed is presented as a sketch in Figure 22. The portion of the trajectory which is omitted was not observable due to the uncertainty of whether the particle would recirculate in the

manner described as the secondary trajectory or proceeding out the underflow opening.

The short circuit flow was readily evident in that particles were observed to progress in the manner depicted in the early part of the trajectory presented in Figure 23 as sketched from visual observation. The sudden change of course noted in this trajectory in the outer core caused the particle to execute loops before proceeding into the apex region.

Except for cases in which the air core was suppressed by sufficient overflow pressures, the general appearance of the particle distribution within the hydrocyclone was essentially independent of the flow rate.

As the overflow pressure was increased sufficiently to suppress the air core, the air core disappeared downward, indicating that a vertical fluid velocity of zero or slightly negative existed at the centerline of the hydrocyclone. This observation is in agreement with those reported by Fontein, van Kooy, and Leninger (46) in a recent study of the operational characteristics of hydrocyclones for various applications.

Any air bubbles of consequence were diverted directly to the outside wall of the overflow tube, down the wall and into the mouth of the tube with the leaving overflow slurry.

Particles were observed traveling the length of the hydrocyclone in the upward moving inner core. A discussion of the possible ways in which the particle could have gotten into the inner core will be given in Chapter VII.

CHAPTER VII

COMPARISON OF ANALYTICAL PREDICTIONS AND EXPERIMENTAL OBSERVATIONS

Particle Trajectories

Digital and analog computer solutions to the differential system of a sphere in hydrocyclone flow for special cases were obtained. Visual observation and photographic technique were employed in the experimental determination of the particle trajectories. Only relatively large particles gave satisfactory contrast for observing and photographing the trajectories. The analytical predictions of spherical particle trajectories to be compared with experimental observation were obtained by numerical solution of the full equations of motion after having obtained operating conditions from the experimental investigation.

The trajectories were identified according to the initial conditions imposed on the numerical solutions. Inlet trajectories were trajectories of particles which were admitted into the hydrocyclone through the entry port and proceeded downward through the buffer region and into the outer core. Secondary trajectories were trajectories of particles coming from the apex region. The trajectories of particles in the short circuit flow were not predicted in this work because of the omission of this region from consideration.

The inlet trajectories were observed visually in the inlet, buffer, and outer core regions. Attempts to obtain photographic evidence of the particle trajectories in these regions for the inlet trajectories were not

successful. The large incremental changes of position during the one turn rotational interval did not allow sufficient image repetition for good photographic analysis of a trajectory. Coupling this with the short exposure time giving satisfactory contrast to the photographs gave only two or three images for a particle in the inlet trajectory. The visual observations indicated that the inlet trajectory predictions were qualitatively in agreement with the actual trajectories except that the particles did not generally strike the wall. An unsuspected inlet trajectory characteristic was observed in the outer core in that the particles appeared to strike the wall in the vicinity of z_1 (see Figure 3) and then proceed downward approximately one fourth of an inch from the cone wall. This phenomenon is attributed to the reduced rotational velocity in this region because of viscous effects. These were neglected in the construction of the analytical model. Entry trajectory observations indicate that the particle proceeds downward at smaller radii than for the predictions made neglecting the lift effects. An occasional particle trajectory was observed adjacent to the wall but this was the exception rather than the rule.

Another unsuspected inlet trajectory characteristic noted intermittently was the behavior presented as a sketch in Figure 23. This phenomenon was observed visually but attempts to photograph the trajectory were unsuccessful. In explaining the reasons for this abrupt change of course experienced by the particle, the wall boundary layer instability regarding radial velocity fluctuations discussed at length by Smith (47) would explain the sudden inward turn that the particle trajectory experiences. The criterion for stability with respect to radial fluctuation is that

$(vr)_r > 0$. This condition is satisfied within the outer core but is violated in the wall boundary layer which has been neglected in this analysis. It is conceivable that the instability of the boundary layer could produce effects that would propagate into the outer core and cause the sudden change of direction in the particle trajectory observed in the experiment. In that these sudden variations of fluid radial velocity were neglected in this analysis, the predictions are not expected to agree with the trajectories of particles experiencing sudden large influxes of fluid. The results of the analog computer for secondary trajectories indicate that looping motion occurs when the system is analogous to an underdamped vibrational system. It must be remembered that the analog predictions are for equations neglecting the lift effects. The looping motion predicted by the analog solution is presented in Figure 16.

Secondary trajectory predictions were obtained numerically by setting initial conditions which would locate the particle in the vicinity of the inner core near the apex region. The initial relative velocity of the particle with respect to the slurry was assumed to be zero for these calculations. The results of these predictions indicate that the ultimate position of the particle trajectory is quite sensitive to the initial radial location of the particle as shown in Figure 24. Visual observations and photographs of the secondary trajectories were made by the technique discussed in the preceding chapter.

Because of the sensitivity of the initial condition of radial location, the lower part of the secondary trajectory predictions cannot be compared with experimental observation with a great deal of precision. The general nature of the secondary trajectories is correctly predicted as

evidenced by the agreement of the predicted trajectories and the trajectory segments taken from the photographs and presented in Figure 24. One unusual result was the trajectory of a particle which had been drawn into the inner core of the hydrocyclone. The secondary trajectory prediction indicated that a particle starting in the inner core would not escape from the inner core prior to reaching the overflow tube entrance. This prediction was verified by visual observation of particles spinning rapidly upward through the inner core at essentially a constant radius and escaping through the overflow tube. In later experimental investigation, attempts to photograph this phenomenon were successful. The photograph is reproduced as Figure 25. The initial portion of the trajectory is readily evident but the light scatter in the inner core obscures the particle image in the middle and upper portions of the hydrocyclone.

Particles were observed to come from the apex region in the vicinity of the inner core indicating that some of the secondary trajectories result from particles reaching the apex region and then being drawn upward by the inner core. Also the instability near the outer wall might account for some of the particles reaching the inner core earlier than if the flow were stable with respect to radial velocity fluctuations.

Particles were observed in equilibrium rotation circles at the position indicated in the time exposure presented as Figure 26. This is to be compared with the equilibrium position observed in the predicted trajectory solution of the analog computer as indicated on Figure 16.

Separation Efficiency

Separation efficiency was defined as the percentage of particles reporting to the underflow. Predictions were made from the particle

trajectory calculations in Chapter V. Experimental results were obtained as discussed in Chapter VI. Comparison of the analytical predictions and the experimental observations is presented in Figure 27. The data presented there as extrapolated from the results of Moder (47) for a 10 per cent slurry split to underflow are for a different hydrocyclone configuration and smaller particle size than used in this investigation. These results are included to corroborate the form of the effect of the specific gravity of the particle with respect to the slurry on the separation efficiency. Differences noted in the experimental observations are attributed to the smaller particle size used and the possibility that the air core was of larger diameter in that study than used in this work.

The deviation noted in the analytical predictions and the experimental observations of the separation efficiencies are attributed to the following:

1. The omission of the short circuit flow from the analytical model resulted in a higher predicted separation efficiency than if the short circuit flow could have been taken into account in that particles lighter than the slurry are readily carried out the overflow by the short circuit flow. As previously discussed, the short circuit flow involves approximately 10 per cent of the inlet flow rate and for the case under consideration, this would imply that an approximate correction could be applied to the predicted separation efficiencies of the order of minus 10 per cent if applicable.

2. The retardation of the tangential fluid velocity component in the wall boundary layer was neglected in the postulation of the fluid velocity components to be used in the trajectory calculations. There would

be two effects brought about by including this retardation that would result in a somewhat lowered separation efficiency. The particles would not have sufficient velocity to reach the wall through the inward moving fluid from a drag characteristic point of view and the lift forces on a spherical particle in this region would be inward, further reducing the probability of the particle reaching the wall. These observations have been essentially corroborated in that particles do not generally progress downward in contact with the wall, but move downward somewhat removed from the wall as visually observed in the experimental program. This limitation of the applicability of the analytical model would result in artificially high separation efficiency predictions. The order of the error introduced by this discrepancy is subject to several operational conditions and any attempt to fix the magnitude would be conjecture.

3. Instability of the fluid flow with respect to radial velocity fluctuations in the wall boundary layer could result in radical changes in the radial velocity and consequently particles could be carried into the inner core region by these fluctuations. The possibility of this occurrence has been discussed and observed particle trajectories similar to the sketch presented as Figure 23 indicate that this phenomenon could result in a reduced separation efficiency, the magnitude of which is not readily ascertainable.

4. In that the apex region was very important in the determination of the separation efficiency characteristics of the hydrocyclone, the exact nature of the velocity distribution in this region is very important in the overall prediction of the separation efficiency. Because of the complex nature of the flow in this region, the velocity distribution used

in the trajectory calculations did not agree with the actual velocity distribution. This discrepancy could conceivably have resulted in a higher separation efficiency prediction in that the particle movement out of the overflow through the inner core would be neglected. This can amount to a considerable portion of the particle rate as observed in the change of separation efficiency from 2 to 90 per cent by changing the size of the inner core for certain conditions of operation.

5. Particle concentration and wall proximity effects were neglected in the trajectory calculations. Both of these conditions result in an increased drag force which would reduce the separation efficiency as compared to the results of the predictions obtained for the simplified model considered here.

Additional refinement of the analytical model is necessary to obtain better predictions of the operating conditions in the hydrocyclone; however, the simplified approach presented may be applicable to determination of separation efficiencies relative to a known condition of operation for a particular hydrocyclone. This suggestion is made on the basis of the similarity of the shape of the analytical and experimental separation efficiency curves as a function of the specific gravity of the particle with respect to the slurry as shown in Figure 27.

CHAPTER VIII

DISCUSSION

Conclusions

Exact analytical treatment of the fluid flow in a hydrocyclone is not feasible at present due to the complex boundaries, entrance and discharge conditions, and the lack of a suitable relationship between the shearing stress and flow conditions for the turbulent regime. An approximate analysis of the fluid flow in a hydrocyclone was made by dividing the flow into five regions for separate consideration. The predicted velocity distribution agrees fairly well with experimental observations of flow patterns as presented in the literature. As a result of this analysis, it was concluded that the downward moving outer core is essentially independent of viscous boundary effects.

The equations of motion of particles in three-dimensional viscous fluid flow were developed and application was made to the prediction of individual particle trajectories in hydrocyclone flow for special cases. All attempts to non-dimensionalize the equations of motion so that a generalized trajectory of the particle could be made were unsuccessful. This means that calculations must be made for each different condition imposed on the particle during its trajectory, thereby eliminating the use of generality of solution in this method. The transverse force produced because of the spin of particles in addition to the relative velocity with respect to the fluid is an important factor in the determination of the ultimate position of the particles in hydrocyclone flow.

Separation efficiency predictions were made from the individual particle trajectory calculations for given operating conditions. Predictions made in this fashion are rather complicated and exclude some of the effects which are significant for some conditions of operation. For instance the short circuit flow was an appreciable factor in the separation characteristics of the hydrocyclone with the conditions of operations used in the comparison in this work. Another important operating variable not accounted for was the slurry split to underflow. This variable effects a different velocity distribution in the hydrocyclone and should be taken into account if significant amounts of the slurry is removed through the underflow discharge. Application of the method would proceed in the same manner after the fluid velocity distribution is determined for the relatively large slurry split to underflow conditions of operation. The effects of particle concentration and boundary proximity on the drag-lift effects were also neglected. Significant changes in particle concentration are experienced in the apex region of the hydrocyclone resulting in radical changes in the drag-lift effects.

Modifications in the method of separation efficiency prediction for a hydrocyclone presented here are necessary to account for the variation of conditions of operation discussed above in order to accurately predict the operating characteristics of a hydrocyclone in a practical application. The simplified approach presented here may be applicable to the determination of separation efficiencies relative to a known condition of operation for a particular hydrocyclone.

The results of the visual studies carried on during the course of this investigation accentuate the relative merit of qualitative observation

of complex flow phenomena by particle tracing techniques. The most enlightening of the visual observations of the particle trajectories in the hydrocyclone was the large percentage of particles caught in the upward moving inner vortex in the apex region and then thrown back into the downward moving vortex before reaching the overflow entrance.

An additional visual observation that particles entrained in the upwards moving inner core were not generally centrifugated back into the outer core before entering the overflow tube led to the criterion of small inner core diameter to increase the separation efficiency. This has been experimentally verified for certain conditions of operation.

The results of this investigation offer an improvement in the knowledge of the mechanisms involved in the operation of a hydrocyclone. The trajectory predictions revealed reasons for the experimentally observed separation efficiency deviations from the anticipated values in the very small specific gravity difference range. Lift force components on the spheres explain why the particles can stay in the large radial acceleration field in the vicinity of the inner core.

Visual observation of the particle trajectories indicated regions in which changes in the analysis are necessary for more accurate prediction of the particle trajectories. The wall boundary layer and the short circuit flow affect the particle trajectories and should be considered in future analyses.

Recommendations

The study of particle trajectories in hydrocyclone flow was made in an effort to gain additional knowledge of the mechanisms involved which

could be applied to the development of a method of separation efficiency prediction for various applications. The following recommendations are made as a result of this study.

1. The agreement of the predicted and observed trajectories for spherical particles in hydrocyclone flow indicated that the flow representation and the equations of motion presented here are in qualitative agreement with the actual phenomena encountered except in the wall boundary layer, short circuit and apex regions. Limitations of the method have been discussed in the preceding section of this chapter and should be considered in the application of this method to the prediction of separation efficiency.

2. Additional studies to determine the exact nature of the flow in a hydrocyclone should be pursued in order that more accurate fluid velocity representations may be employed in the determination of the operating characteristics of the hydrocyclone.

3. A possible configuration modification which would probably eliminate some of the inefficiency introduced near the apex of the hydrocyclone is presented as a sketch below. Theory suggests that the rotating surface would throw particles to the outside wall rather than cause them to be drawn in toward the center by the boundary layer that is developed on a stationary plate or in the apex of a cone. Physical implementation and proper control of the underflow rate will likely present difficulties for certain conditions of application but this design modification should be considered as a possible means of improving the effectiveness of the hydrocyclone where applicable and a developmental program should be implemented to overcome the aforementioned difficulties.

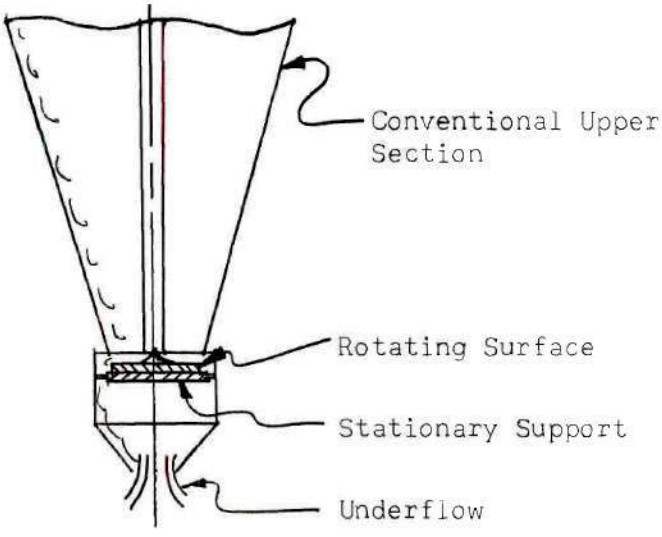

The fluid adjacent to the rotating surface would supply energy to maintain the rotary motion. This configuration modification should result in an increased separation efficiency by elimination of some of the inner core entrapment in the apex region and reduced wear by virtue of the increased diameter of the discharge and the accompanying reduced fluid velocities.

4. Further consideration should be given to elimination of the short circuit flow as a means to effect an improvement in the separation efficiency of the hydrocyclone.

5. The hydrocyclone should be operated with pressure conditions such that the air or vapor core will be as small as practical limitations permit in order to reduce the inefficiencies resulting from particles being carried out the overflow by the inner core.

6. Vacuum pressure application to the underflow should be considered for reducing the diameter of the inner core in order to improve the separation efficiency of the hydrocyclone. This would reduce the level

of the overflow pressure requirements and consequently the pumping costs in an installation.

7. Studies directed toward extension of the transverse force prediction to higher Reynolds number for spinning spheres which are in relative motion with a fluid should be executed in order to obtain a better relationship for the prediction of particle trajectories including this effect.

8. The equations of motion of particles in three-dimensional fluid flow should be considered in the application of particle tracer techniques to fluid flow analyses in order to ascertain the effects of the relative motion of the particle with respect to the fluid on the results of the study.

9. Flow visualization studies should be made for cases that are not readily amenable to conventional experimental probing analyses.

10. Development of particles which are self luminous for particle trajectory analyses to eliminate the contrast difficulties encountered in this work should be undertaken.

11. Consideration should be given to implementing the solution of systems of ordinary differential equations having one independent variable on suitable electrical analog computing equipment.

APPENDIX A

ILLUSTRATIONS

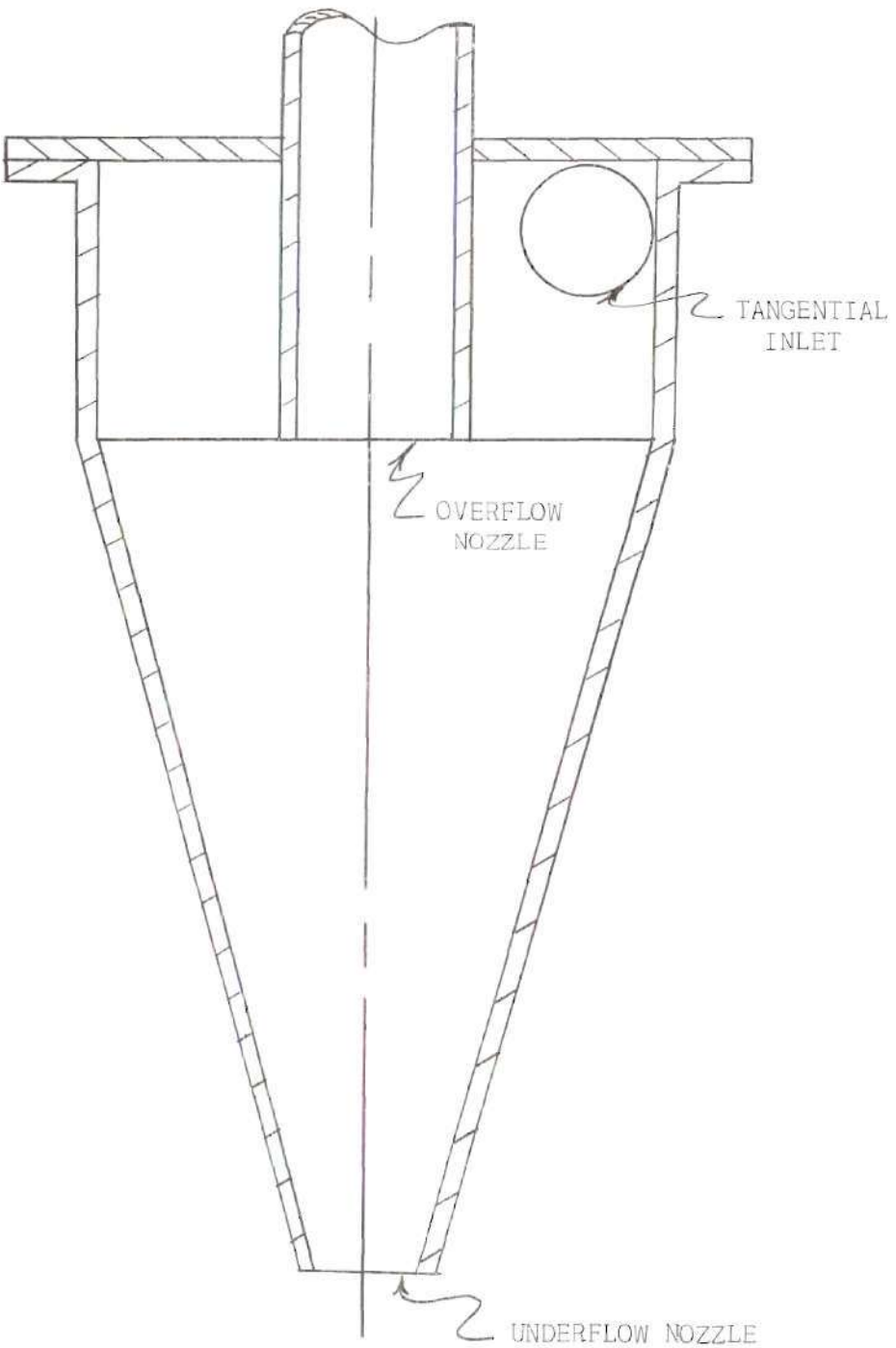

Figure 1. Cross Section of a Conventional Hydrocyclone

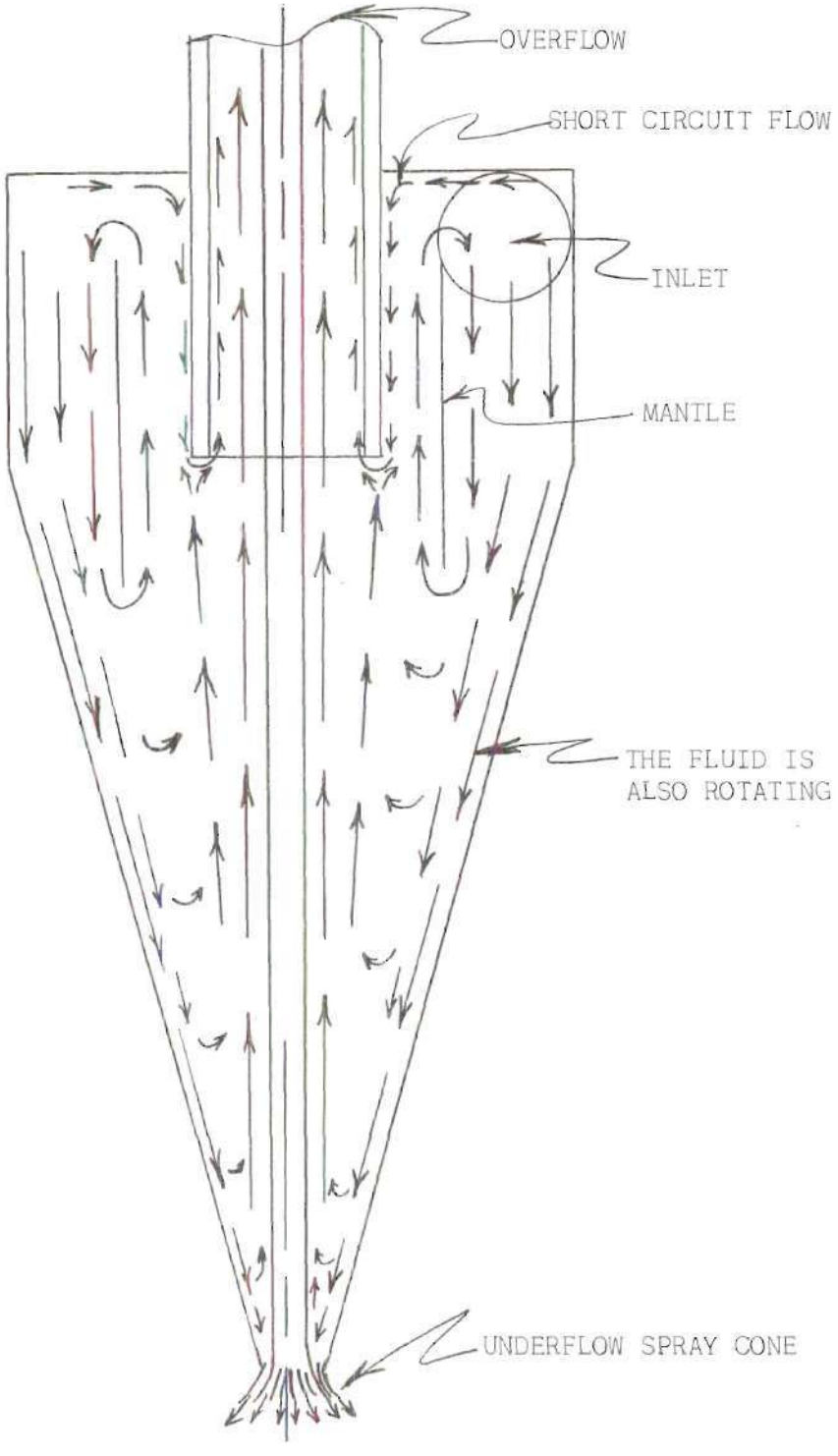

Figure 2. Descriptive Flow Patterns Based on Vertical and Radial Components of Velocity in a Hydrocyclone

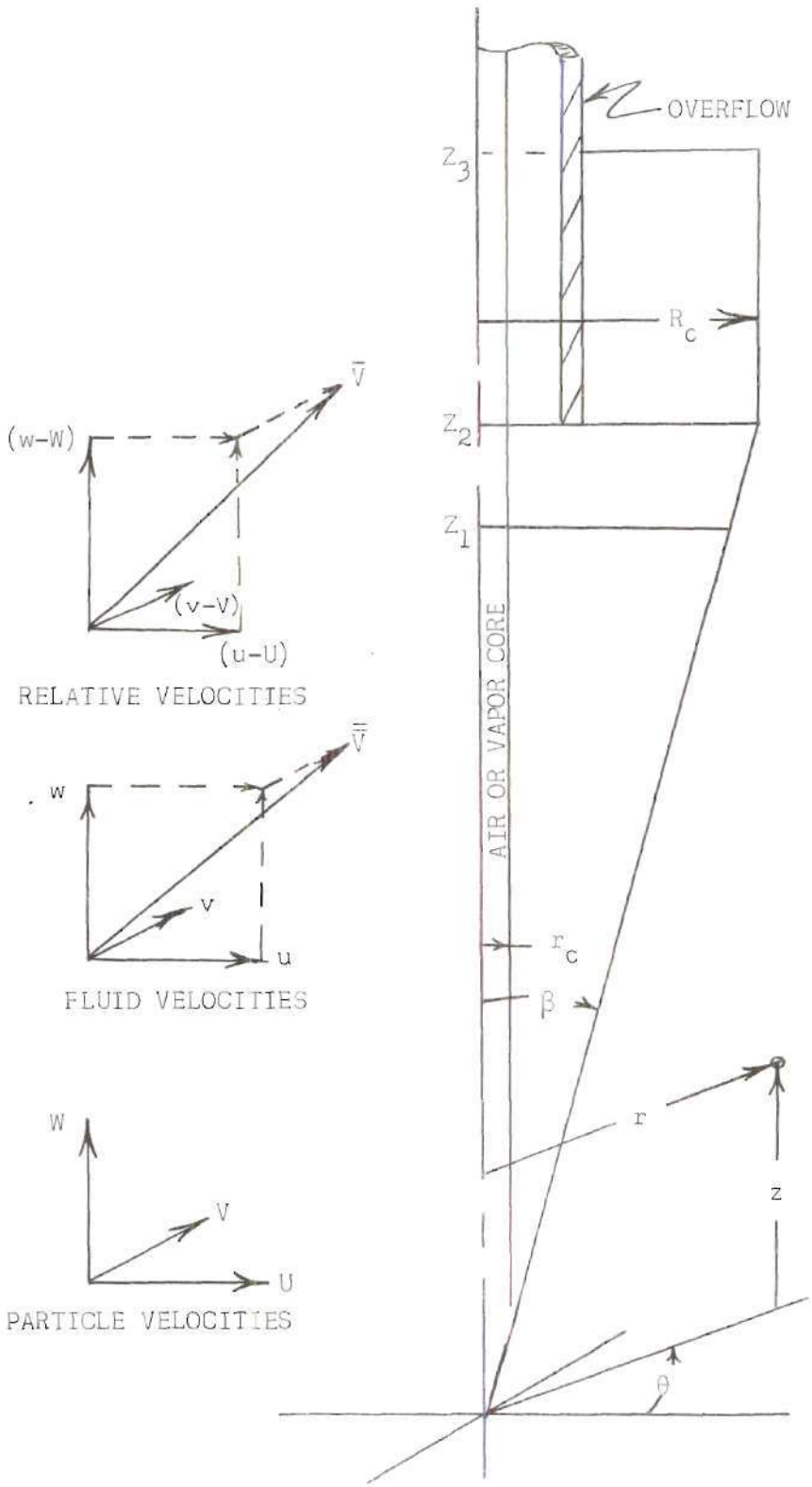

Figure 3. Coordinate System and Velocity Vectors

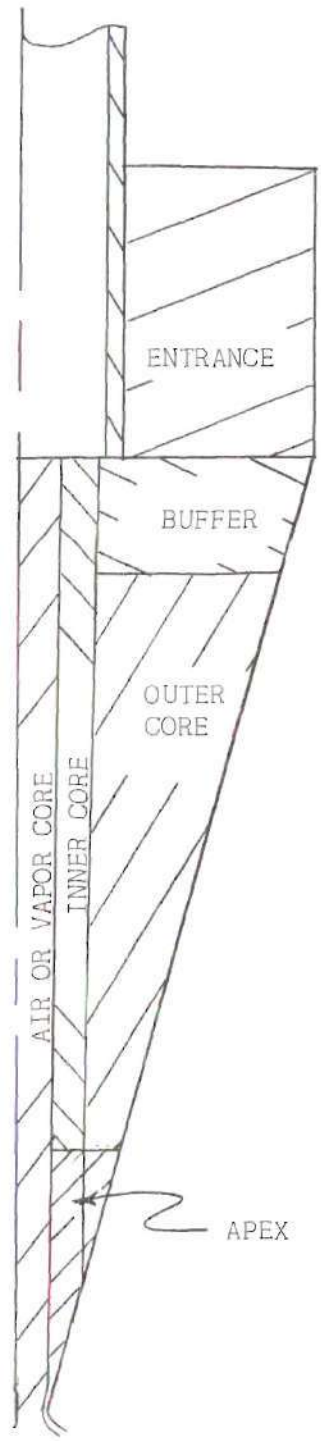

Figure 4. Regions of Flow in the Conventional Hydrocyclone

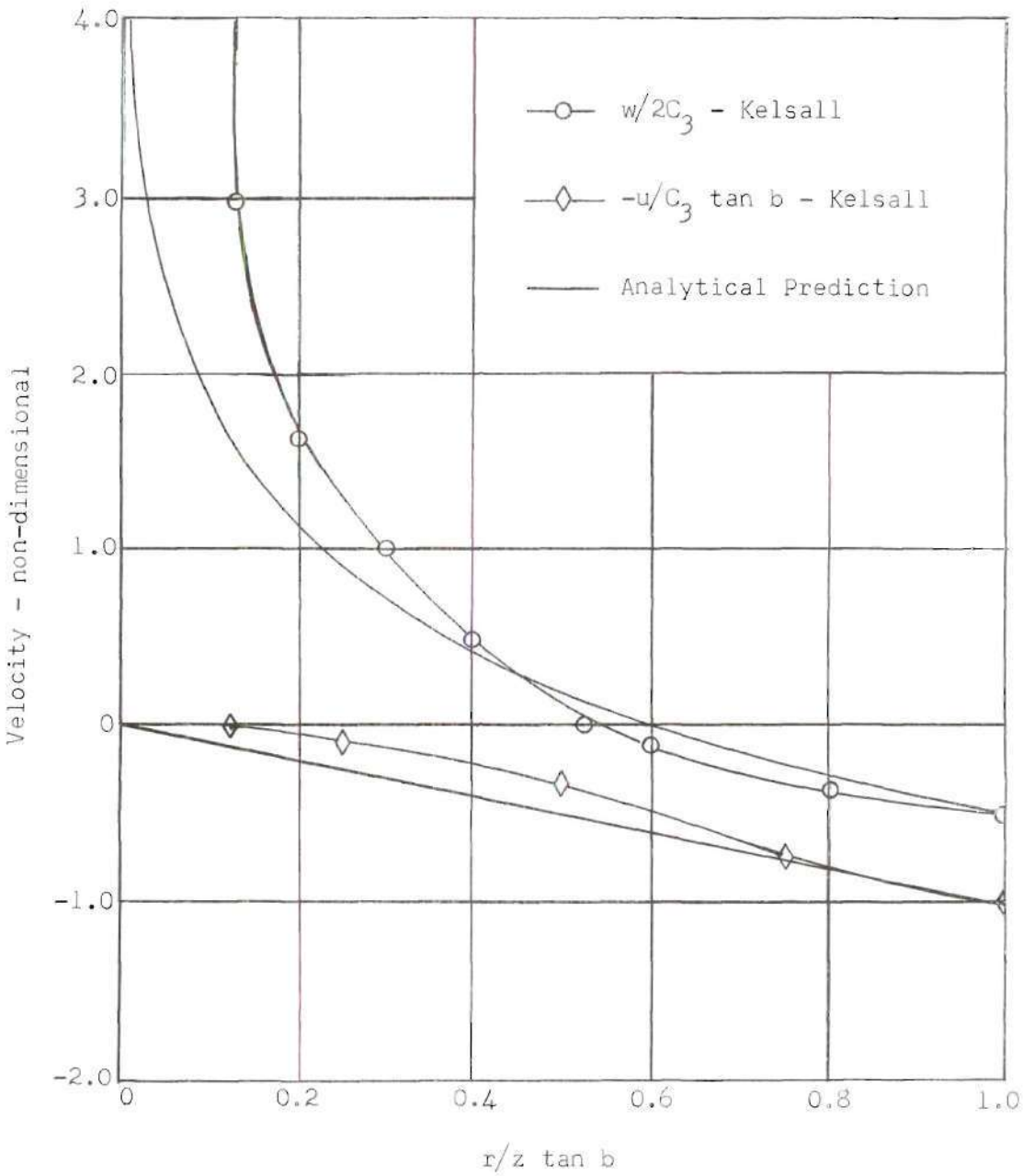

Figure 5a. Comparison of Predicted and Experimental Fluid Velocity Components

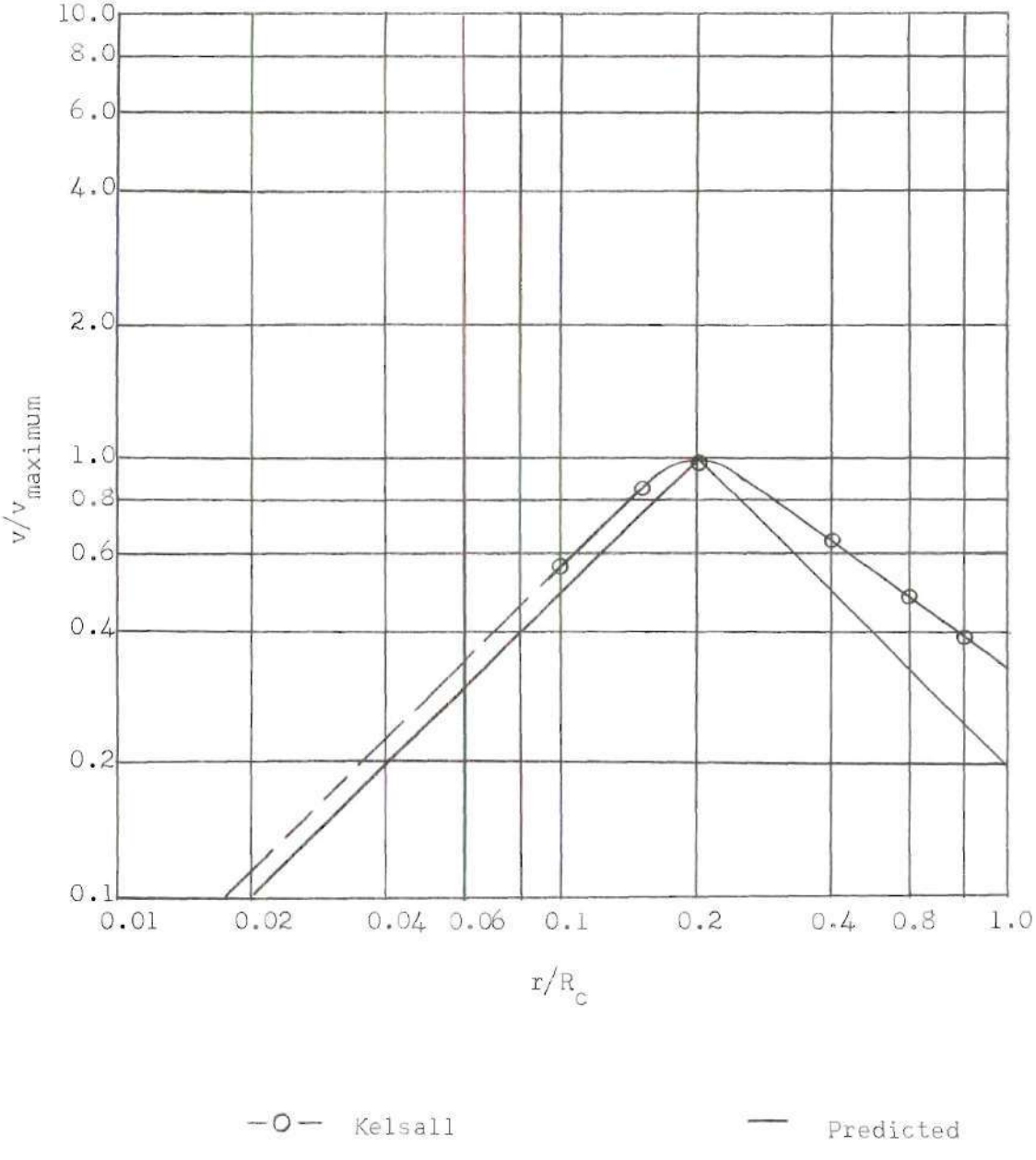

Figure 5b. Comparison of Predicted and Experimental Fluid Velocity Components

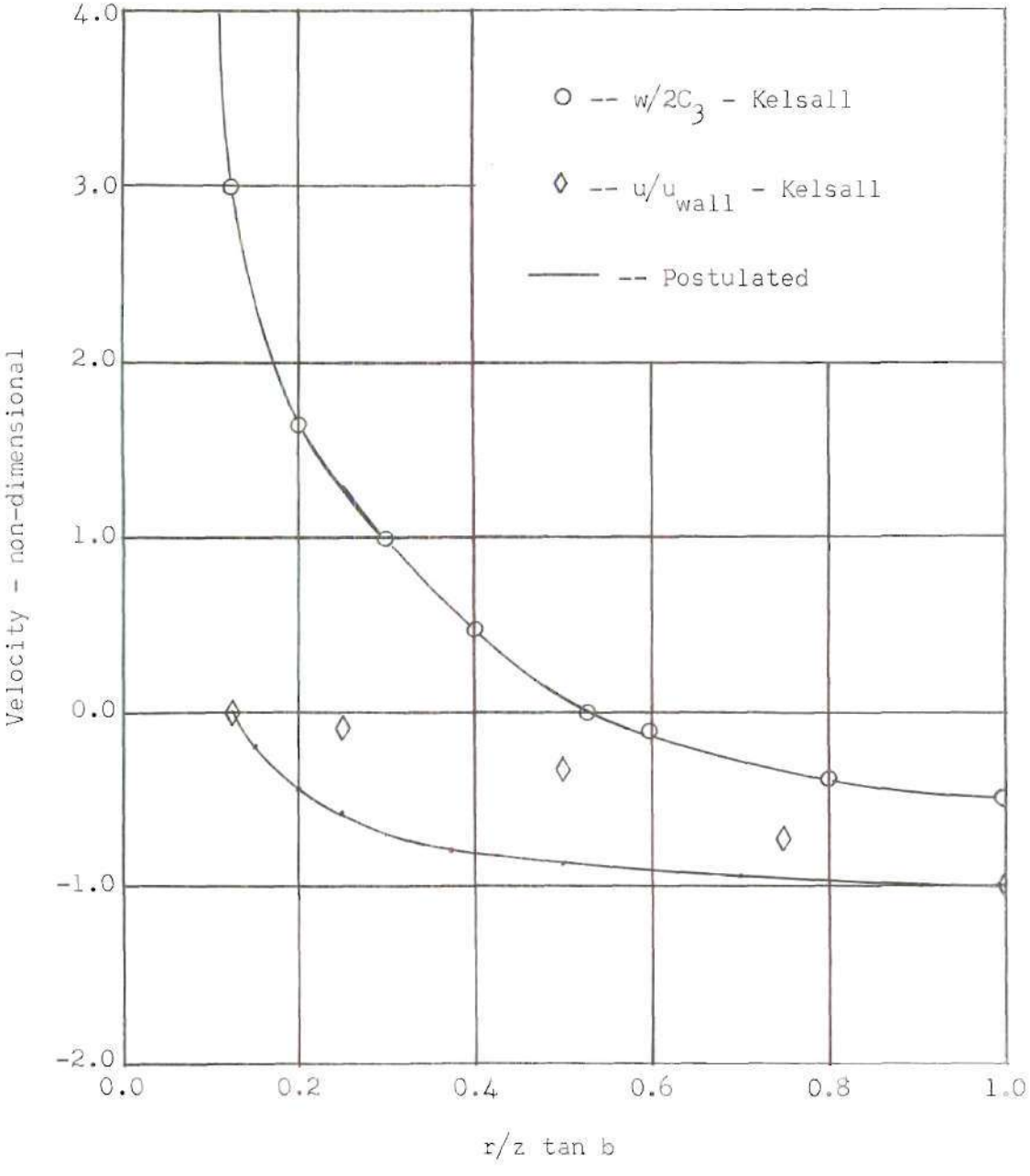

Figure 6a. Comparison of Postulated and Experimental Fluid Velocity Components

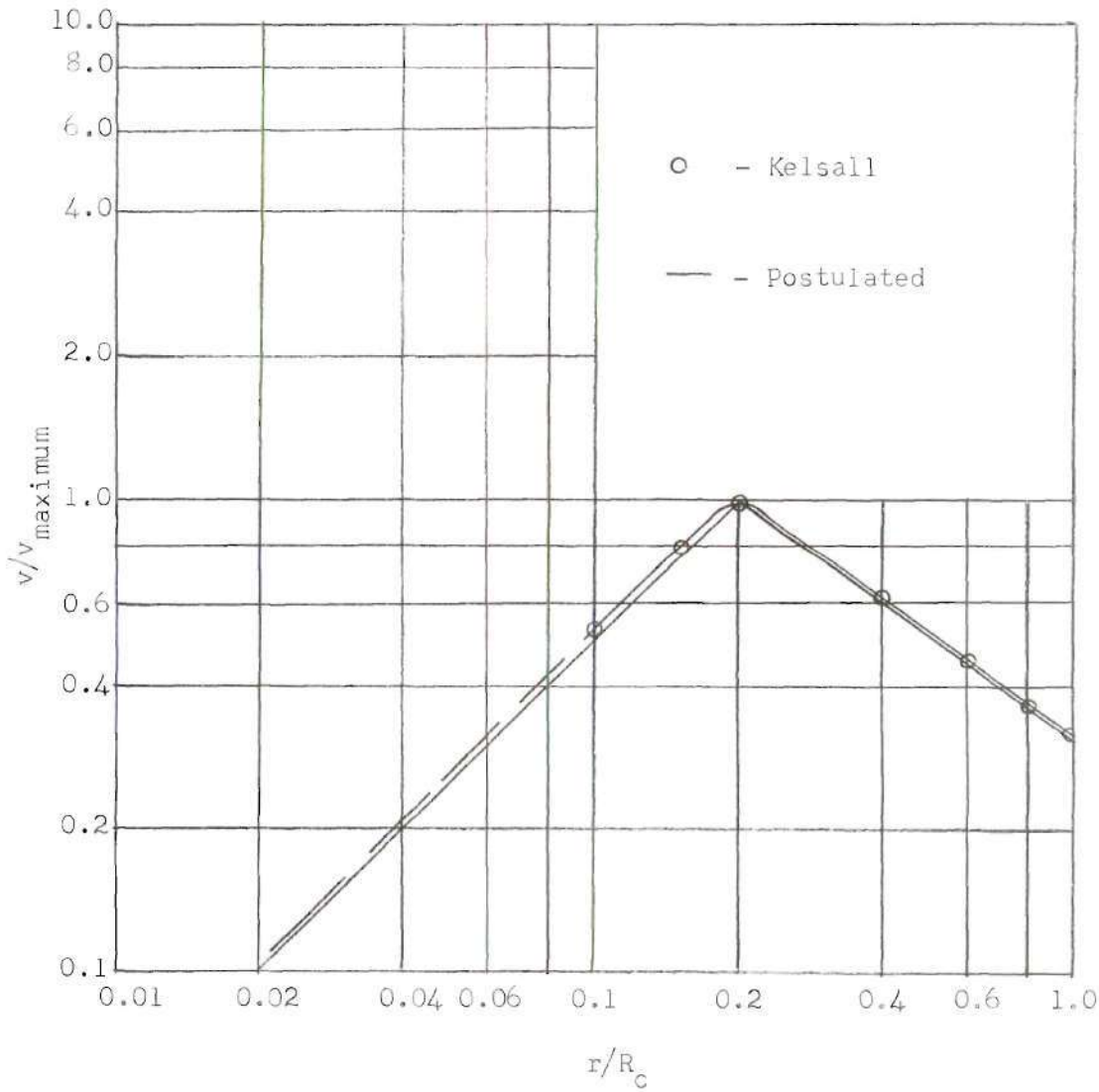

Figure 6b. Comparison of Postulated and Experimental Fluid Velocity Components

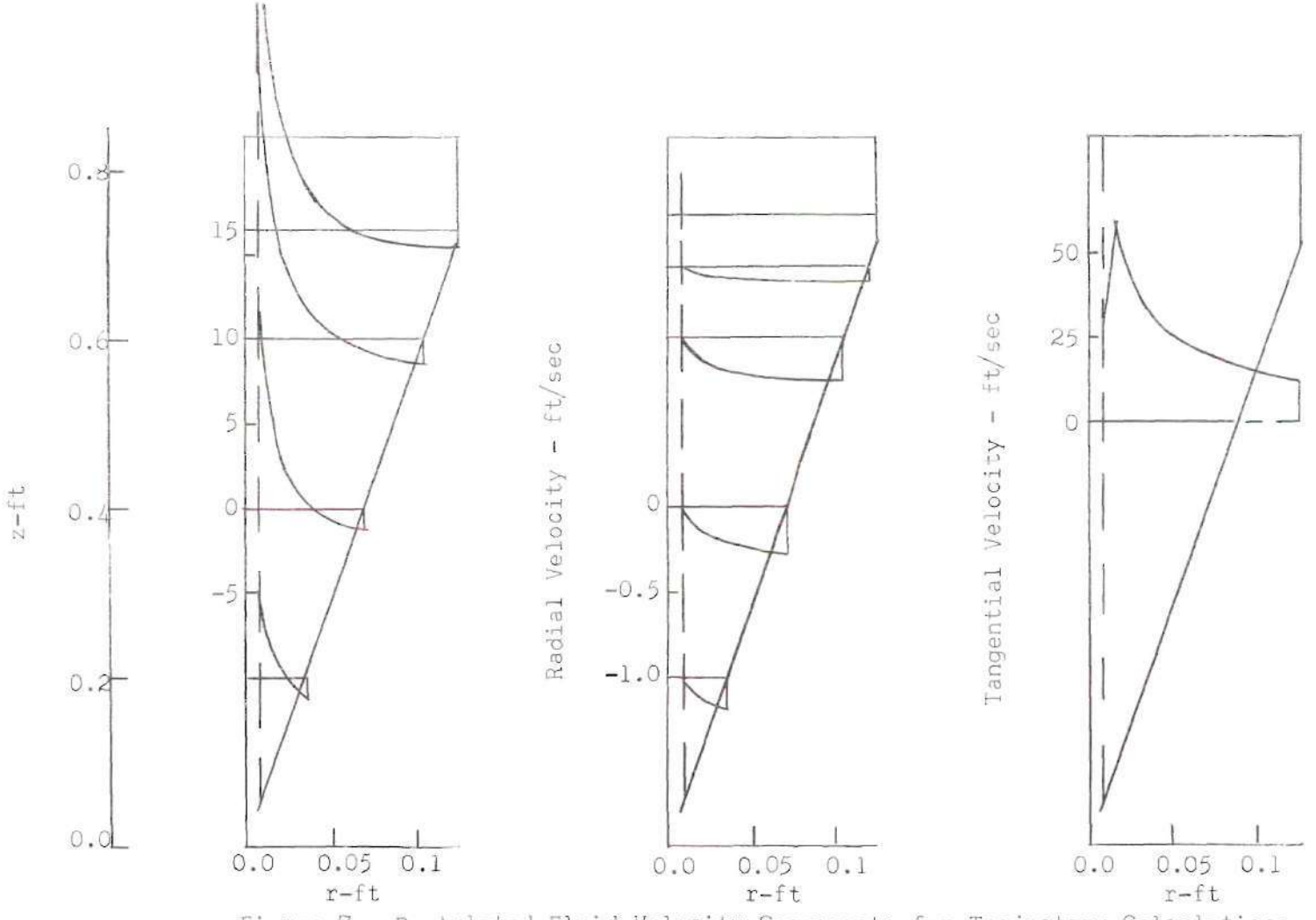

Figure 7. Postulated Fluid Velocity Components for Trajectory Calculations

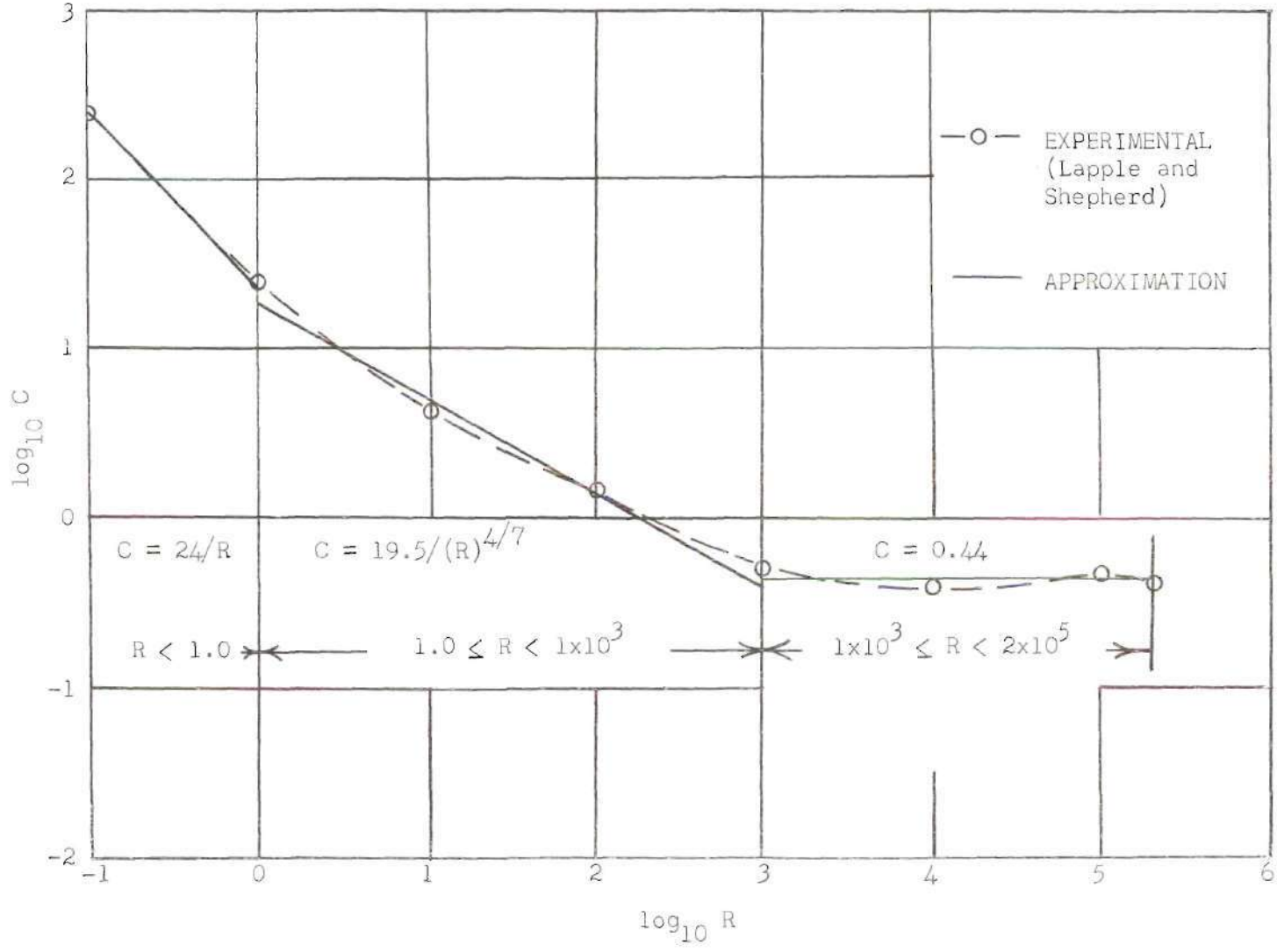

Figure 8. Comparison of Approximations with Experimental Values for the Drag Coefficient for a Sphere

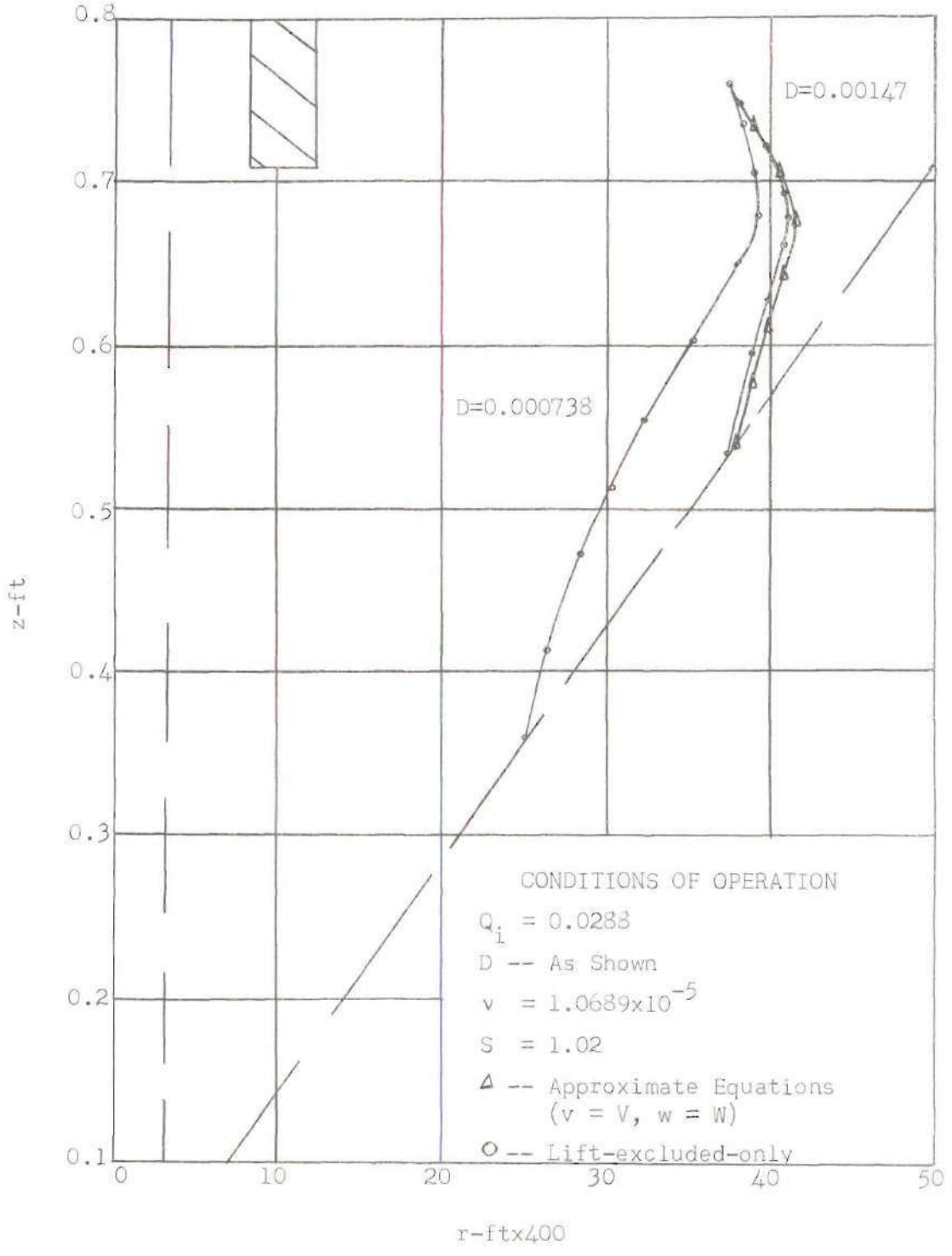

Figure 9. Comparison of Predicted Trajectories for Approximate and Lift-excluded-only Solutions

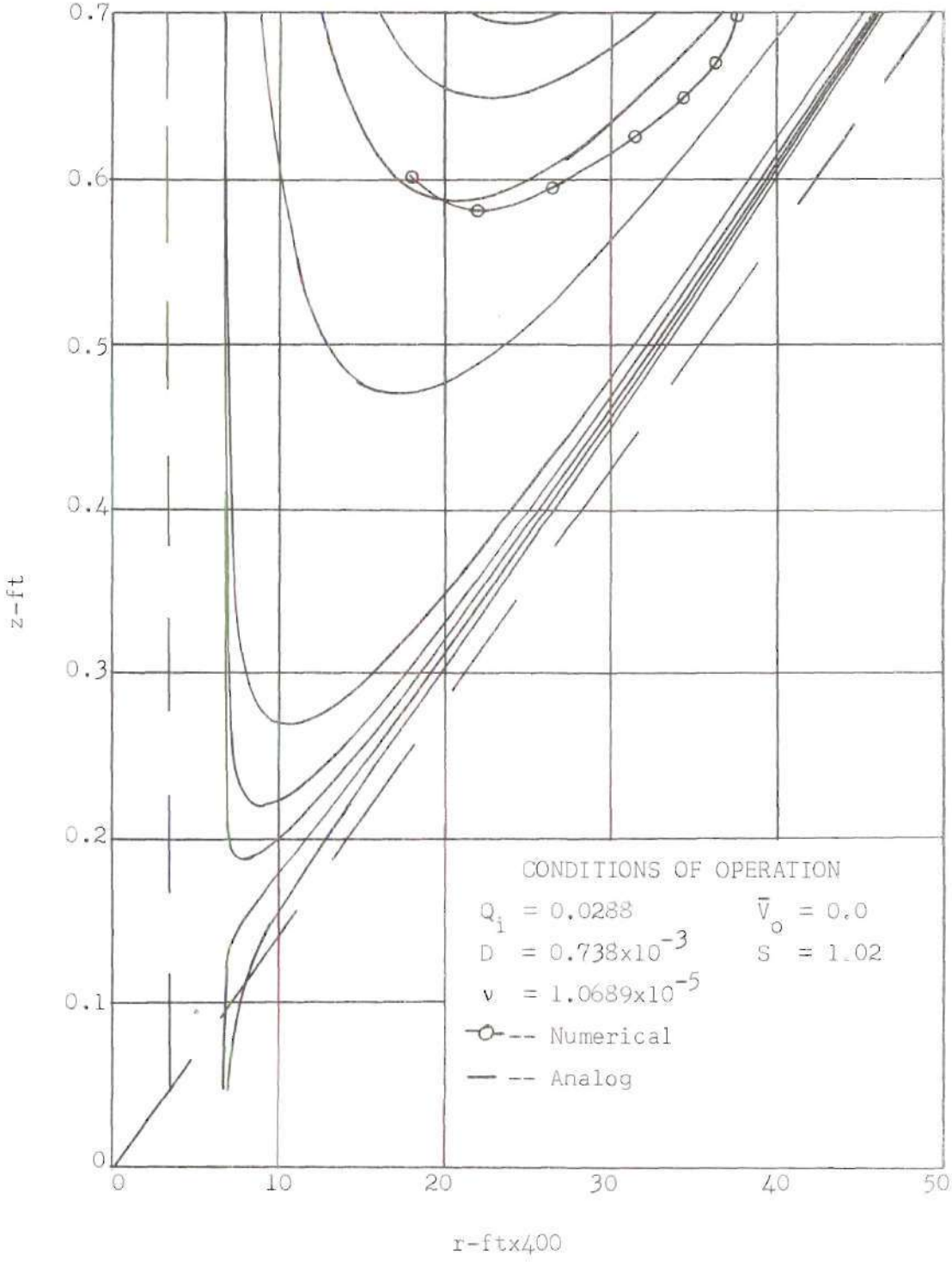

Figure 10. Predicted Trajectories for Particles Remaining in the Stokes Regime

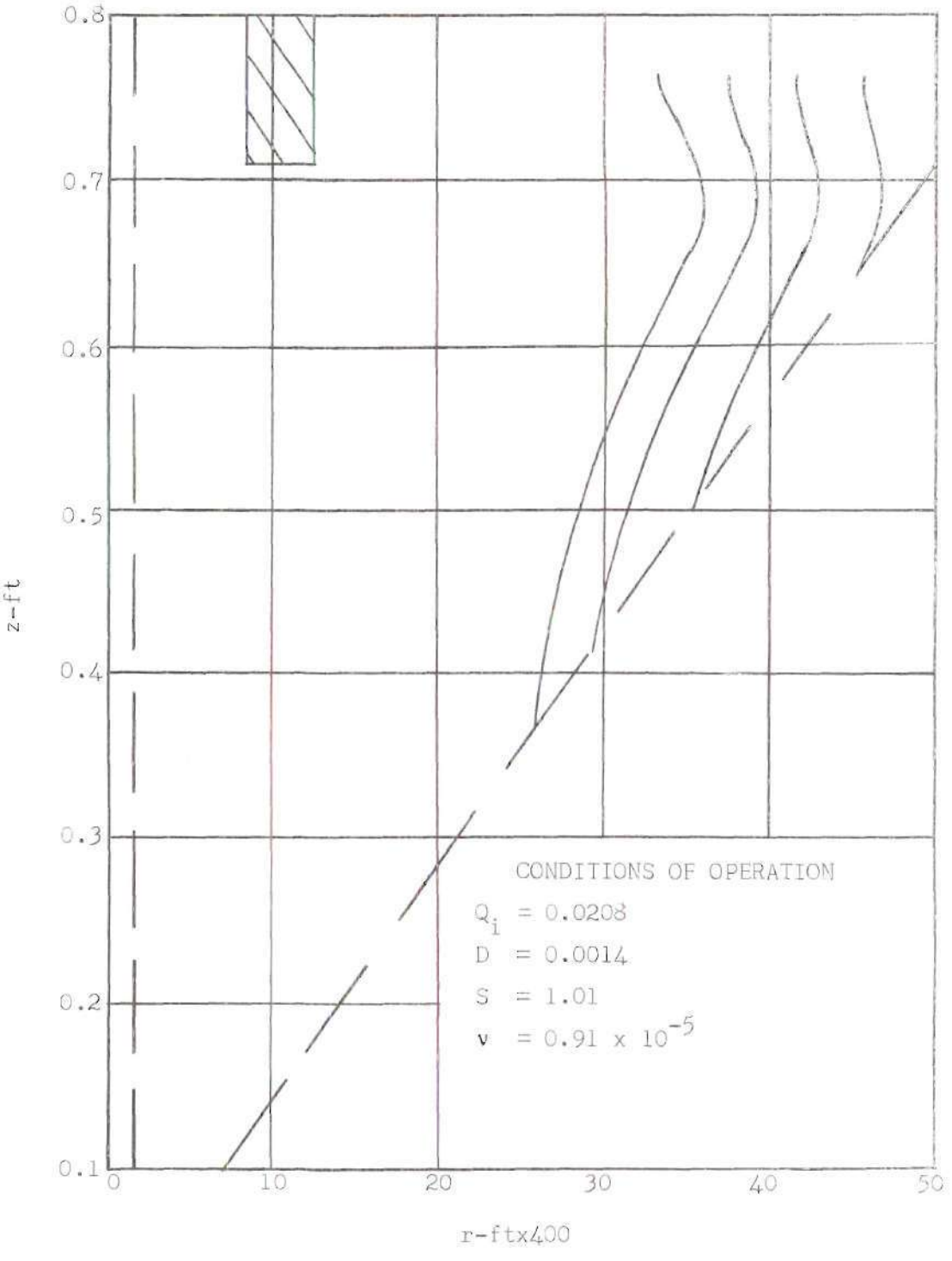

Figure 11a. Predicted Particle Trajectories—Numerical Solution—Condition I

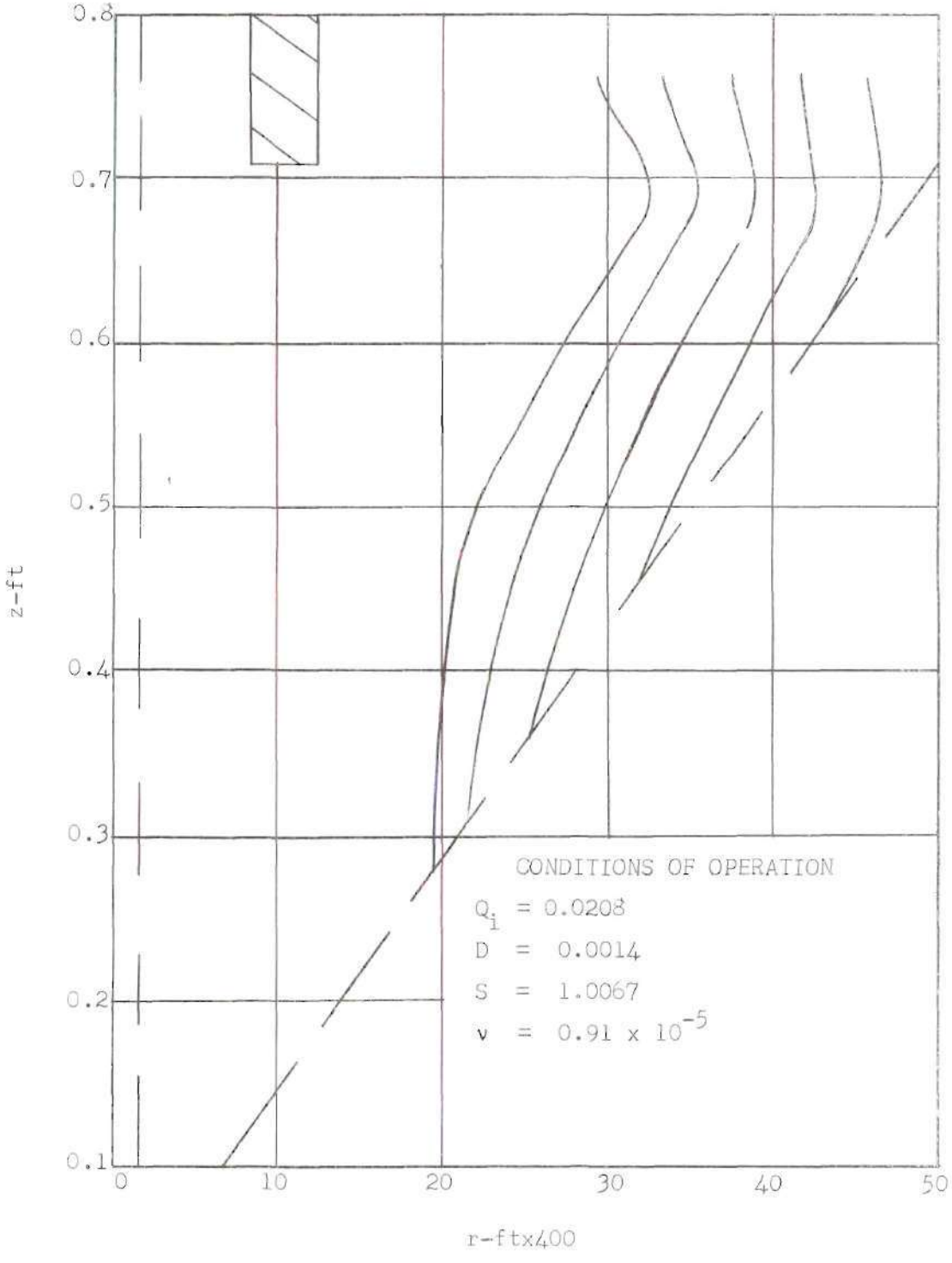

Figure 11b. Predicted Particle Trajectories—Numerical Solution—Condition II

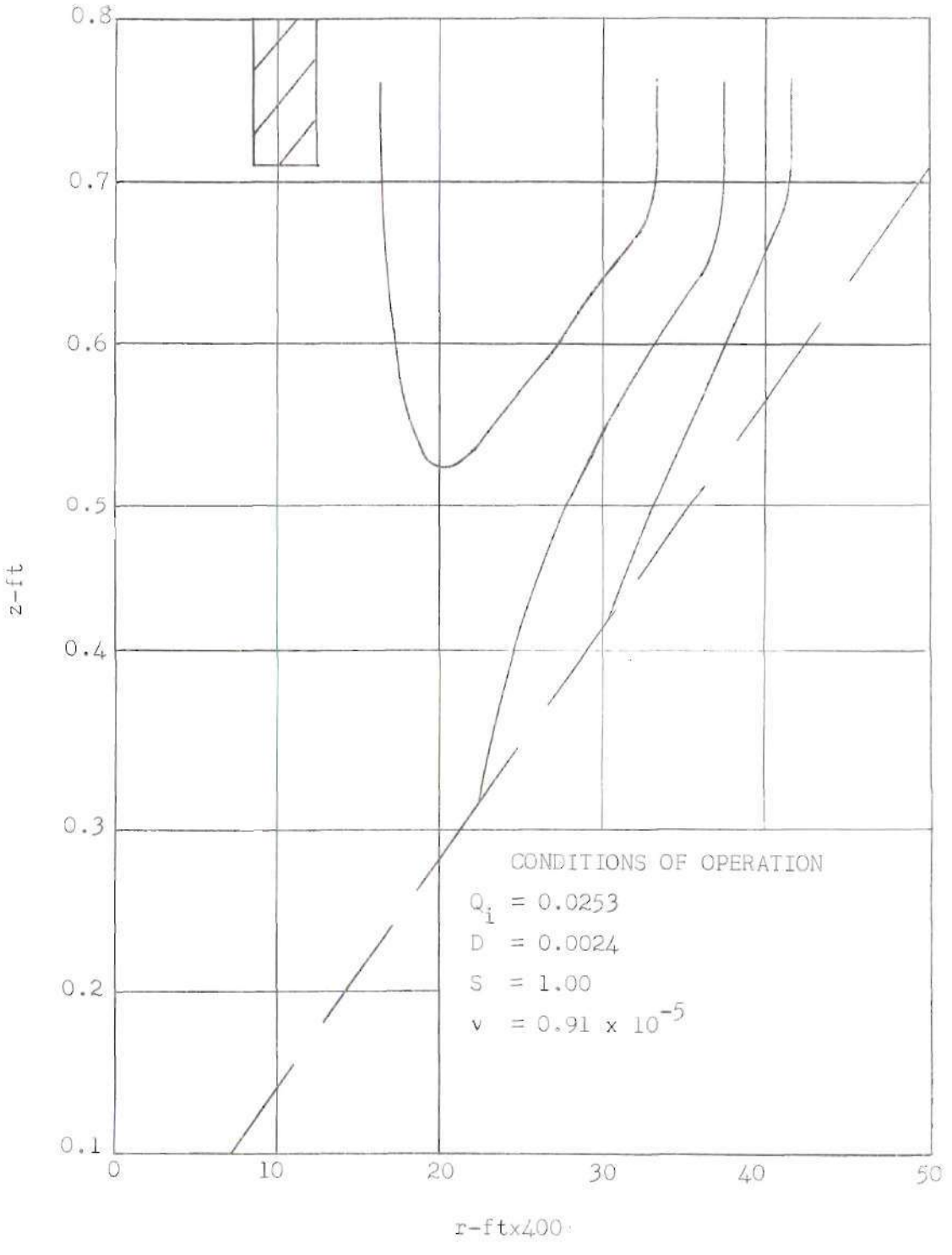

Figure 12a. Predicted Particle Trajectories—Numerical Solution—Conditions III

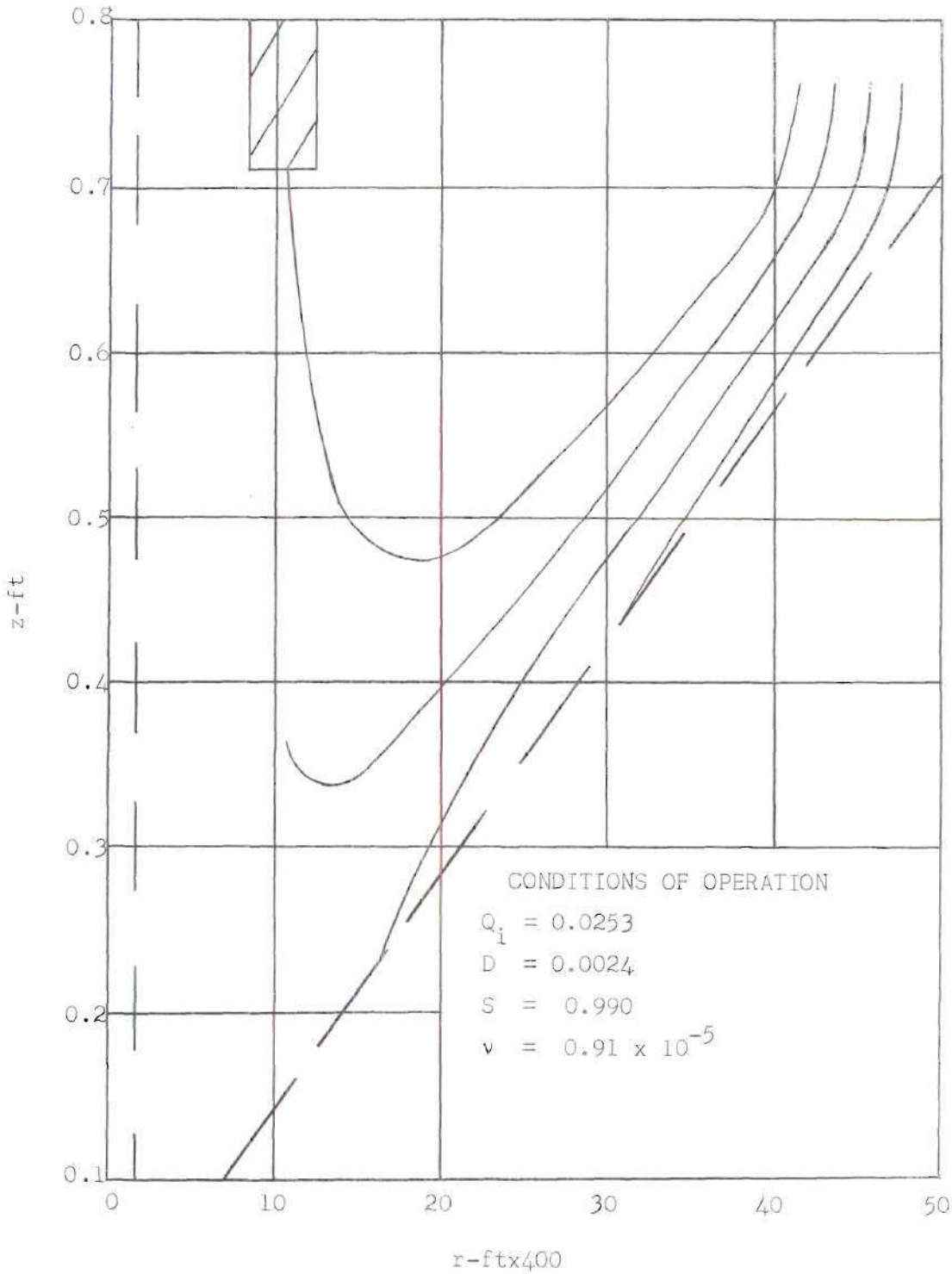

Figure 12b. Predicted Particle Trajectories—Numerical Solution—Conditions III

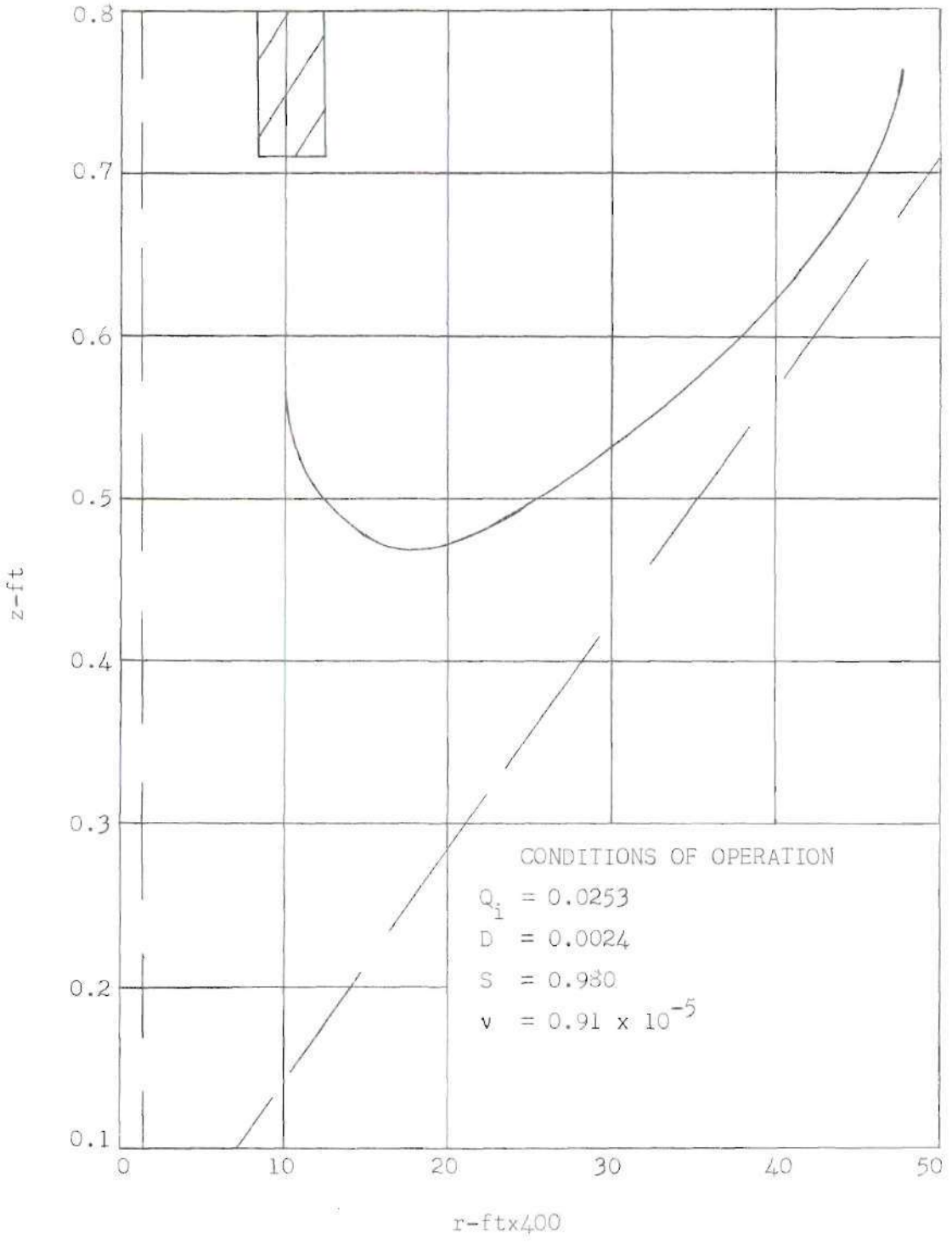

Figure 12c. Predicted Particle Trajectories—Numerical Solution—Conditions III

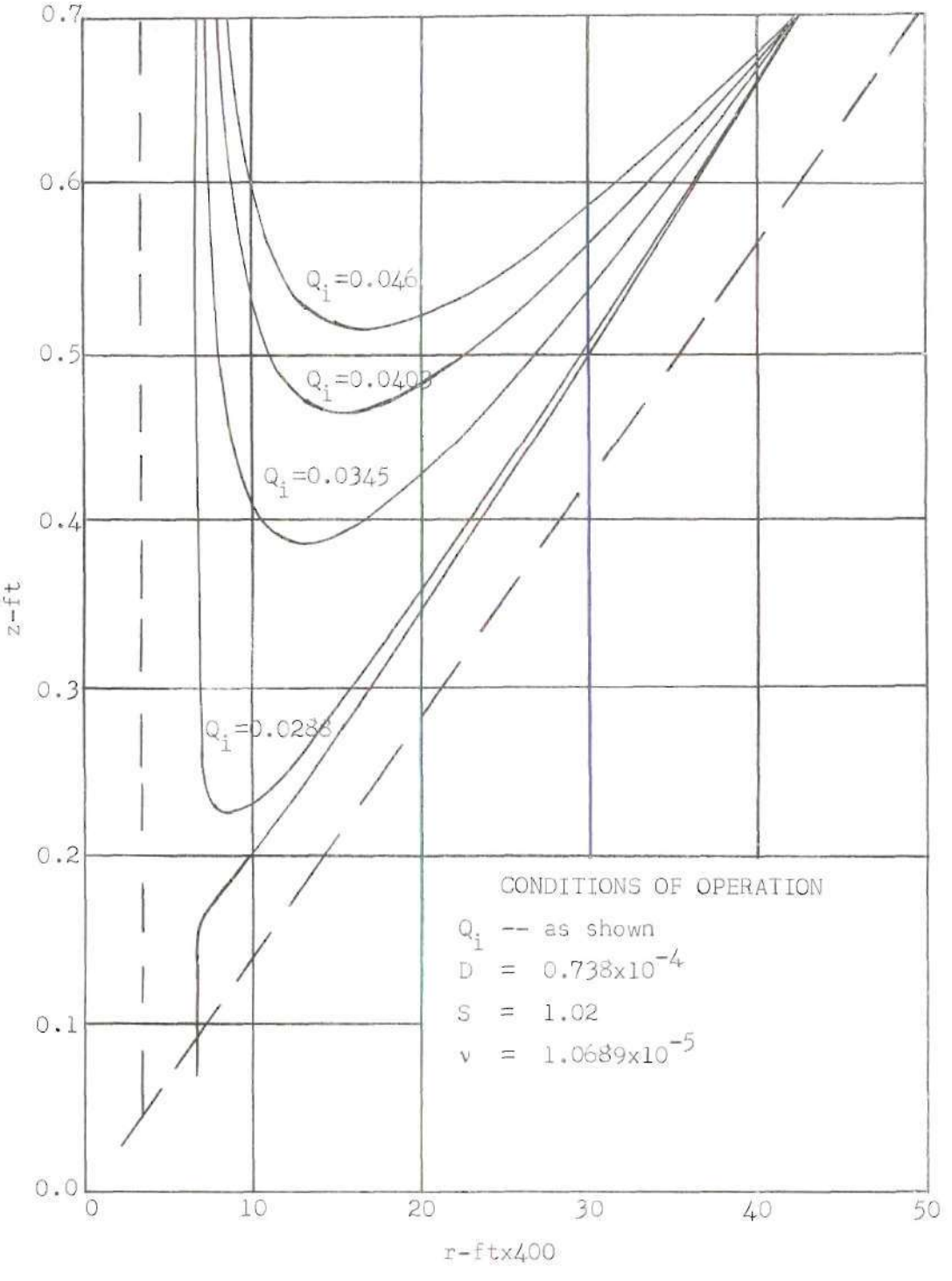

Figure 13. Effect of Flow Rate on Small Particle Trajectories

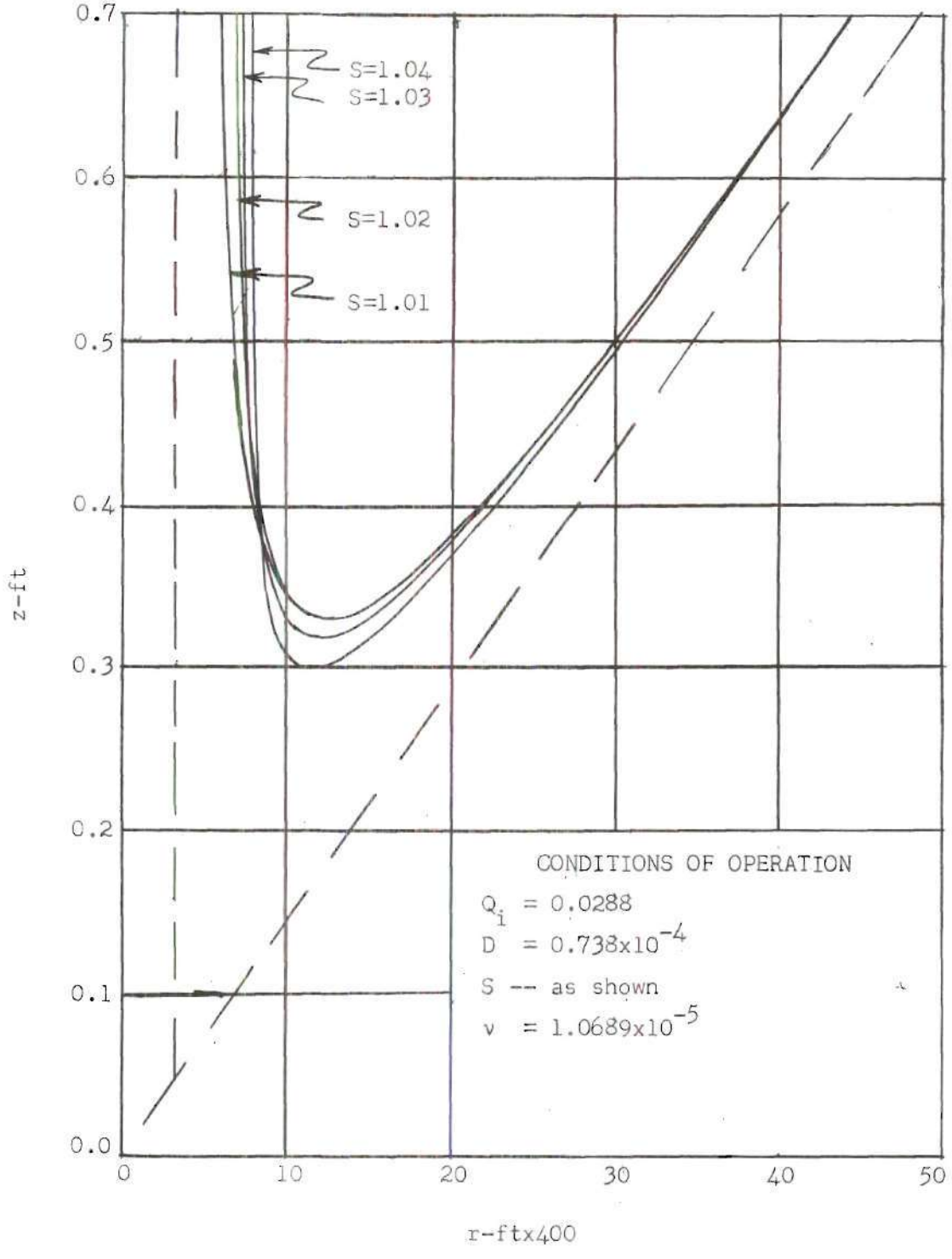

Figure 14. Effect of Specific Gravity on Small Particle Trajectories

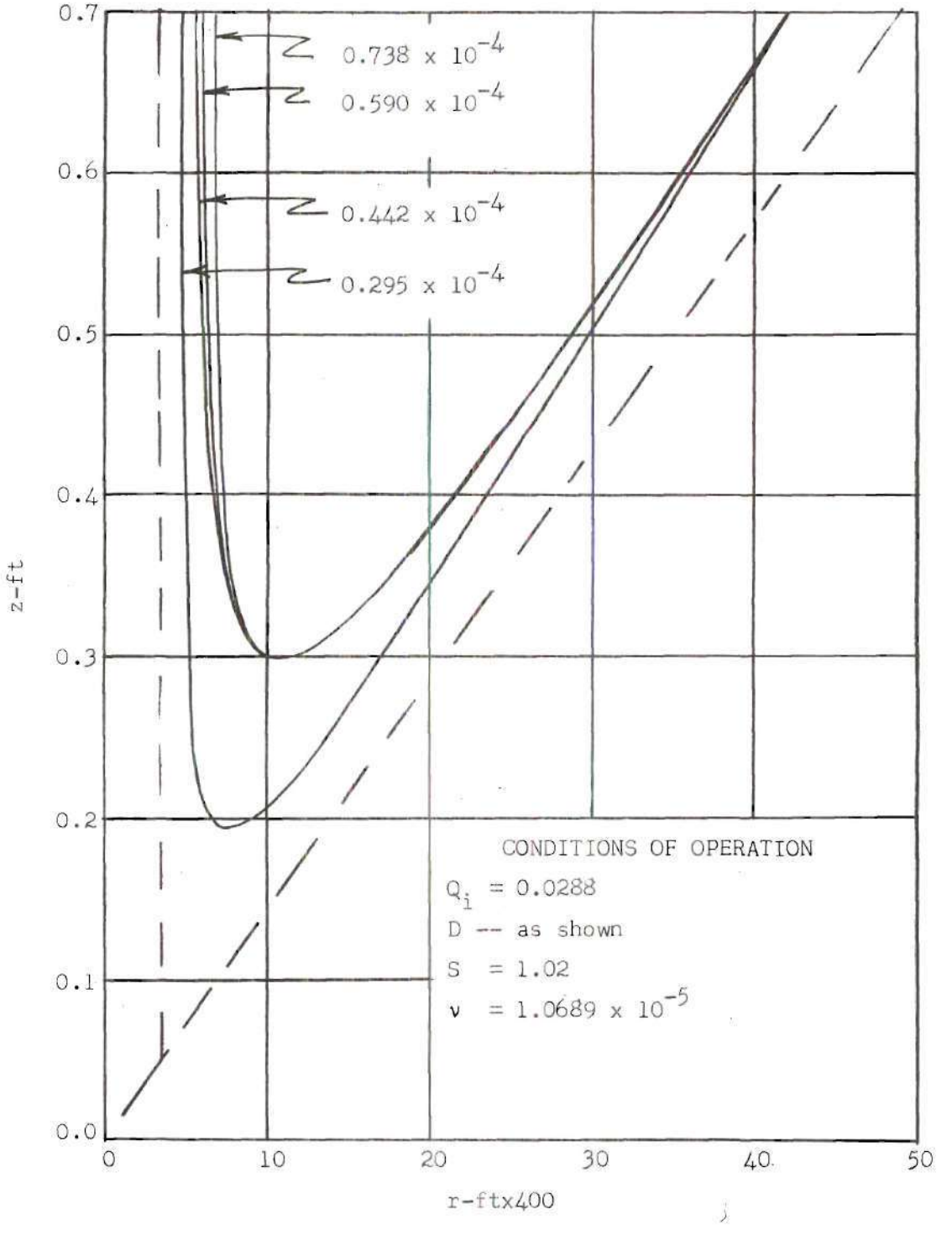

Figure 15. Effect of Sphere Diameter on Small Particle Trajectories

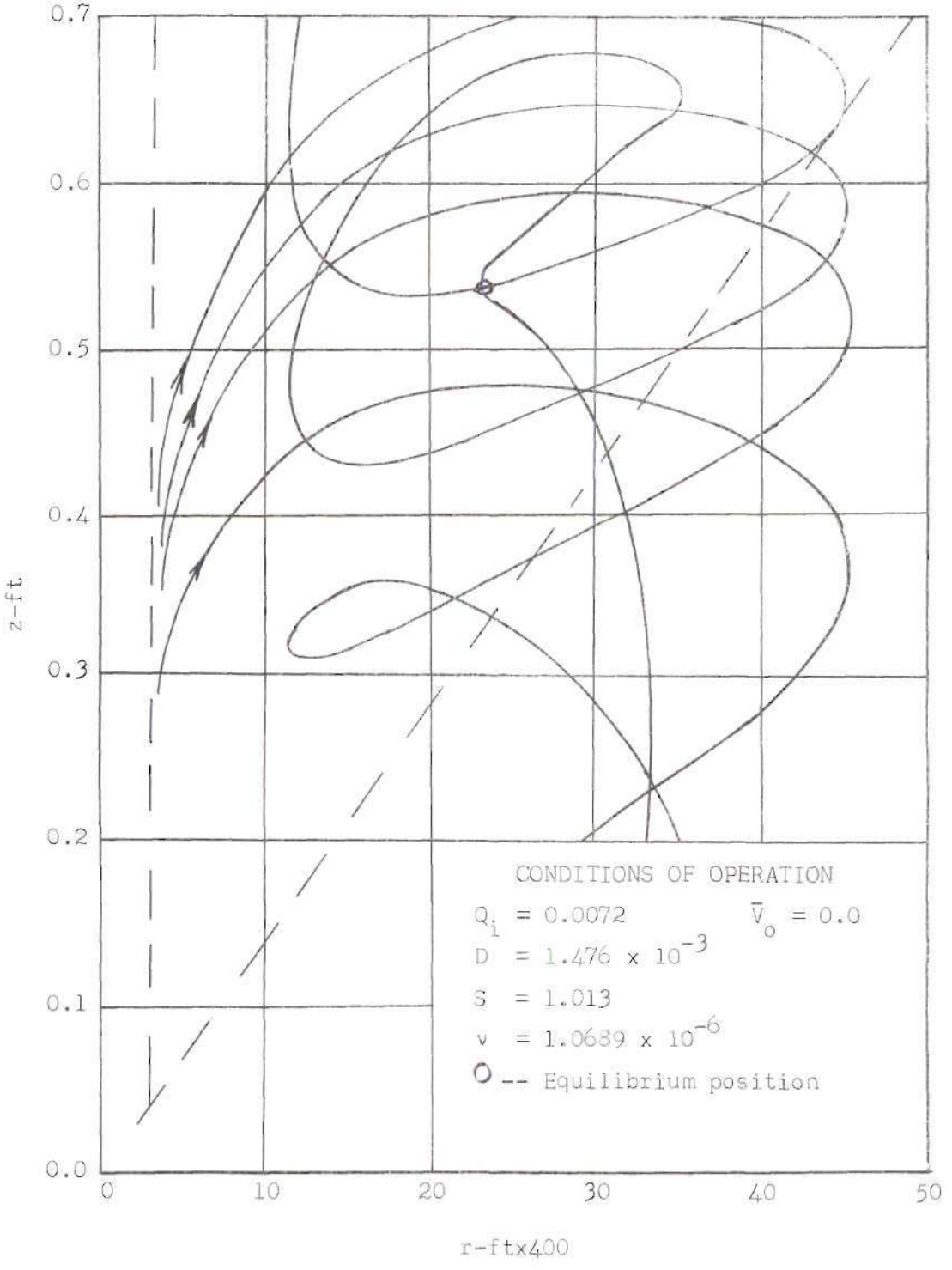

Figure 16. Secondary Trajectories—Analog Solution

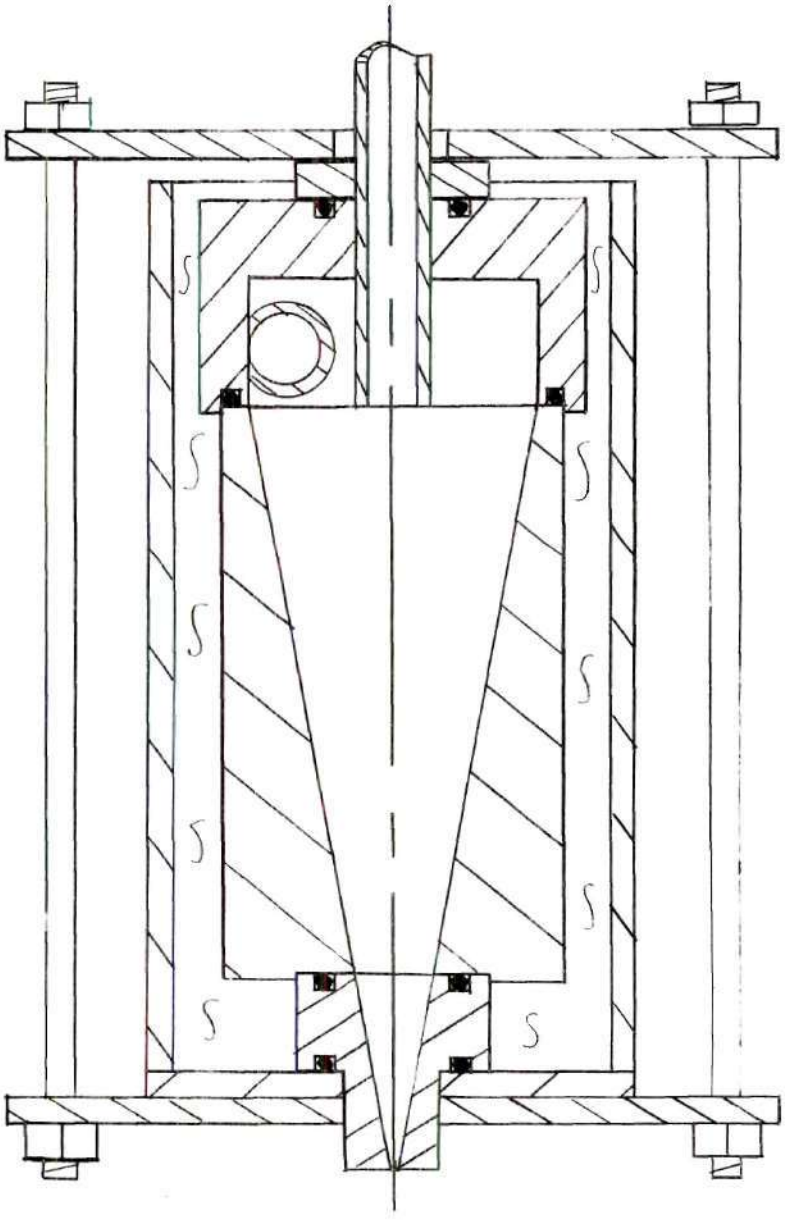

Scale: 1" = 2"

Figure 17. Cross Sectional View of the Hydrocyclone Used

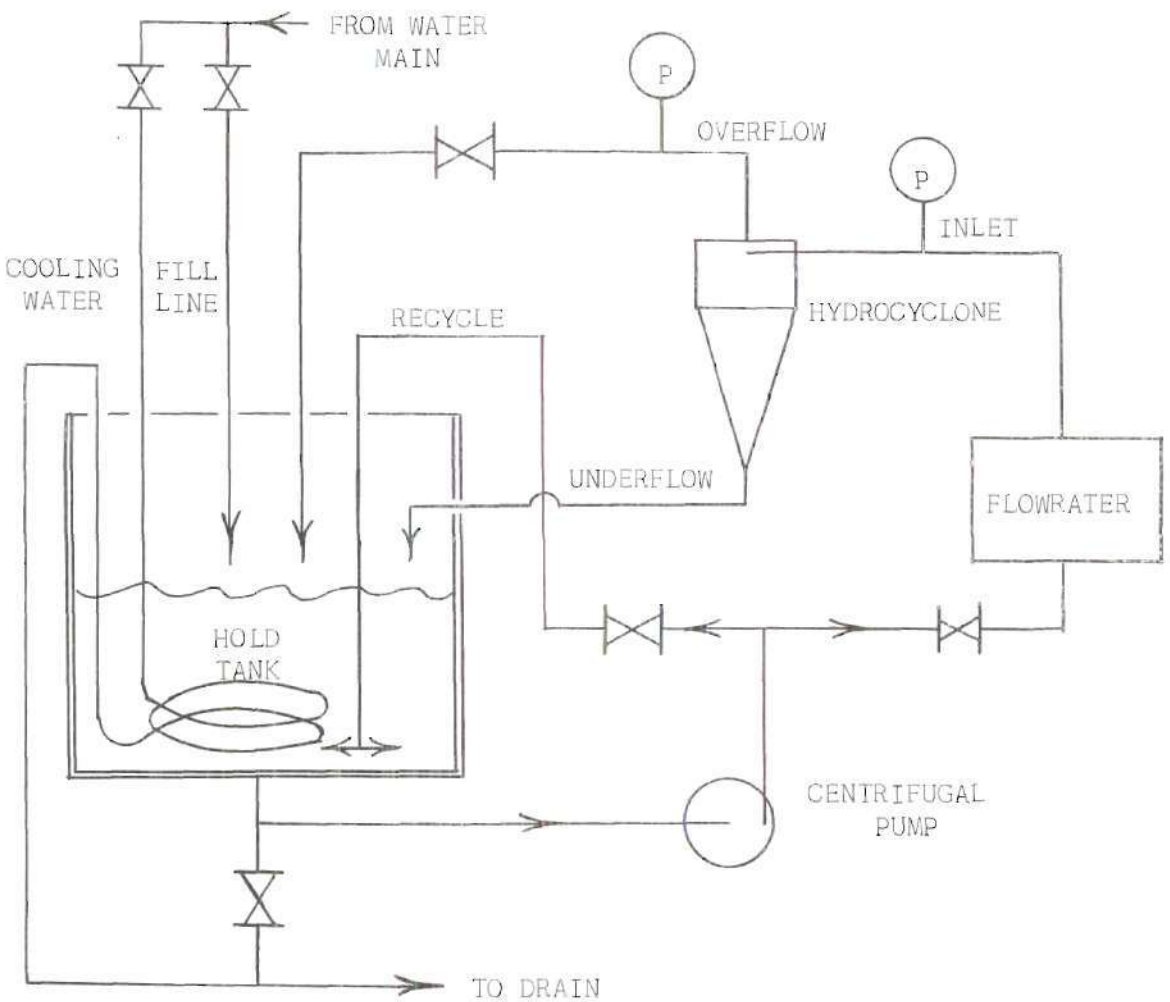

Figure 18. Schematic Diagram of Flow System

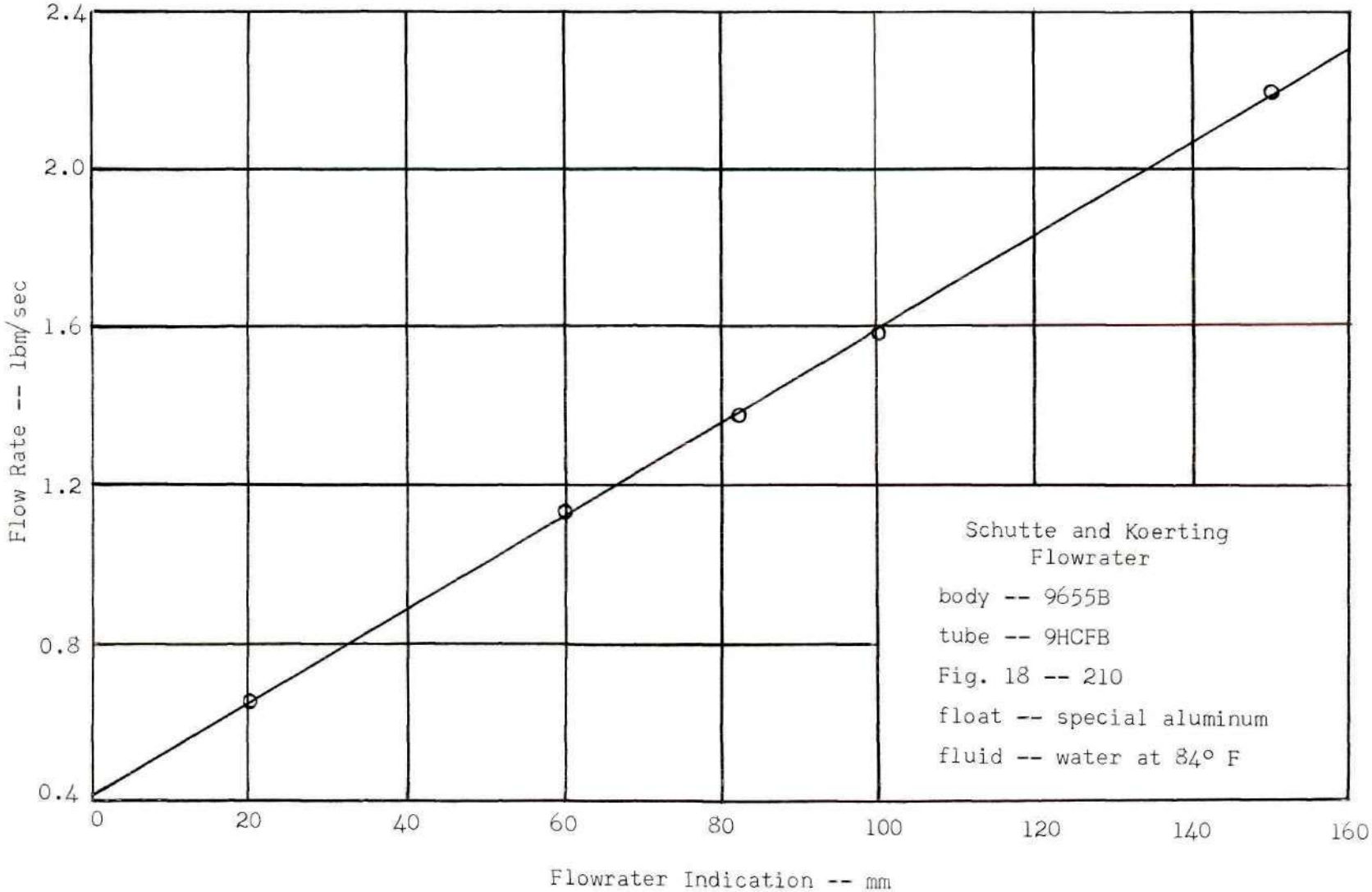

Figure 19. Calibration of Flowrater

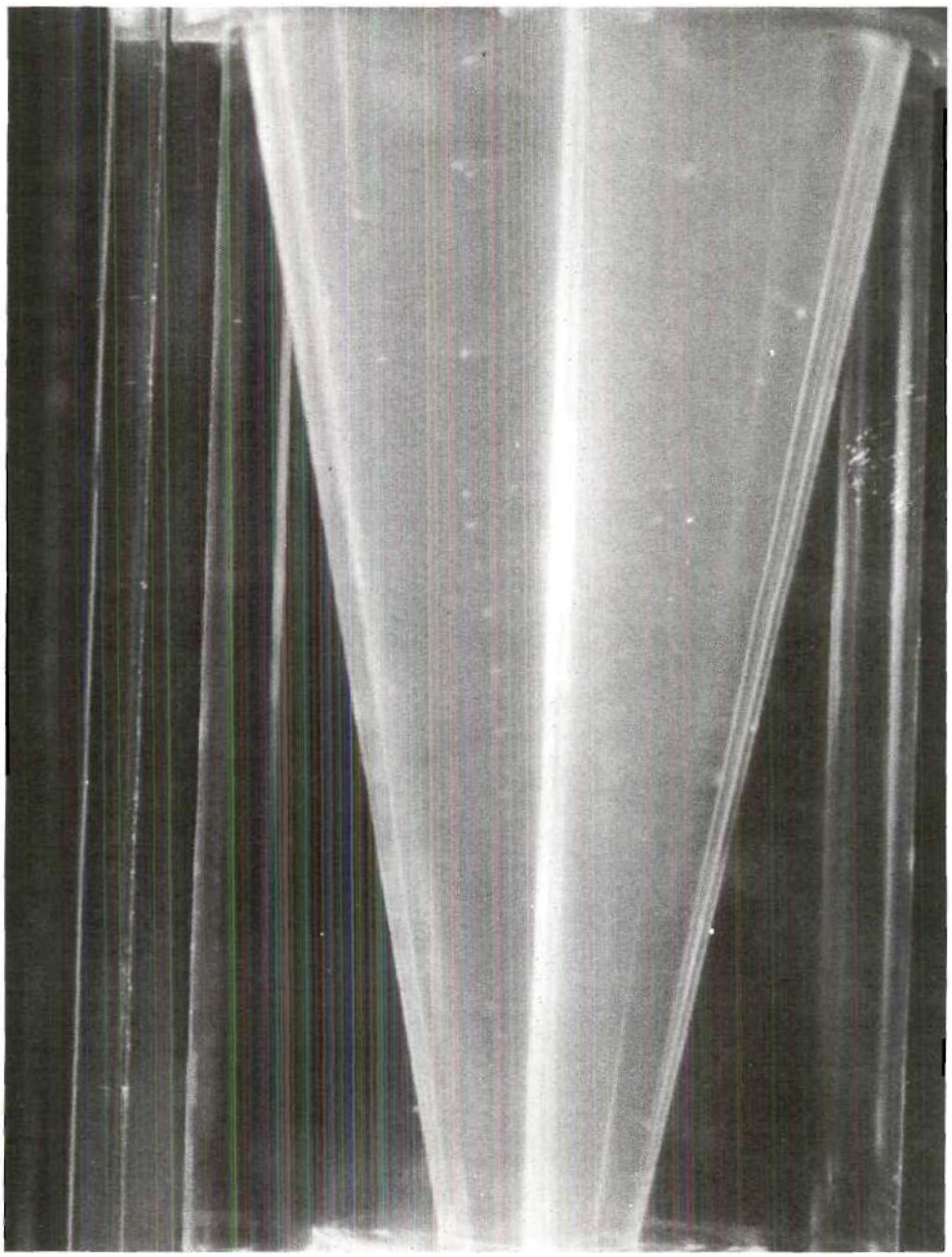

Figure 20. Typical Particle Trajectory Photograph--
Slit Illumination.

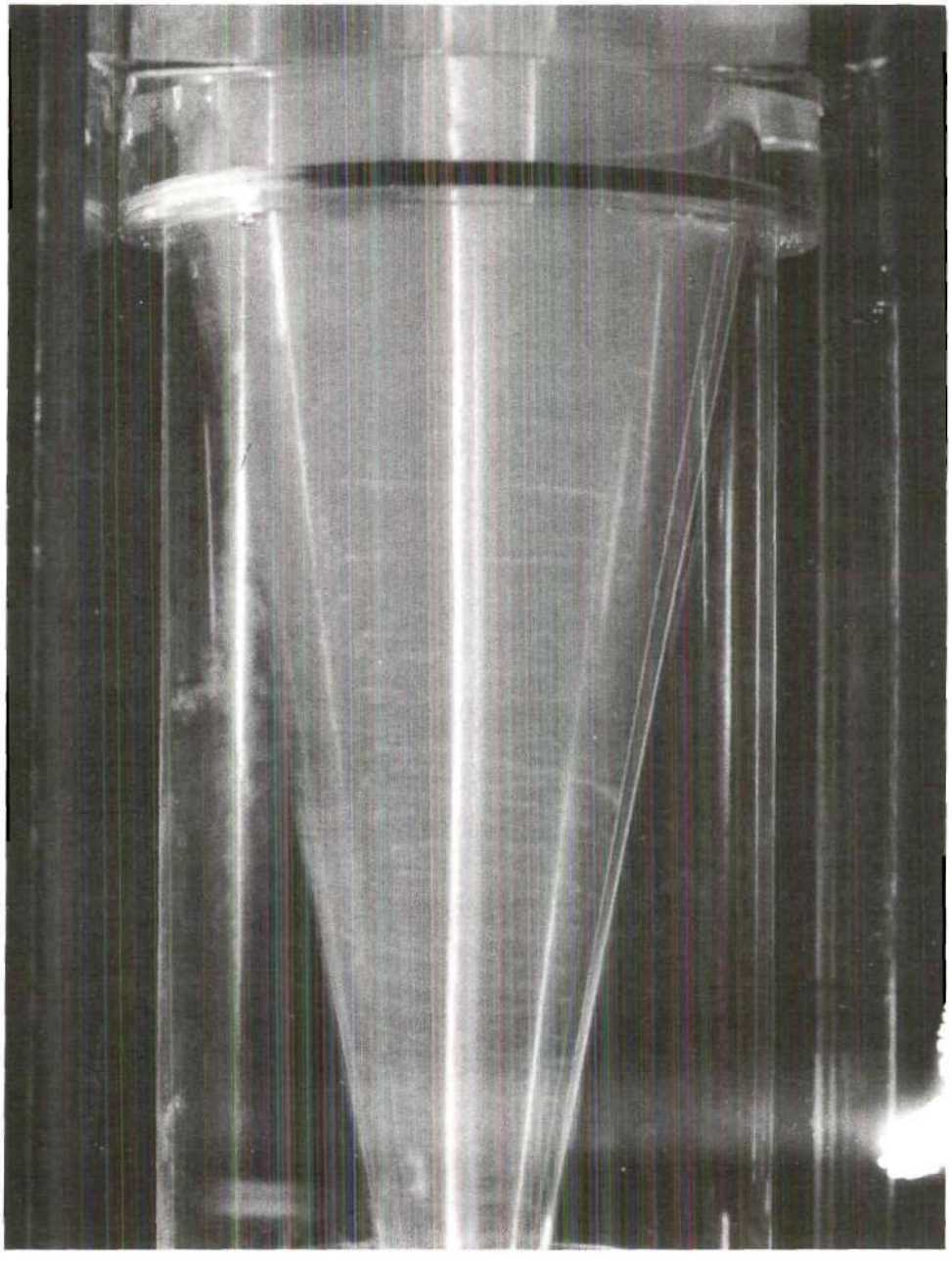

Figure 21. Typical Particle Trajectory Photograph--
Full Illumination.

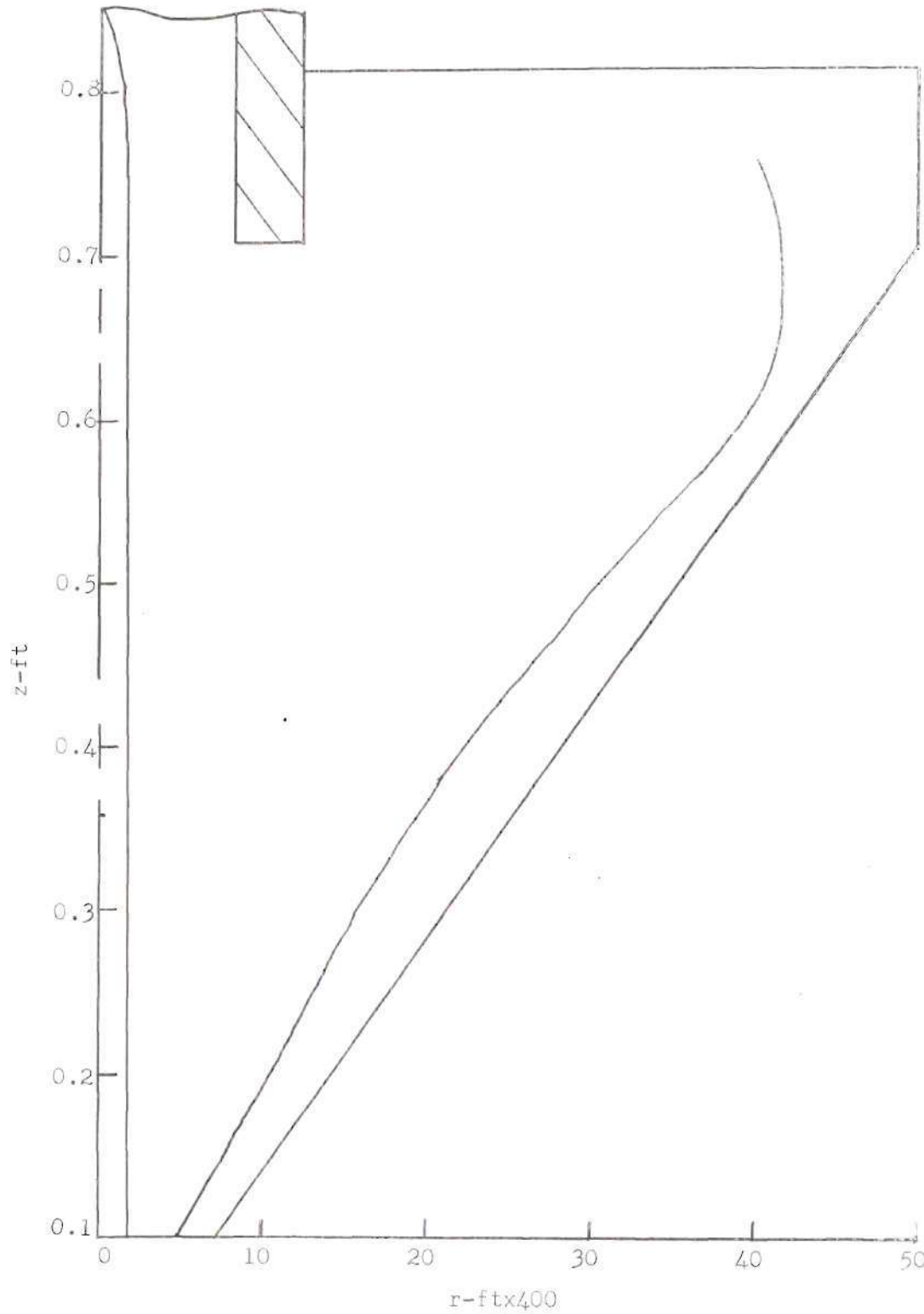

Figure 22. Sketch of a Typical Inlet Particle Trajectory

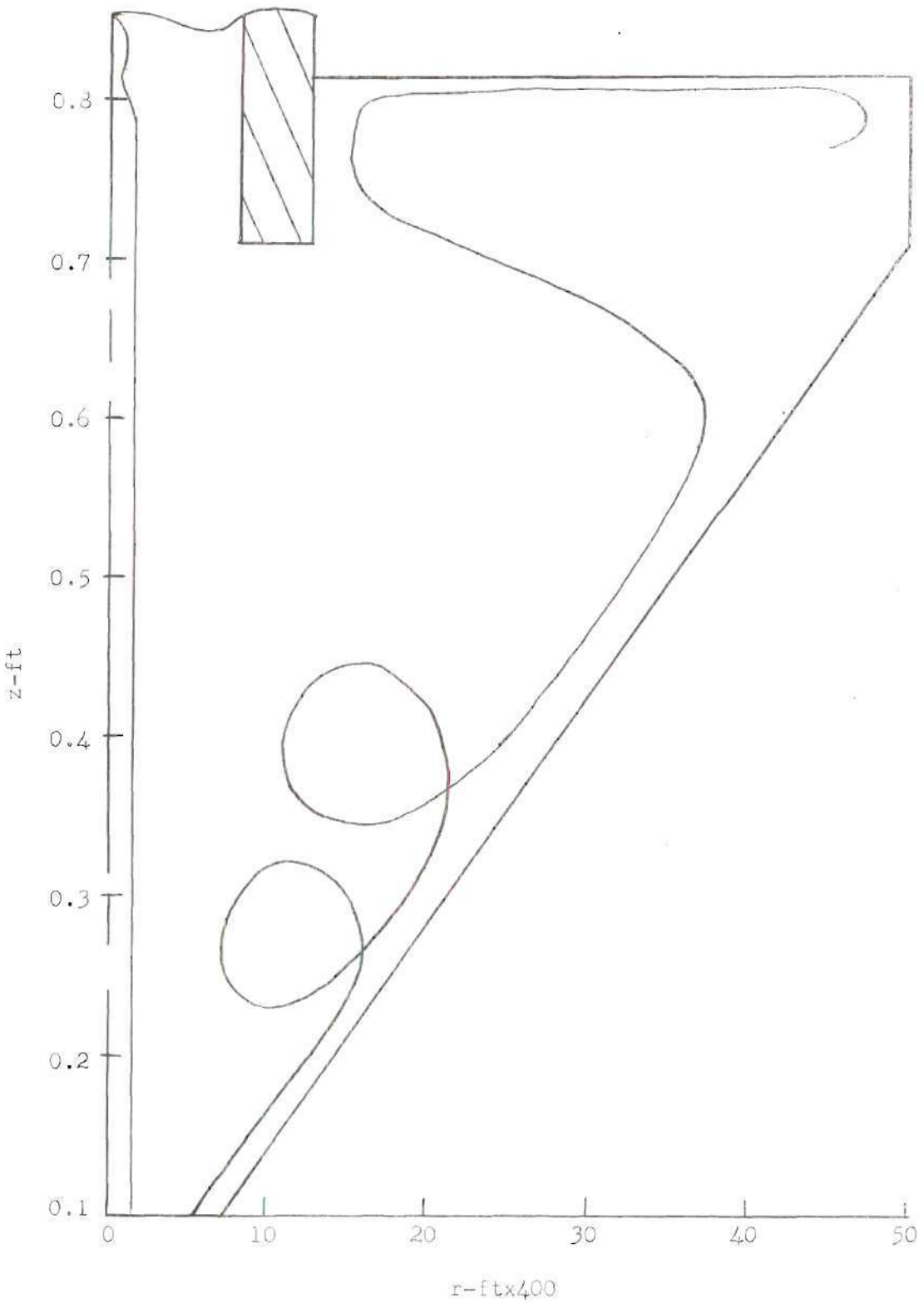

Figure 23. Sketch of an Exceptional Inlet Particle Trajectory

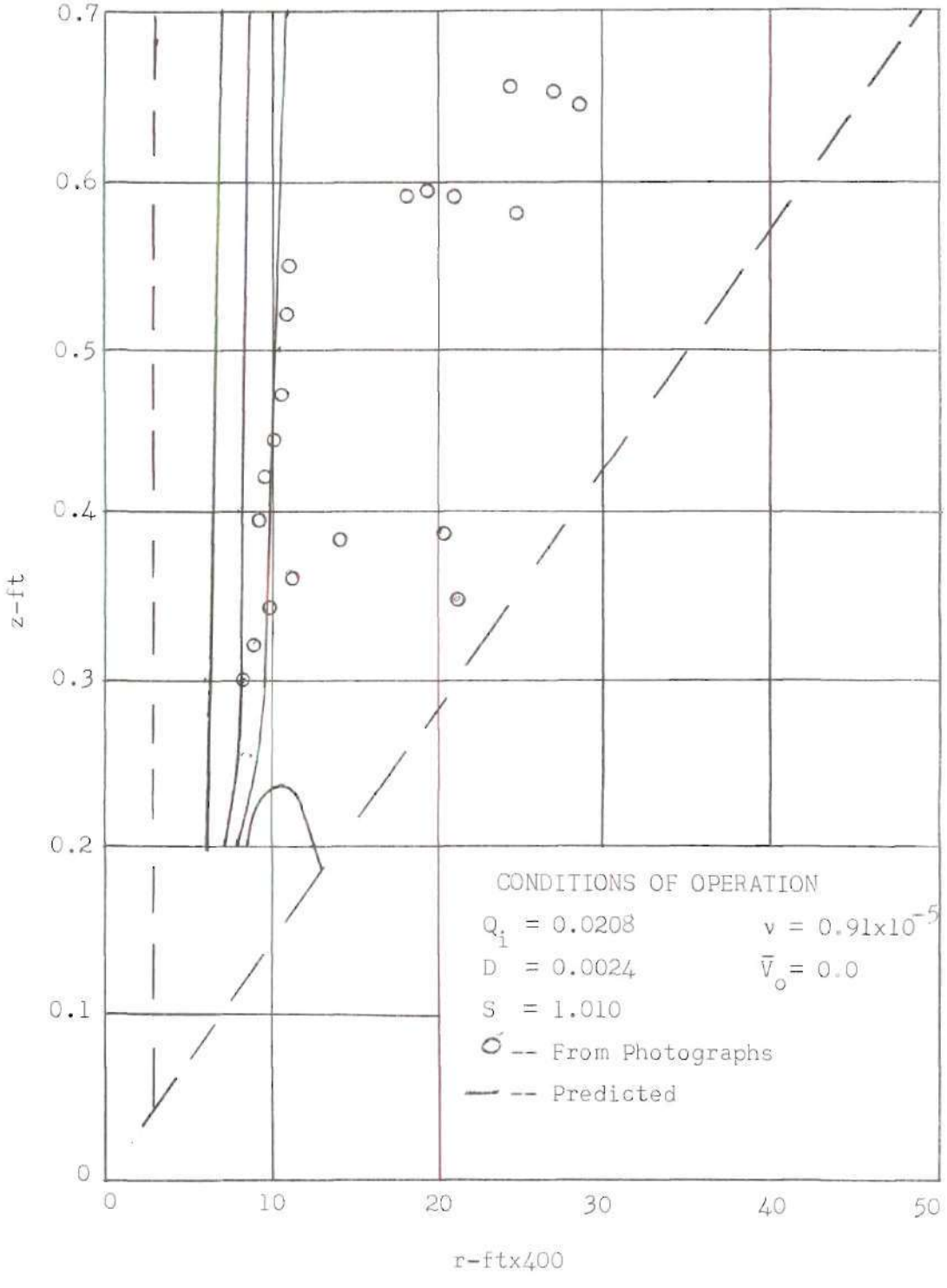

Figure 24. Comparison of Predicted and Observed Secondary Trajectories

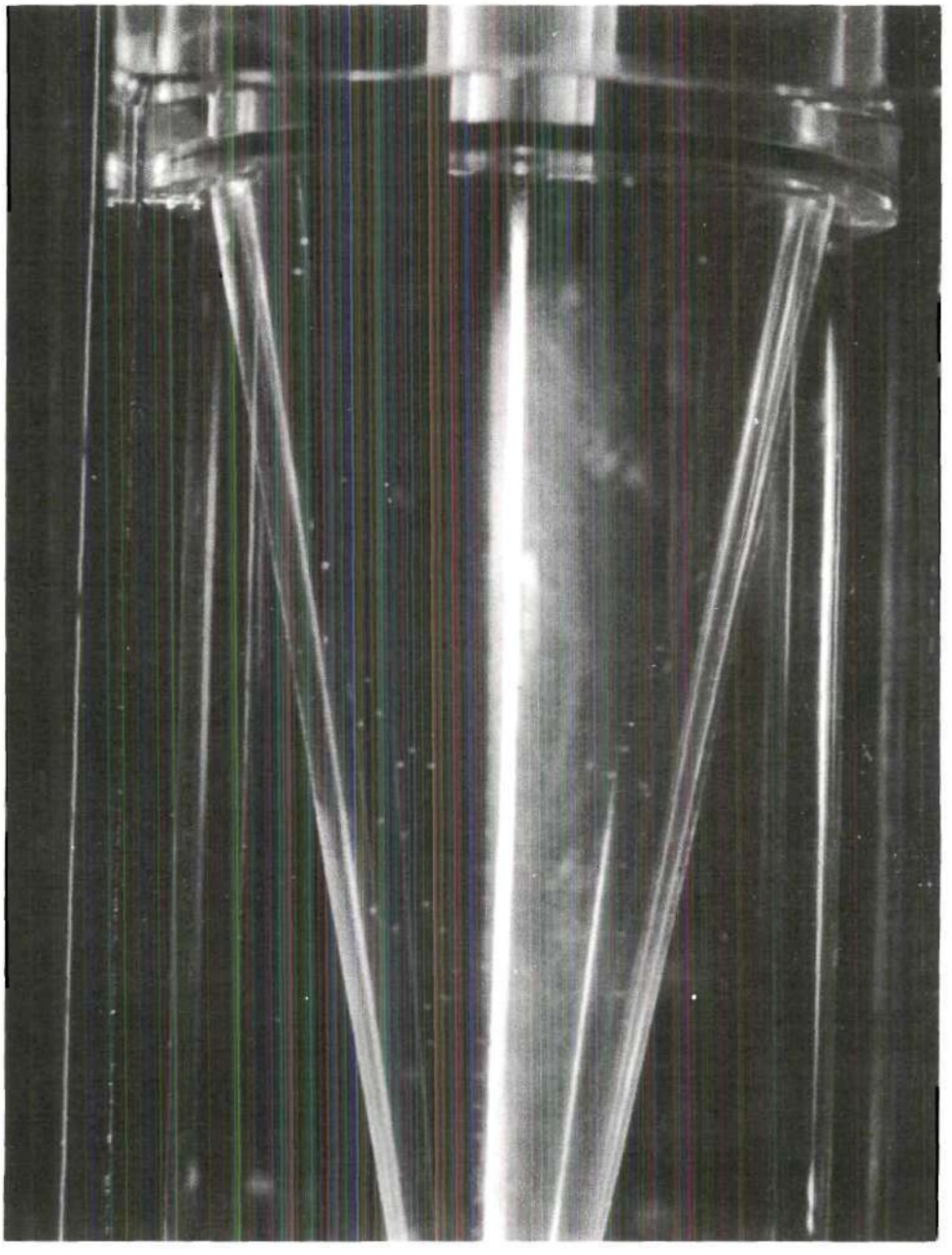

Figure 25. Inner Core Trajectory.

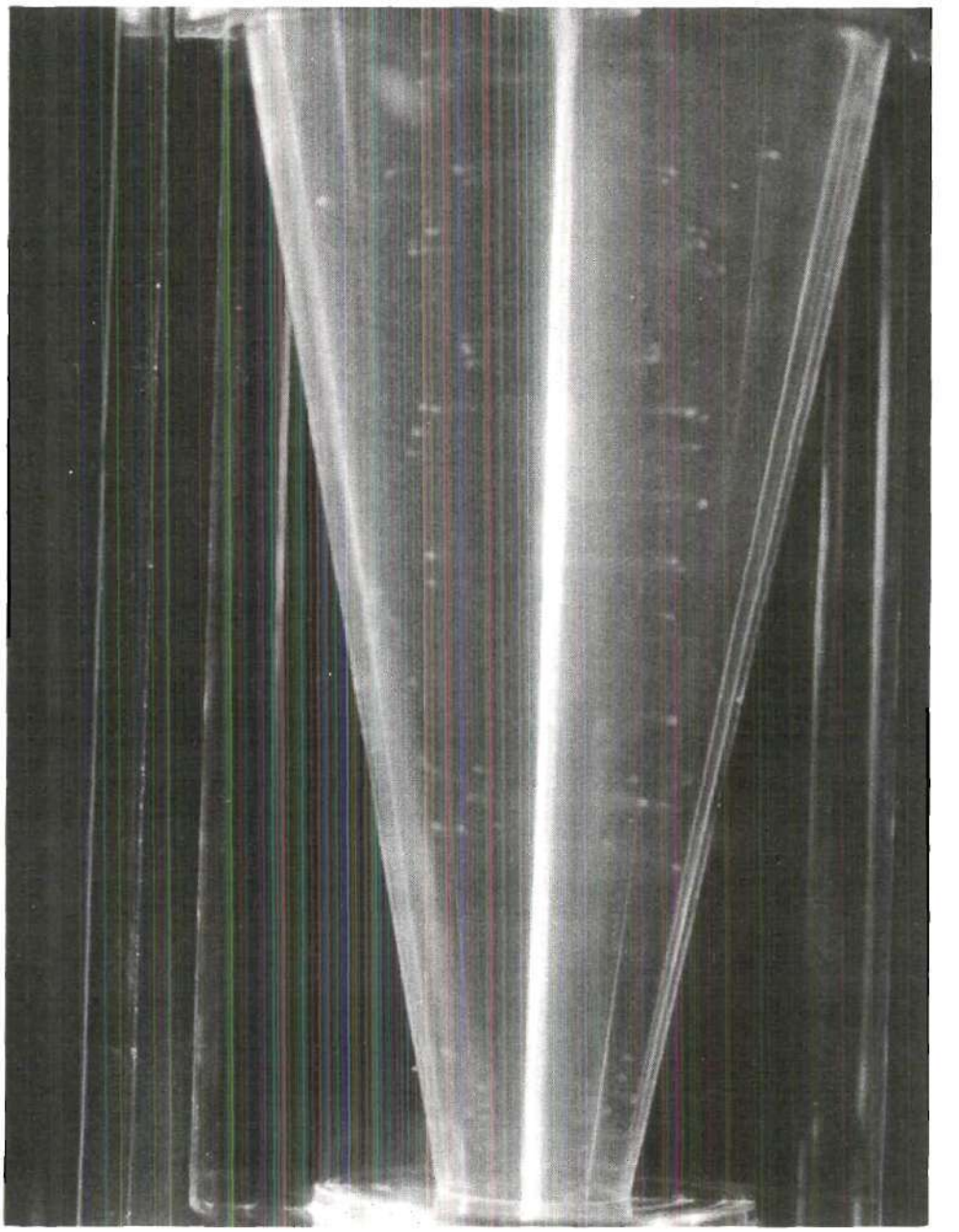

Figure 26. Equilibrium Positions of Particles.

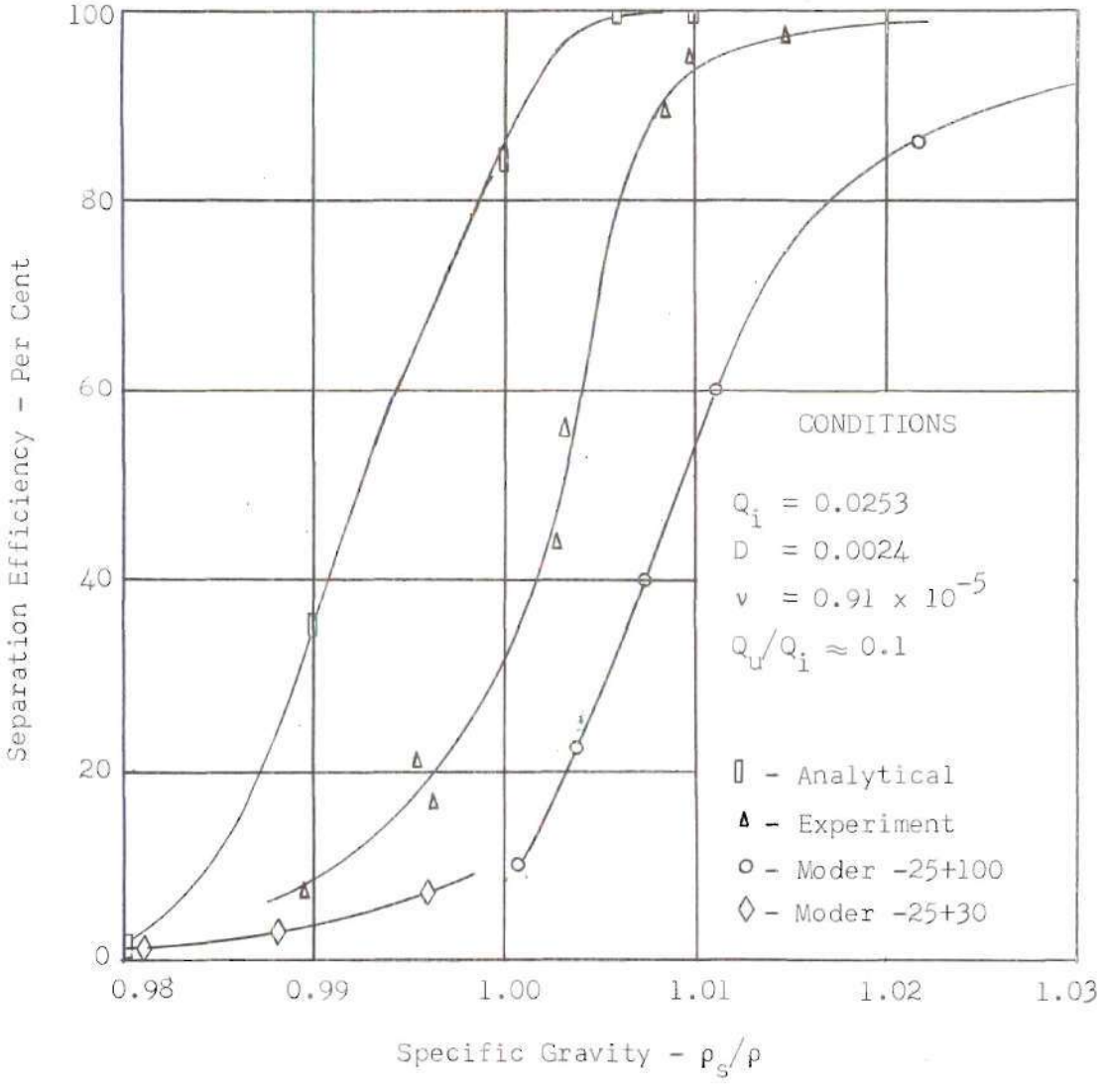

Figure 27. Comparison of Experimental and Analytical Separation Efficiency

APPENDIX B

DIGITAL COMPUTER PROGRAM

Numerical solution of the equations of motion for a sphere in hydrocyclone flow was implemented through the use of the "Algol" language for the compiler used on the Burroughs 220 Data Processing System of the Rich Electronic Computer Center at the Georgia Institute of Technology. A calculation flow chart for development of the program is presented as Figure 28 and presents only the major sequence of steps involved in the iterative procedure employed. The program used and an example of the typical output results are presented for the convenience of future investigators in this area.

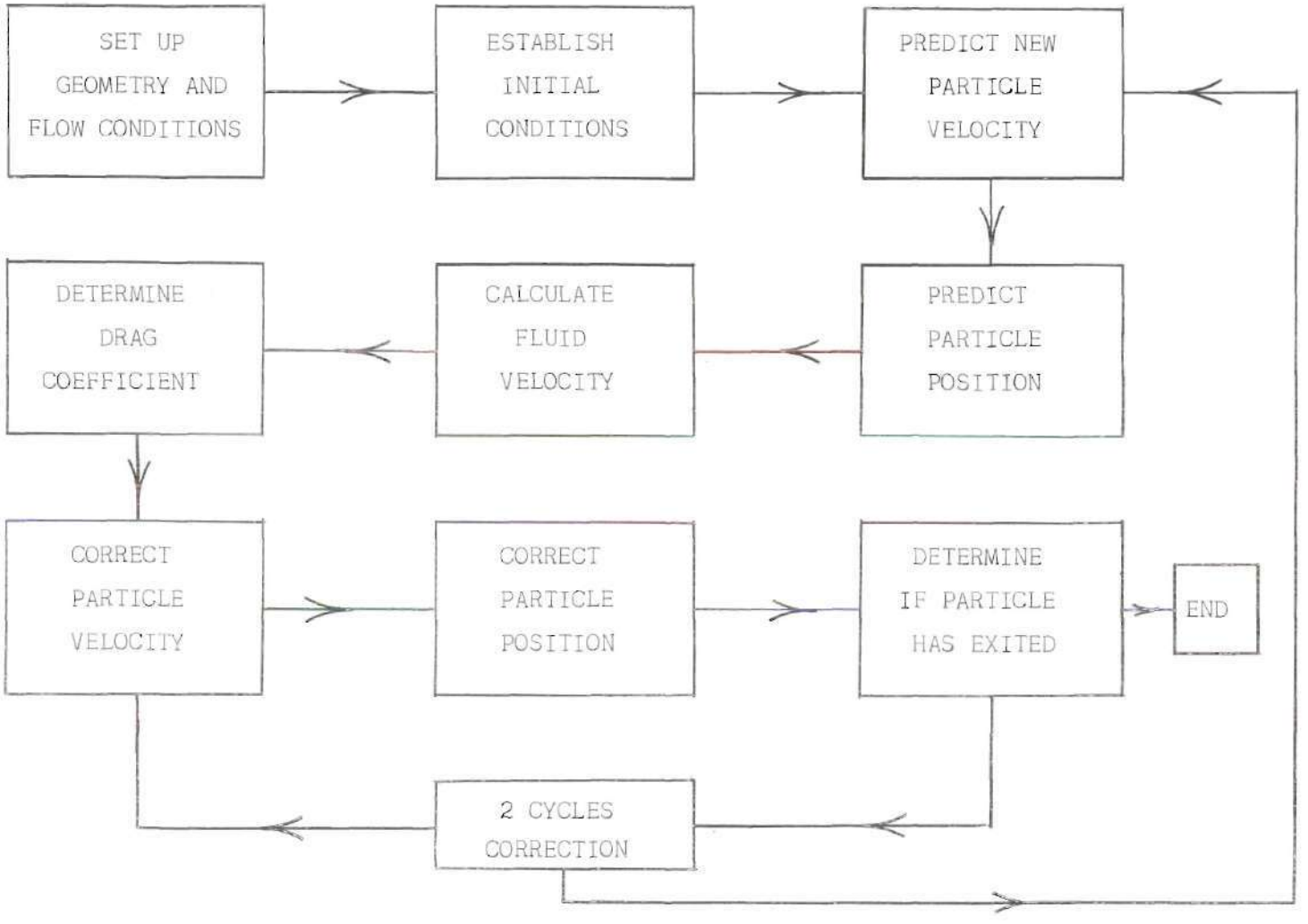

Figure 28. Calculation Flow Diagram for Numerical Solution

```
   COMMENT C W BOUCHILLON  ME DEPT  EXT 458                                  $
COMMENT    COMPUTER PROGRAM FOR SOLUTION OF THE FULL EQUATIONS OF
           MOTION FOR SPHERICAL PARTICLES IN HYDROCYCLONE FLOW               $
        B = 10.0                                                             $
        TB = 0.17633   $   RC1  =  0.00833   $   RC2  =  0.0167             $
        QI = 0.0253  $  RC3 = 0.125  $  RC4 = 0.0208   $
        G = 32.2                                                             $
        PI = 3.1415927                                                       $
        Z0 = RC1/TB                                                          $
        Z2 = RC3/TB                                                          $
        Z1 = 0.93.Z2                                                         $
        Z3 = Z2 + 0.1042  $
        R4 = 0.5(0.5(Z1+Z2)TB+RC1)                                           $
        R5 = RC3 - R4  $
        NU = 0.91**-5           $
        DIA  =  0.0024                                                       $
        K = RC2*-1.8                                                         $
      RSPG = 1.02   $  N = 0.4       $  ENTER TRAJ                           $
        READ ($$ANY)                                                         $
    SUBROUTINE TRAJ $ BEGIN
   COMMENT  INITIAL CONDITIONS OF PARTICLE TRAJECTORIES                      $
        BEGIN  AR = RC3 - N.0.05208333                                       $
        DT = 0.00001                                                         $
        SG  =  1.0/RSPG       $
        WRITE ($$ANS3,FMT3)                                                  $
        TIME = 0.0                                                           $
        C1  =  66.44.QI                                                      $
        AZ = Z3 - 0.0521                                                     $
        C3 = (2.0.QI)/(PI(Z1.TB-RC1)(Z1.TB-RC1))                             $
        AVFR = 0.0                                                           $
        AVFT = C1(AR*-0.8)                                                   $
        AVFZ = C3(((Z2.TB+RC1)/AR)-2.0-(0.5(TB/AR)(Z2-Z1)))                  $
        AVPR = 0.0   $  AVPT = AVFT $  AVPZ = AVFZ  $
        AT = 0.0                                                             $
        AVR = 0.0                                                            $
        ACDV = 0.0                                                           $
```

```
        WRITE ($$TOP1)                                                    $
        WRITE ($$ANS1,FMT1)                                               $
        CNT = 0.0                                                         $
   COMMENT  PREDICT NEW PARTICLE VELOCITY                                 $
PRED..      CVPR = (((AVPT.AVPT - RSPG.AVFT.AVFT)/AR)
                    ((0.75.ACDV)(AVFR-AVPR)/DIA)(RSPG))DT                 $
        CVPT = (((0.75.ACDV.RSPG)(AVFT-AVPT)/DIA)-((AVPR.AVPT)/AR))DT     $
        CVPZ = ((G)(RSPG-1.0) + ((0.75.ACDV.RSPG)(AVFZ-AVPZ)/DIA))DT      $
   EITHER IF AR LEQ RC2   $ BEGIN
        CVPR = CVPR + 0.375.RSPG((C3(AVFZ-AVPZ)(AZ.TB+RC1)/AR.AR)
           2.0.C1.K(AVFT-AVPT))DT                                         $
        CVPT = CVPT + 0.75.C1(AVFR-AVPR)RSPG.DT   END                     $
     OTHERWISE  $  BEGIN
        CVPR = CVPR
           .375.RSPG((C3(AVFZ-AVPZ)(AZ.TB+RC1)/AR.AR) - 0.2.C1(AVFT-
        AVPT)/AR*1.8) DT       $
        CVPT = CVPT + 0.075.C1(AVFR-AVPR)(AR*-1.8)RSPG.DT   END  $
    CVPZ = CVPZ - 0.375.C3.RSPG.DT(AVFR-AVPR)(AZ.TB+RC1)/AR.AR    $
        BVPR = AVPR + CVPR                                                $
        BVPT = AVPT + CVPT                                                $
        BVPZ = AVPZ + CVPZ                                                $
   COMMENT   PREDICT NEW PARTICLE POSITION                                $
        BR = AR + (0.5)(AVPR + BVPR)DT                                    $
        BT = AT + (0.5)(AVPT/AR + BVPT/BR)DT                              $
        BZ = AZ + (0.5)(AVPZ + BVPZ)DT                                    $
   COMMENT   CALCULATE FLUID VELOCITY AT NEW POSITION                     $
CORR..    EITHER IF BR LEQ RC2                                            $
        BVFT = C1.BR(RC2*-1.8)                                            $
        OTHERWISE $ BVFT = C1(BR*-0.8)                                    $
   EITHER IF BZ GEQ Z2                                                    $
   BEGIN BVFZ = (C3)(((Z2.TB+RC1)/BR)-2.0-0.5(TB/BR)(Z2-Z1))              $
        BVFR = 0.0                  END                                   $
      OR IF BZ GEQ Z1                                                     $
   BEGIN  BVFZ = (C3)(((BZ.TB+RC1)/BR) - 2.0
        -(TB/BR)(0.5(BZ-Z1)+(Z2-Z1)(SIN((BZ-Z1)PI/(Z2-Z1)))/2.0.PI))      $
        S = SIN (0.5.PI(BZ-Z1)/(Z2-Z1))                                   $
```

```
      BVFR=(-C3•TB)((1•0-(RC1/BR))(1•0-S•S))END                                $
   OTHERWISE $ BEGIN BVFZ = (C3)(((BZ•TB+RC1)/BR)-2•0)                         $
      BVFR = (-C3•TB)(1•0 - (RC1/BR))     END                                  $
   COMMENT  DETERMINE THE RELATIVE VELOCITY AND DRAG COEFFICIENT               $
      BVR = SQRT ((BVFR-BVPR)(BVFR-BVPR)+(BVFT-BVPT)(BVFT-BVPT)
        (BVFZ-BVPZ)(BVFZ-BVPZ))                                               $
      BRDVR=BVR•DIA/NU  $
    EITHER IF BRDVR LEQ 1•0                                                   $
      BCDV = 24•0•NU/DIA                                                      $
     OR IF BRDVR LEQ 1000•0                                                   $
      BCDV = (19•5)((NU/DIA)*0•5714)(BVR*0•4286)                              $
     OR IF BRDVR LEQ 200000•0                                                 $
      BCDV = 0•45•BVR                                                         $
   OTHERWISE $  BCDV = 0•2•BVR                                                $
   COMMENT  CORRECT CHANGE IN PARTICLE VELOCITY ON THE INTERVAL               $
      CN = CN + 1•0  $  IF CN LEQ 2•0   $
BEGIN   DVPR = (0•5•CVPR) + (0•5)(((BVPT•BVPT - RSPG•BVFT•BVFT)/AR)
          ((0•75•BCDV)(BVFR-BVPR)/DIA)(RSPG))DT
              (0•5•RSPG)(BVR-AVR)(BVFR+AVFR-BVPR-AVPR)/(AVR+BVR)  $
      DVPT = (0•5•CVPT) + (0•5)(((0•75•BCDV)(BVFT-BVPT)/DIA)(RSPG)
        - (BVPR•BVPT/BR))DT
              (0•5•RSPG)(BVR-AVR)(BVFT+AVFT-BVPT-AVPT)/(AVR+BVR)  $
      DVPZ = (0•5•CVPZ)  + (0•5) ((G)(RSPG-1•0) + ((0•75•BCDV)(RSPG)
        (BVFZ-BVPZ)/DIA))DT
              (0•5•RSPG)(BVR-AVR)(BVFZ+AVFZ-BVPZ-AVPZ)/(AVR+BVR)  $
   EITHER IF BR LEQ RC2   $ BEGIN
      DVPR = DVPR +0•1875•RSPG((C3(BVFZ-BVPZ)(BZ•TB+RC1)/BR•BR)
        2•0•C1•K(BVFT-BVPT))DT                                                $
      DVPT = DVPT +0•375•C1(BVFR-BVPR)RSPG•DT   END                           $
    OTHERWISE  $  BEGIN
      DVPR = DVPR
        •1875•RSPG ((C3(BVFZ-BVPZ)(BZ•TB+RC1)/BR•BR) - 0•2•C1(BVFT-
      BVPT)/BR*1•8) DT       $
      DVPT = DVPT +0•0375•C1(DVFR-BVPR)(BR*-1•8)RSPG•DT   END  $
   DVPZ = DVPZ -0•1875•C3•RSPG•DT(BVFR-BVPR)(BZ•TB+RC1)/BR•BR    $
      BVPR =AVPR +DVPR $  BVPT = AVPT + DVPT  $  BVPZ = AVPZ + DVPZ $
```

```
   COMMENT  CORRECT PARTICLE POSITION                                    $
        BR = AR + (0.5)(AVPR + BVPR)DT                                   $
        BT = AT + (0.5)(AVPT/AR + BVPT/BR)DT                             $
        BZ = AZ + (0.5)(AVPZ + BVPZ)DT                                   $
        GO TO CORR  END                                                  $
        CN = 0.0  $
    CONT.. CNT=CNT+1.0 $
        TIME = TIME + DT                                                 $
   COMMENT  DETERMINE IF THE PARTICLE HAS DEPARTED THE CLEANER           $
        IF  (BZ GTR Z2)  AND  ((BR LSS RC4) OR (BR GTR RC3))             $
        BEGIN  N= 0.9  $  GO TO LAZY            END                      $
        IF (BZ LEQ Z2)  AND  ((BR LSS RC1)  OR  (BR GTR BZ.TB))          $
        GO TO LAZY                                                       $
        IF BZ  LEQ  Z0                                                   $
        GO TO LAZY                                                       $
        IF BZ GEQ Z3  $  BEGIN  N = 0.9  $  GO TO LAZY      END          $
        IF TIME GTR   5.0                                                $
        GO TO LAZY                                                       $
        IF CNT EQL 20.0  $  BEGIN  WRITE ($$ANS2,FMT1)  $  CNT = 0.0     $
        IF DT LSS 0.0010 $  DT = 2.0.DT    END  $
        AVFR =BVFR  $  AVFZ =BVFZ  $  AVFT =BVFT  $
                          AR = BR  $  AT = BT  $  AZ = BZ                $
        AVPR = BVPR  $  AVPT = BVPT  $  AVPZ = BVPZ  $
        ACDV  =  BCDV  $  AVR  = BVR     $
   COMMENT  CONTINUE THE TRAJECTORY DETERMINATION                        $
        GO TO PRED                                                       $
   COMMENT  END FOR THE TRAJECTORY DETERMINATION                         $
   LAZY..  WRITE ($$ANS2,FMT2)              END                          $
FORMAT TOP1(B4,*TIME*,B7,*R*,B9,*THETA*,B8,*Z*,B7,*REY-NO.*,B5,
*PVR*,B7,*PVZ*,B7,*PVT*,W6)                                              $
FORMAT FMT1 (X8.4,X12.8,X12.6,X11.7,X10.3,X10.5,X11.4,X11.4,W0)          $
FORMAT FMT2 (X8.4,X12.8,X12.6,X11.7,X10.3,X10.5,2X11.4,W6,W1)            $
FORMAT FMT3(B22,*TABLE II.  TRAJECTORIES IN HYDROCYCLONES*,W6,B20
,*CONDITIONS OF OPERATION- CONE ANGLE = *,X7.3,* DEGREES,*,W0,B20,*VISC
OSITY = *,F15.6,* FT SQ/SEC,  INLET FLOW RATE = *,X6.3,* GPM*,W0,B20,*
PARTICLE DIAMETER =*,X9.5,* , SPECIFIC GRAVITY = *,X8.4,W0)              $
```

```
  OUTPUT ANS1 (TIME,AR,AT,AZ,ARDVR,AVPR,AVPZ,AVPT)                    $
  OUTPUT ANS2 (TIME,BR,BT,BZ,BRDVR,BVPR,BVPZ,BVPT)                    $
OUTPUT ANS3 (B,NU,(QI.450.0),DIA,SG)                                  $
 LZY=0.0   RETURN END TRAJ                          $
INPUT ANY (BODY,S)                                                    $
FINISH                                                                $
```

TABLE II. TRAJECTORIES IN HYDROCYCLONES

CONDITIONS OF OPERATION- CONE ANGLE = 10.000 DEGREES,
VISCOSITY = .910000,-05 FT SQ/SEC, INLET FLOW RATE = 11.385 GPM
PARTICLE DIAMETER = .00240 , SPECIFIC GRAVITY = .9803

TIME	R	THETA	Z	REY-NO.	PVR	PVZ	PVT
.0000	.10416667	.000000	.7609980	.000	.00000	-1.0538	10.2651
.0002	.10416647	.019709	.7607874	.799	-.00302	-1.0537	10.2652
.0006	.10416417	.059128	.7603660	2.386	-.00904	-1.0535	10.2654
.0014	.10415229	.137976	.7595234	5.485	-.02079	-1.0532	10.2666
.0030	.10410128	.295763	.7578389	11.261	-.04267	-1.0526	10.2717
.0062	.10390455	.612051	.7544722	20.748	-.07846	-1.0515	10.2912
.0126	.10325173	1.249610	.7477523	31.865	-.11948	-1.0478	10.3532
.0254	.10156372	2.552887	.7344423	37.144	-.13632	-1.0296	10.5045
.0510	.09810776	5.285610	.7087845	37.409	-.13498	-.9727	10.8053
.0766	.09407004	8.207278	.6843224	28.073	-.20056	-.9402	11.1896
.1022	.08767283	11.443543	.6612004	30.428	-.28541	-.8496	11.8644
.1278	.08033067	15.194343	.6411324	33.172	-.28264	-.7209	12.7356
.1534	.07315688	19.610401	.6244110	36.235	-.27839	-.5805	13.7291
.1790	.06609693	24.875915	.6117425	40.325	-.27262	-.4014	14.8948
.2046	.05922165	31.247400	.6043269	45.342	-.26403	-.1670	16.2671
.2302	.05260359	39.076241	.6038518	51.736	-.25252	.1453	17.8886
.2558	.04631756	48.847972	.6127271	60.175	-.23809	.5705	19.8090
.2814	.04043628	61.236127	.6344884	71.732	-.22104	1.1634	22.0847
.3070	.03509865	77.172049	.6743132	78.703	-.18310	1.9584	24.7342
.3326	.03058219	97.643232	.7350310	101.087	-.16169	2.8115	27.6010
.3582	.02656757	123.903050	.8175263	111.913	-.15065	3.6548	30.8932

APPENDIX C

ANALOG COMPUTER PROGRAM

Solution of the reduced equations of motion for spherical particles in hydrocyclone flow for special cases were obtained by using an electrical analog computer for the integration of the system of equations applicable to the special cases. An abbreviated list of symbols used in drawing the circuit diagrams representing the computer components is presented below. This will enable the reader to interpret the circuit diagrams presented as Figures 29 and 30 provided basic electronic symbols are already known.

The circuit diagram for the solution of the special case of small particles -- $R < 1.0$ -- as used in this work is presented as Figure 29. The equations of motion of the particle for this case were presented as Case I of the Analog Computer Solutions in Chapter IV as equations 99 through 101. These equations were transformed into a machine parameter set of equations with the initial conditions as given below.

$$(R_m)_{TT} = 1480\,(R_m^{-2.6}) - 86.5\,(R_m)_T - 80\,R_m^{-1} - 24.0$$

$$Z_T = 1.58\,\{[(0.7052\,Z + 0.04)/(R_m)] - 2.0\}$$

$$\theta_T = 1172\,(R_m^{-1.8})$$

with the initial conditions

$$R_m(o) = 25.25 \qquad \theta(o) = 0.0$$

$$(R_m)_T(o) = 0.0 \qquad z_1(o) = 0.709$$

where

$$R_m = 400\ r\ , \quad Z = 100\ z\ , \quad \text{and} \quad T = 400\ t$$

were used in the transformation of the equations of motion into the machine parameter representation.

Case II as discussed in the Analog Solutions section of Chapter IV had the characteristic equations of motion presented by equations 102 through 105. These equations were transformed into a machine parameter set of equations with the initial conditions as given below. The circuit depicted in Figure 30 gave the solution to this differential system.

$$(R_m)_{TT} = 9.6 \times 10^6 \left(R_m^{-2.6}\right) - 15850 \left[0.342 - 1.14/(R_m) + (R_m)_T/80\right] C \bar{V}$$

$$Z_{TT} = 39.70\ C \bar{V} \left[1.94\ (0.704\ Z + 3.32 - 2\ R_m)/(R_m) - Z_T/20\right]$$

with the initial conditions

$$R_m(o) = 40.0 \qquad Z(o) = 0.709$$

$$(R_m)_T(o) = 0.0 \qquad Z_{TT}(o) = 0.0$$

where

$$R_m = 400\ r\ , \quad Z_1 = 100\ z\ , \quad \text{and} \quad T = 5\ t$$

were used in the transformation of the equations of motion into the machine parameter representation.

Because the relationship RxC(R) appeared in both the r and z equations for Case II, it was convenient to generate this relation as a function of R. An additional advantage was gained in that RxC(R) was readily represented as several straight line segments on a diode function generator by offsetting the zero position as indicated in Figure 31. The value of the slope of the RxC(R) function at R = 0.0 was too large to be represented by the diode function generator without the offset employed. The monotonically decreasing slope was more readily negotiated by the buildup effect of the segments coming from the offset zero position.

Symbolism for Analog Computer Components

Integrating Amplifier

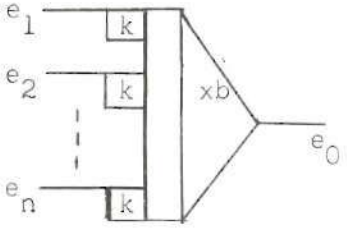

$$e_0 = -b \int_0^t \sum_{i=1}^{n} k\, e_i \, dt$$

Summing or Inverting Amplifier

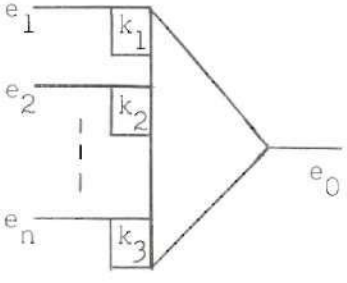

$$e_0 = -\sum_{i=1}^{n} k_1 e_i$$

Special Purpose Amplifier

(Used for output of special components, etc.)

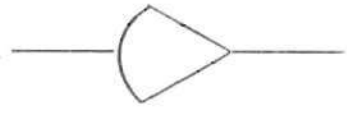

$$e_0 = -e_i$$

Potentiometer

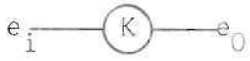

$e_0 = K e_i$

Electro-Mechanical Resolver

(Multi-purpose, e.g.: $e_{0_j} = k e_{i_j}$; $e_0 = k e_1/e_2$; $e_0 = k e_1 e_2$;
$e_0 = k e_1 \sin e_2$; etc.)

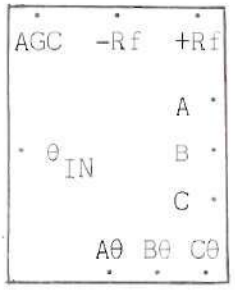

Diode Function Generator

(Straight line approximation to functions of one variable)

$e_0 = f(e_i)$

Fixed Diode Function Generator

(Generates Given Functions Such as Sin, Cos, etc.)

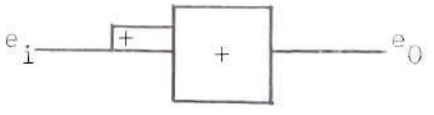

e.g., $e_0 = k \log_{10} e_i$

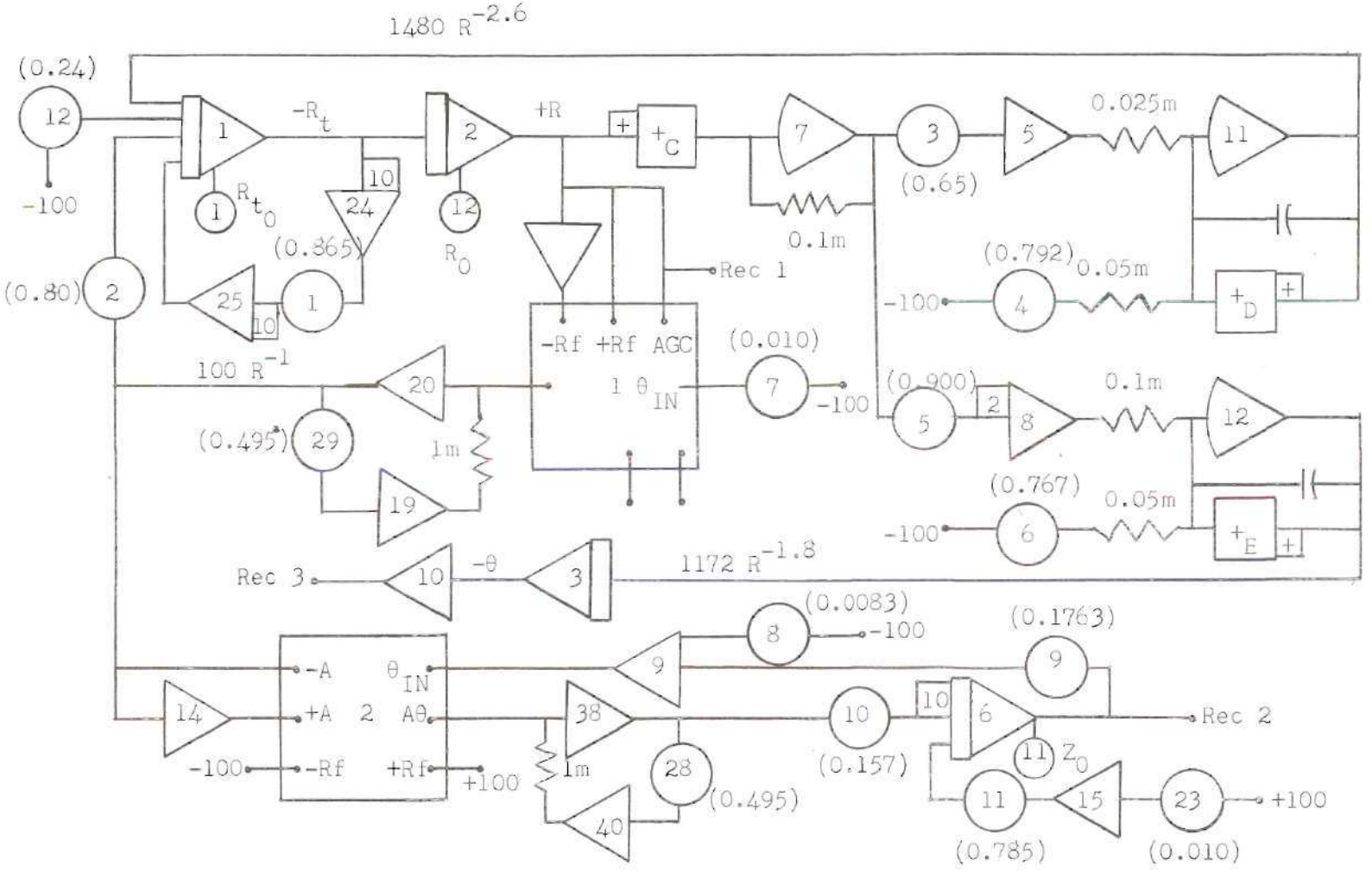

Figure 29. Schematic Diagram for Analog Computer—Case I

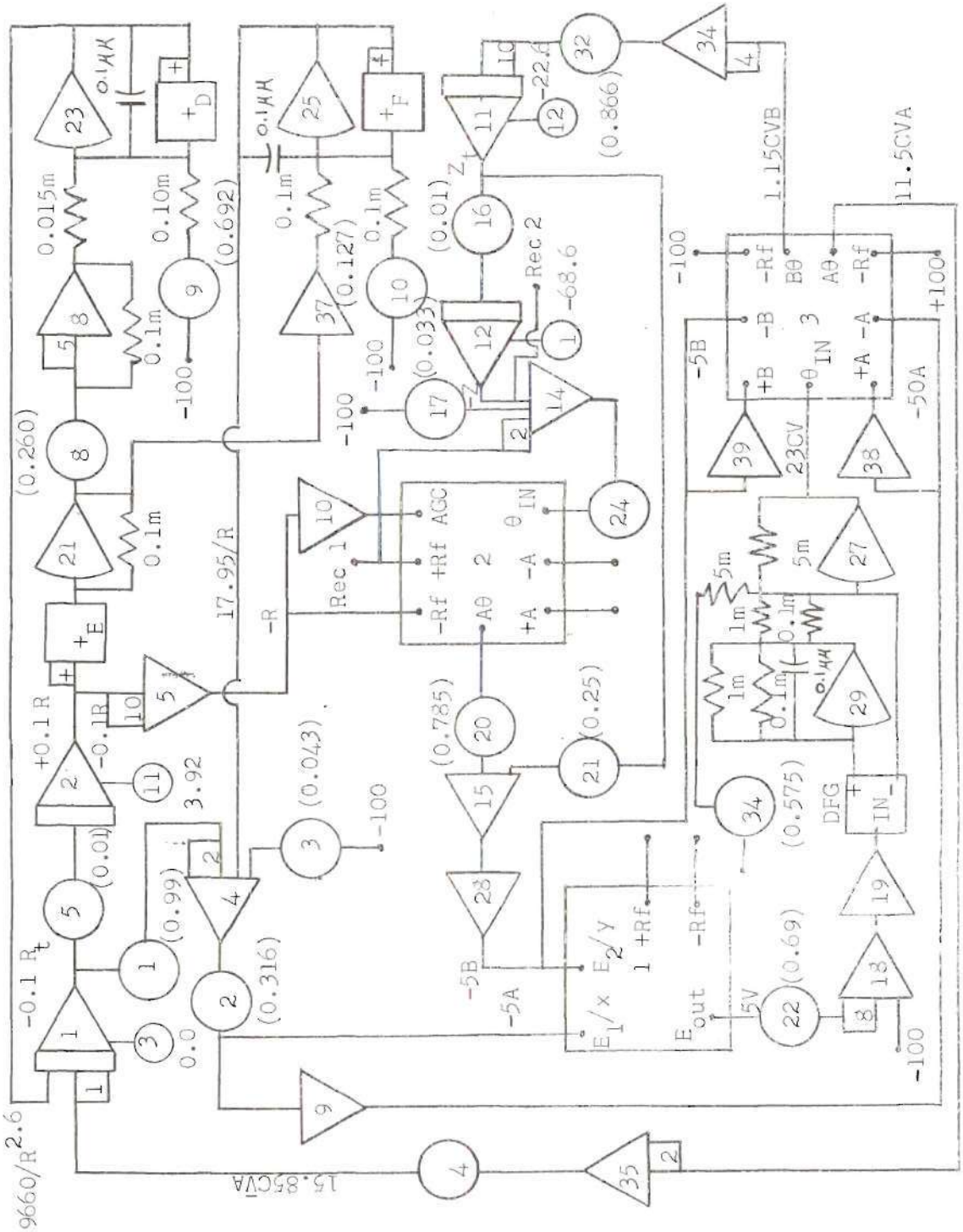

Figure 30. Schematic Diagram for Analog Computer—Case II

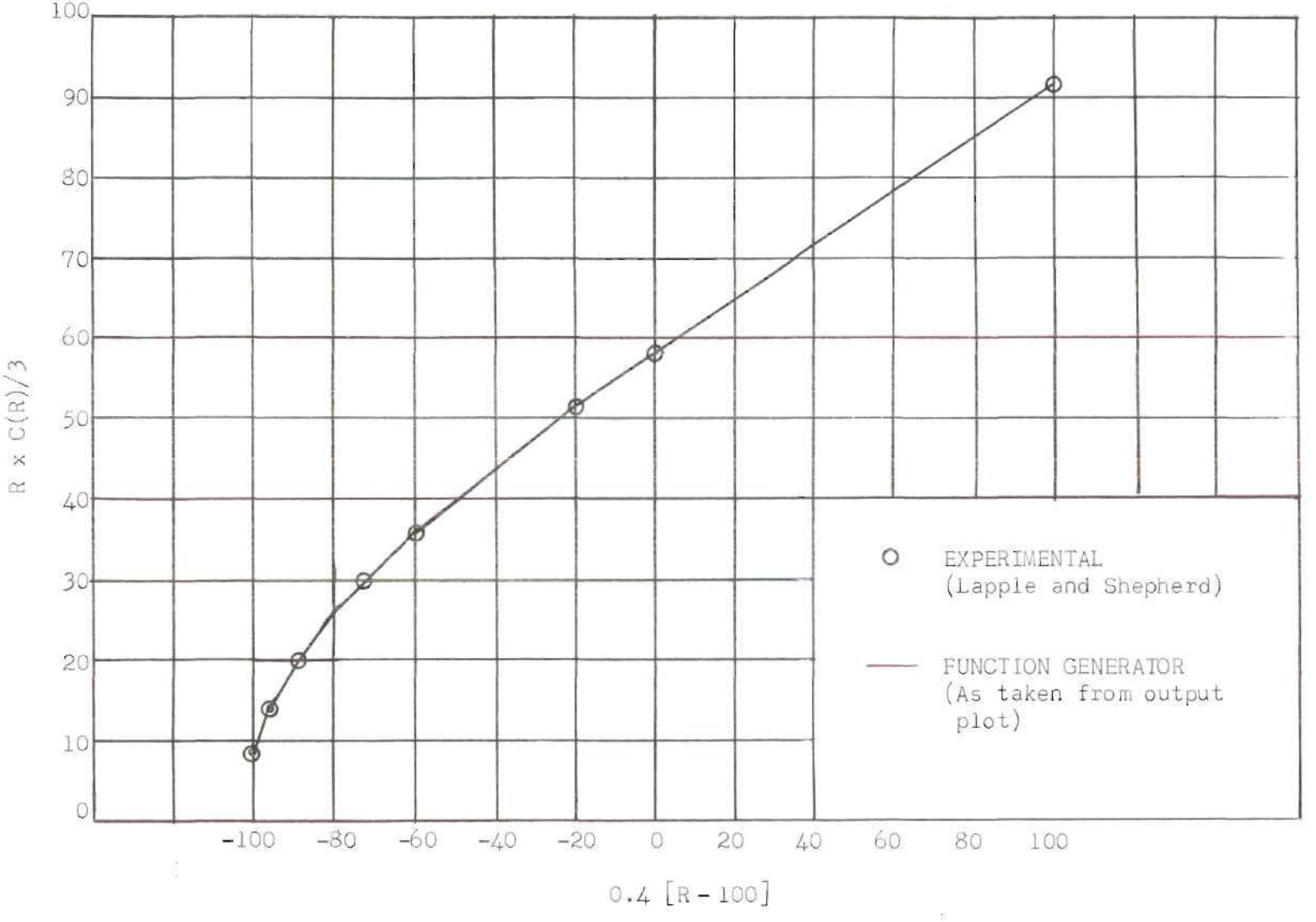

Figure 31. Diode Function Generator Representation of R x C(R)

BIBLIOGRAPHY

Literature Cited

1. Broer, L. J. F., "Symposium Cyclonen," De Ingenieur, Vol. 65, No. 38, 1953, Ch. 77.

2. Winternitz, F. A. L., "Probe Measurements in Three Dimensional Flow," Aircraft Engineering, Vol. 28, No. 330, August, 1956, pp. 273-8.

3. Ter Linden, A. J., Ionindustrie-Zeitung, Vol. 77, No. 49, 1953, p. 49.

4. Shepherd, C. B. and Lapple, C. E., "Flow Pattern and Pressure Drop in Cyclone Dust Collectors," Industrial and Engineering Chemistry, Vol. 31, 1939; id., Vol. 32, 1940.

5. Smith, J. L., Jr., "An Experimental Study of the Vortex in the Cyclone Separator," American Society of Mechanical Engineers Paper No. 61-WA-189.

6. Bradley, D. and Pulling, D. J., "Flow Patterns in the Hydraulic Cyclone and Their Interpretations in Terms of Performance," Transactions of the Institution of Chemical Engineers, Vol. 37, No. 1, 1959, p. 34.

7. Kelsall, D. F., "A Study of the Motion of Solid Particles in a Hydraulic Cyclone," Trans. Inst. Chem. Engr., Vol. 30, 1952, p. 87.

8. Moder, J. J. and Dahlstrom, D. A., "Fine Size, Close Specific Gravity Solid Separation with the Liquid-Solid Cyclone," Chemical Engineering Progress, Vol. 48, No. 2, February, 1952, p. 75.

9. Bradley, D., "A Theoretical Study of the Hydraulic Cyclone," The Industrial Chemist, Vol. 34, September, 1958, p. 473.

10. Tarjan, G., "Beitrag zur Theorie und Praxis des Hydrozyklons," Aufbereitungs-Technik, No. 12, 1961, p. 447.

11. Lapple, C. E. and Shepherd, C. B., "Calculation of Particle Trajectories," Industrial and Engineering Chemistry, Vol. 32, May, 1940, p. 605.

12. Kriebel, A. R., "Particle Trajectories in a Gas Centrifuge," Trans. A.S.M.E., J. Basic Engr., Vol. 83, Series D, No. 3, September, 1961, p. 333.

13. Calder, K. L., "Some Theoretical Aspects of the Rotating Drum Aerosol Chamber," BWL Technical Study No. 13, October, 1958, Army Biological Warfare Laboratory, Frederick Md. ASTIA AD-207-865.

14. Swanson, W. M., "The Magnus Effect: A Summary of Investigations to Date," Trans. A.S.M.E., J. Basic Engr., Vol. 83, Series D, No. 3, September, 1961, p. 461.

15. Rubinow, S. I. and Keller, J. B., "The Transverse Force on a Spinning Sphere Moving in a Viscous Fluid," Journal of Fluid Mechanics, Vol. 11, 1961, p. 447.

16. Lord Rayleigh, "On the Motion of Solid Bodies Through Viscous Liquid," Philosophical Magazine, Sixth Series, Vol. 21, No. 126, June, 1911, p. 697.

17. Bradley and Pulling, op. cit., p. 36.

18. Kelsall, op. cit., p. 87.

19. Schlichting, H., Boundary Layer Theory, Pergamon, New York, 1955, p. 463.

20. Kelsall, op. cit., p. 94.

21. Ibid.

22. Schlichting, op. cit., p. 155.

23. Kelsall, op. cit., p. 104.

24. Bradley and Pulling, op. cit., p. 36.

25. Kelsall, op. cit., p. 98.

26. Ibid., p. 97.

27. Ibid.

28. Ibid.

29. Bradley, op. cit., p. 474.

30. Lapple and Shepherd, op. cit., p. 606.

31. Ibid., p. 605.

32. Ibid.

33. Lamb, Sir Horace, Hydrodynamics, Dover, New York, 1932, p. 642.

34. Rayleigh, op. cit., p. 704.

35. Swanson, loc. cit.

36. Swanson, op. cit., p. 464.

37. Rubinow and Keller, op. cit., p. 461.

38. Ibid., p. 454.

39. Ibid., p. 456.

40. Ibid.

41. Kelsall, op. cit., p. 89.

42. Lapple and Shepherd, op. cit., p. 611.

43. Moder and Dahlstrom, op. cit., p. 77.

44. Hodgman, C. D., Handbook of Chemistry and Physics, Chemical Rubber, Cleveland, Ohio, 36th Edition, p. 1852.

45. Fontein, F. J., van Kooy, J. G., and Leninger, H. A., "The Influence of Some Variables in Hydrocyclone Performance," British Chemical Engineering, June, 1962, p. 410.

46. Ibid.

47. Smith, J. L., Jr., "An Analysis of the Vortex Flow in the Cyclone Separator," A.S.M.E. Paper No. 61-WA-188.

48. Moder, op. cit., p. 79.

Other References

1. Milne-Thompson, L. N., Theoretical Hydrodynamics, The MacMillan Co., New York, 1950, p. 415.

2. Luneau, J. L., "Influence of Acceleration upon the Resistance of Movement in Fluids," Publications Scientifiques et Techniques du Ministry de l' Air, France, No. 363, 1960.

3. Kunz, K. S., Numerical Analysis, McGraw-Hill, New York, 1957.

4. Landweber, L., "On a Generalization of Taylor's Virtual Mass Relation for Rankine Bodies," Quarterly of Applied Mathematics, Vol. 14, No. 1, 1956.

5. Landweber, L. and Yih, C. S., "Forces, Moments, and Added Maddes for Rankine Bodies," Journal of Fluid Mechanics, Vol. 1, Part 3, 1956.

VITA

Charles Wesley Bouchillon was born in Winston County near Louisville, Mississippi on July 17, 1931. He attended elementary and high school at Louisville, graduating in 1949. A Bachelor of Science in Mechanical Engineering degree was granted to him by Mississippi State College in June of 1953. After graduation, he joined the structures development group of Chance Vought Aircraft Corporation at Dallas, Texas, serving as a Junior Engineer until going on active duty as a Second Lieutenant in the Antiaircraft Artillery for a two-year period beginning in January of 1954. He was relieved from active duty as a First Lieutenant in January of 1956 and entered the Graduate Division of the Georgia Institute of Technology shortly thereafter. A Master of Science in Mechanical Engineering degree was awarded to him in June of 1959.

His summer employment included experience in the fields of area mensuration by aerial photography with Production Marketing Association at Sardis, Mississippi, pipeline construction with Station Construction Company at Batesville, Mississippi, and petroleum filtration research with Plantation Pipeline Company in Atlanta, Georgia. While at the Georgia Institute of Technology, he was a part-time Instructor in the School of Mechanical Engineering during the regular school sessions of 1958 through 1961 inclusive. Also he was associated with their Engineering Experiment Station as Research Associate on an industrially sponsored research and developmental program and was Project Director of this program during 1960 to 1962.

He is currently an Associate Professor of Mechanical Engineering at Mississippi State University.

He is a member of Tau Beta Pi and Omnicron Delta Kappa and an associate member of Sigma Xi.

The former Barbara Scott Owens of Headland, Alabama became his wife in 1958 and they have a daughter and a son.